INTEGRATION OF A COORDINATING SYSTEM WITH CONVENTIONAL METROLOGY IN THE SETTING OUT OF MAGNETIC LENSES OF A NUCLEAR ACCELERATOR

FRED J. WILKINS

November 1989

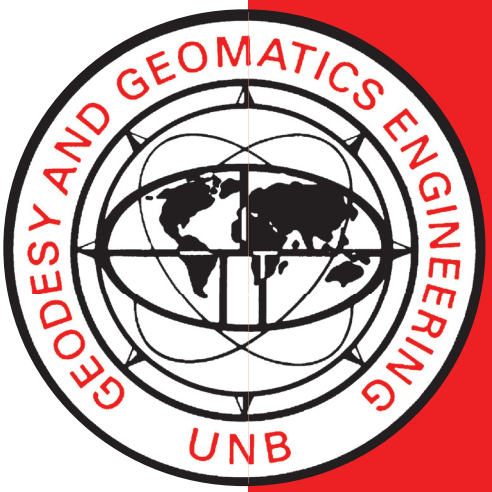

TECHNICAL REPORT
NO. 146

PREFACE

In order to make our extensive series of technical reports more readily available, we have scanned the old master copies and produced electronic versions in Portable Document Format. The quality of the images varies depending on the quality of the originals. The images have not been converted to searchable text.

INTEGRATION OF A COORDINATING SYSTEM WITH CONVENTIONAL METROLOGY IN THE SETTING OUT OF MAGNETIC LENSES OF A NUCLEAR ACCELERATOR

Fred J. Wilkins

Department of Surveying Engineering
University of New Brunswick
P.O. Box 4400
Fredericton, N.B.
Canada
E3B 5A3

November 1989
Latest Reprinting January 1994

PREFACE

This technical report is a reproduction of a thesis submitted in partial fulfillment of the requirements for the degree of Master of Science in Engineering in the Department of Surveying Engineering, September 1989. The research was supervised by Dr. Adam Chrzanowski, and funding was provided partially by the Natural Sciences and Engineering Research Council of Canada, the Atomic Energy of Canada Ltd., and by the National Research Council of Canada's Industrial Research Assistance Program agreement with Usher Canada Ltd.

As with any copyrighted material, permission to reprint or quote extensively from this report must be received from the author. The citation to this work should appear as follows:

Wilkins, F.J. (1989). *Integration of a coordinating system with conventional metrology in the setting out of magnetic lenses of a nuclear accelerator.* M.Sc.E. thesis, Department of Surveying Engineering Technical Report No. 146, University of New Brunswick, Fredericton, New Brunswick, Canada, 163 pp.

Abstract

Industrial metrology is a discipline of engineering surveys that requires the utmost in achievable accuracies. The instrumentation used in traditional industrial metrology requires long painstaking procedures with very skilled craftsmen to obtain the required results. The introduction of electronic theodolites has changed the approach and the flexibility of industrial surveys.

The development of coordinating systems, electronic theodolites interfaced to a microcomputer, provides the capabilities for on line data gathering with simultaneous processing in all three dimensions. The existing requirements for conventional metrology of having to access particular lines of sight can be neglected, without loss of accuracy and with the addition of redundancy, to obtain the coordinate solutions. In addition, groups of targets can be analysed in virtual real time by determining coefficients for a particular surface from a least squares fitting. However, the coordinating system and the conventional techniques each have their own assets, with the integration of the two techniques into a single system allowing for the full exploitation of each's assets.

A coordinating system, precision three dimensional coordinating system ("P3DCS"), has been developed at UNB, as a by-product of a project involving the setting out of components forming a portion of a nuclear accelerator. The algorithms that have been developed and used for the software development are presented with emphasis placed on obtaining the optimal accuracies from the system.

The UNB coordinating system was integrated with traditional metrology techniques in the successful completion of the setting out of Phase II of the Tandem Accelerator Superconducting Cyclotron ("TASCC") for Atomic Energy of Canada Ltd. ("AECL"). This phase of TASCC involved the precision three dimensional alignment of 67 magnets, both bending and focussing, to tolerances less than 0.1 mm in the transverse and 0.2 mm in the along beam line from their nominal locations.

Table of Contents

List of Illustrations

page

List of Tables

Acknowledgements

There are no research projects that can be concluded without the help and support of many individuals, whose contributions deserve proper acknowledgement.

Firstly, I would like to thank my supervisor, Dr. Adam Chrzanowski, for providing the opportunity for me to partake in one of his many research projects and supplying some of the financial resources available to him from the Natural Science and Engineering Research Council of Canada. His endless supply of patience and knowledge were drawn upon many times throughout the research activity as well as in the preparation of this manuscript. In times of need the opportunities for discussion, encouragement, and friendship were always available irregardless of his very busy schedule and other commitments.

Additional financial support for these studies has been obtained from contract agreements between Atomic Energy of Canada Ltd. with the University of New Brunswick and Usher Canada Ltd. In particular, I would like to thank Dr. Hermann Schmeing of AECL for his willingness to disregard his initial reservations, which allowed the involvement of UNB in the TASCC project.

All surveying projects that involve field work require additional personnel to help complete the various tasks. In this respect I would like to acknowledge the contributions of James Secord, Mark Rohde, Peter Stupan, and Pablo Romero for their excellent field work as well as that from their technical knowledge.

Finally, the most precious acknowledgement of all is that to my wife Adela and our daughter Danielle. Together they have forfeited countless number of evenings and weekends to allow me the necessary time to perform the work and complete this manuscript.

1. Introduction

Industrial metrology is a field of engineering surveys that requires the utmost in achievable accuracies and almost invariably depends on the results being in real time. Traditional methods of metrology have involved alignment telescopes, wires (invar, piano, etc.), calibrated bar sections (for distance), jig transits, autocollimating instruments, machinists levels (of varying sensitivities and lengths) and other such instrumentation, which when properly calibrated and used by skilled craftsmen are very capable of fulfilling the accuracy requirements for most industrial applications.

Positioning of components forming particle accelerators has long been a developing ground for instrumentation used in industrial metrology and consequently surveying in general. This is due to the very stringent accuracy requirements of the assemblies, bordering on or going just beyond the capabilities of the most technologically advanced instrumentation and methodologies. This in turn, creates very time consuming and subsequently expensive measurement techniques being performed by very skilled craftsman.

The European Organization for Nuclear Research ("CERN") has been the most influential in this expansion of technology throughout their various projects, spanning back to the construction of the Proton Synchrotron in 1954-59 (Gervaise, 1974) and covering the Super Proton Synchroton constructed in 1971-76 (Gervaise, 1976). CERN's prestigious surveying group can be credited with the discovery of the problem involving the elongation of invar wire with use, first detailed studies of the trilateration method of positioning stations, and inventing of the "distinvar" (Gervaise, 1976). The findings of this group have not only been used at other construction sites involving accelerators, but

the ramifications of their results can also be seen throughout the various surveying disciplines.

In recent years the imaginative surveying groups have taken the approach of developing special accessories to complement existing optical tooling instrumentation. For example, the surveying group at Los Alamos National Laboratory has constructed special wedges to install a skewed accelerator beam line (Bauke et al., 1985) and a special sine bar to install deflection mirrors at a particular skewed angle (Bauke et al., 1983). The accessories were required to be able to create an oblique reference plane, which is not easily accomplished with typical jig transits and alignment telescopes because of their reference dependence on local gravity.

However, traditional mechanical optical instrumentation normally requires an elaborate and time consuming set up and measurement procedure, which makes it very unsatisfactory for applications that need an almost real time interaction and involve a variety of instrument locations, such as a setting out survey. An additional disadvantage of traditional methods is the inability to determine easily the shape of various objects and surfaces (planes, paraboloids, cubes, etc.), which is an application commonly required in today's industrial environment. Modern technology has responded to alleviate the above limitations with the development of electronic theodolites, which when interfaced to a microcomputer allow on line data gathering and complete automation of the setting out of desired components using coordinates. This allows all of the design information to be kept on file in the microcomputer, which gives on line access to the information corresponding to a particular element which facilitates computing corrections for its setting out. This method has been successfully deployed at the Stanford Linear Accelerator Center (SLAC) in setting out their new linear collider, which involves the positioning of about 1000 magnets at various compound angles (Friedsam, 1985; Oren and Ruland, 1985; Curtis et al., 1986; Oren et al., 1987).

Prior to the introduction of electronic theodolites optical-mechanical theodolites monopolized the measurement of angles. The characteristics and behaviour of these instruments are well known, in all conditions of measurement, and peculiarities could be removed or minimized by proper observing procedures. Parallelling the development of new technologies are unknown behaviours and new characteristics of the instruments involved and the electronic theodolite is no exception to this generality. Well established rules of measurement and methods of a priori determination of angular accuracies, with optical mechanical instruments, must now be reanalysed for their validity with electronic theodolites.

The need for the reanalysis comes mainly from the use of various electronic methods and components to obtain the circle readings in electronic theodolites, which may lead to inconsistencies in measurement due to premature ageing of the electronics involved. A possibility of the inconsistencies being dependent on the type of theodolite, temperature, and time is analogous to the situation involving the crystal oscillators of electronic distance meters ("EDM"). New calibration procedures for this new technology must be developed to ensure that the optimum observational accuracy is being achieved, if these instruments are to be used in the very demanding industrial metrology environment.

Two electronic theodolites interfaced to a microcomputer allow the three dimensional (x, y, z) coordinate triplet of any targetted point to be determined almost instantaneously. By determining a number of coordinate triplets of targetted points located on an object or surface its geometric representation can be determined in virtually real time. This discussion clearly indicates the necessity of having a software package or a combination of software modules to complete the various tasks involved. The tasks start with the computer interface, contain a variety of options that govern the process, and end, in the most general case, with an estimation of parameters defining the shape, dimensions, position, and orientation of an analysed object or surface. It can be appreciated that a great

deal of software is required to create a general system easily adaptable to any application, with a minimal amount of effort.

Two of the major suppliers of survey instruments, Kern (recently acquired by Wild-Leitz) and Wild Heerbrugg, each have their own software packages, "ECDS2" and "RMS2000", respectively, designed for use in an industrial metrology environment. Both systems are very impressive, especially in their file management and operator interfaces, but have some shortcomings in their overall technical performances that are not negligible at the magnitude of accuracy usually sought in metrological applications. It is these shortcomings that has prompted the development of a precision three dimensional coordinating system ("P3DCS") at the Department of Surveying Engineering of the University of New Brunswick ("UNBSE"). The author has been involved in the development and industrial implementation of the UNB system from its very conception.

The initial development of the system was an attempt to emulate the commercially available software to determine the parameters defining the geometric shape (vertex, focal length, and coefficients) as well as the surface irregularities of a ~1 meter diameter circular parabolic antenna in virtual real time. The experiment was expected to give standard errors of a few hundreths of a millimetre for all three coordinates of each targetted point. The final results showed some inconsistencies, that when analysed were contributed to defects in the data gathering algorithms being duplicated and the handling of the instrumental errors, collimation and index, which are unique for every theodolite.

These results initiated a complete revision of the algorithms used in the data gathering procedure, which were then incorporated with the original version of the software package to form the basis of P3DCS. The software has since been expanded upon to add various options to make it a much more versatile package capable of handling a multitude of industrial related tasks. Most recently the package has been implemented in a project involving the precision three dimensional alignment of components forming a

portion of a tandem accelerator superconducting cyclotron ("TASCC") for Atomic Energy of Canada Ltd. ("AECL") at their Chalk River Nuclear Laboratories ("CRNL").

Though the use of electronic theodolites in semi-automatic 3D positioning systems has already found many industrial applications, it is still a new technology which requires a thorough evaluation and clarification of concepts involved. Therefore, the main objectives of this thesis has been to clarify the basic concepts of 3D positioning, evaluate the achievable accuracy, and give guidelines for an optimal use of the coordinating systems with electronic theodolites. This is accomplished by using as an example, the development of the UNB P3DCS system and its application in the setting out surveys at AECL's Chalk River facilities.

To gain an understanding of how the very high accuracies required in setting out accelerator components can be achieved using a coordinating system, requires an in depth description of the various components comprising a system. The accuracy a system is capable of obtaining is limited by the measurement accuracy of the electronic theodolites, hence, they are discussed at length in Chapter 2. Although not directly a system component, the three dimensional network geometry created by the combination of target and theodolite locations is critical, if optimum accuracies are to be achieved and is discussed in Chapter 3. Chapter 4 introduces the various algorithms that have been developed, involving the theodolite interface to the parametric least squares adjustment, which all together allow the process to be automated for real time results. The primary objective of this thesis, integrating traditional techniques with the coordinating system for the aforementioned TASCC project, is discussed in detail in Chapter 5. Conclusions and recommendations are contained in the final chapter, Chapter 6.

2. Electronic Theodolites

Coordinating system packages have been developed due to the introduction of electronic theodolites. Methodologies employed in the algorithms comprising the systems have been practiced and perfected with various types of angular measuring devices (i.e. polimetrum, plane tables, quadrants, optical-mechanical theodolites, etc. (Deumlich, 1982)), since triangulation was first introduced by Willebrod Snellius in 1615 (Encyclopedia Brittanica, 1970). Electronic theodolites with a microcomputer allow the entire process of triangulation to be automated, from the data collection to the rigorous solution of final coordinate results using least square techniques.

The electronic theodolites have improved the angle measuring capabilities of optical theodolites by removing operator reading errors by using digital displays, removing the effects of residual tilt of the vertical axis by correcting displayed horizontal circle readings for the effects of mislevelment (e.g. Kern E2, Wild T2002, and Wild T3000 theodolites), and removing or significantly reducing circle graduation and eccentricity errors by using more of the circle for each individual measurement. However, each of these improvements requires the use of eletronic circuits, oscillators, and light emitting and photo sensing devices, which may be prone to loss of effectiveness or intensity with accumulated age and use.

This chapter deals with the topic by first introducing the two methods of electronic angular measurement developed and implemented by the two commercial companies, Kern and Wild, in the electronic theodolites used with their software packages. The two methods have been discussed thoroughly in the literature by Katowski and Salzmann (1983) and by Münch (1984), and will be reiterated here to achieve completeness on the topic. The discussion on electronic theodolites will be limited to the models manufactured by Wild and

Kern due to the focus of this thesis being on coordinating systems of which the two companies together, hold almost a monopoly in the industrial marketplace.

A comparison of electronic and optical-mechanical theodolites is required to show the similarities between the two and to emphasize the slight differences. An indication of the types of errors to expect from both, with an estimation of their magnitudes is imperative to prevent unexpected results and inconsistencies from appearing in the computed quantities.

2.1 Electronic Circle Measurement

One of the first instruments capable of electronic angle measurement, the Zeiss RegElta 14, was made available to the surveying community in 1968 (Cooper, 1982). The manufacturer's specifications for the RegElta 14 claimed a standard deviation of about 3" in the measurement of a direction. Since that time both Kern and Wild have perfected their own styles of electronic circle measurement in their development of single second electronic theodolites. Both companies, before their merger in 1988, were competing for control in the surveying markets requiring the automated gathering of precision measurements, of which industrial metrology is part. The dynamic style of measurement developed by Wild and used on their T2000, T2002, and T3000 theodolites vastly differs from the static approach adopted by Kern on their E1 and E2 models, therefore, the two systems will be separated and discussed individually.

2.1.1 The Wild Dynamic System

The same measuring system originally developed on the T2000 is also being used on the latest generation of theodolites, T2002, and T3000 (Wild Heerbrugg Ltd., 1987). The Wild system methodology parallels that used in their development of Electronic Optical Distance Meters ("EODM"), as both have been developed in conjunction with "SERCEL"

(Société d'Etudes, Recherches et Construction Electroniques) and employ some of the same principles for determining phase changes (Katowski and Salzmann, 1983).

The circles themselves are glass with a radius of 26 mm and are divided into 1024 uniformly spaced sections. Each section contains a line of reflective material which covers half of the section while the remaining half is left transparent. There are four sensors or light barriers (as Wild calls them) located around the edges of each circle. Each sensor consists of an infrared light emitting diode and a receiving diode. Two of the sensors, describing the zero of the theodolite (horizontal circle) or the zenith (vertical circle), are in fixed locations on diametrically opposite sides of the circles. The remaining two sensors, also diametrically opposite each other, revolve around the circles with the alidade (horizontal) or telescope (vertical) and define the spatial direction of the telescope. Figure 2.1 illustrates the location of just two of the sensors positioned around the circle with L_S being one of the static sensors and L_R one of the revolving sensors, but each of the remaining two duplicate sensors, as mentioned previously, would be located diametrically opposite its complement. This method of defining the angle requires that the revolving sensors L_R be capable of passing freely by the static sensors L_S, therefore, each type is located on opposite edges of the glass circle (L_R inside edge and L_S outside edge) as shown in Figure 2.1.

The angle to be measured is labelled in Figure 2.1 as φ and contains a certain number of full sections n, each of angle φ_o, and a partial section, of angle $\Delta\varphi$, which gives the simple relationship in equation (2-1).

$$\varphi = n \cdot \varphi_o + \Delta\varphi \qquad (2\text{-}1)$$

This equation is analogous to that involved in distance measurement with an EODM only now the quantities are angular instead of wavelengths. Two different frequencies must be measured, a coarse and a fine measurement, to resolve the two unknowns, n and $\Delta\varphi$

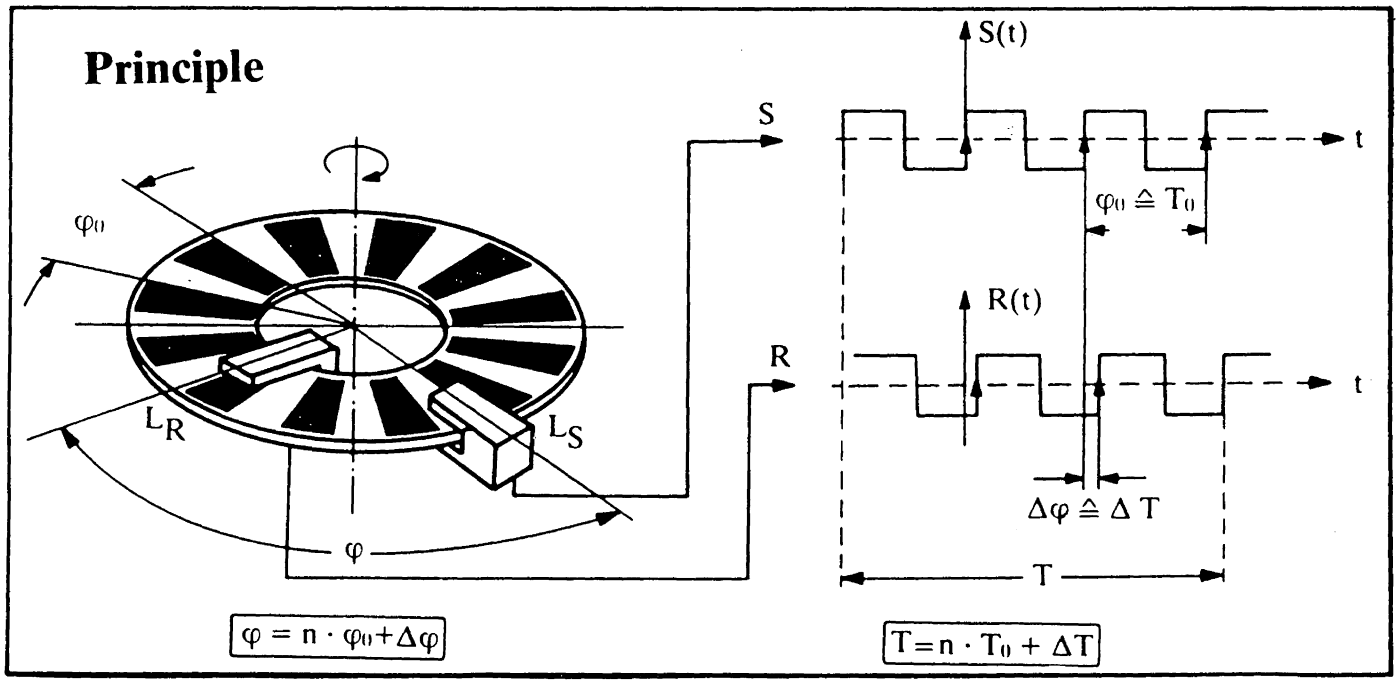

Figure 2.1 The Wild Dynamic Measuring System
(Katowski and Schneider, 1987b)

respectively, that are contained in the equation. Obviously, as with EODM, the accuracy of the observation itself depends on how accurately the fine measurement can be made, which is used to determine $\Delta\varphi$.

When the theodolite is prompted for a horizontal angle measurement it responds by turning on a motor that spins the horizontal circle at a constant rate. The fine measurement is made when two of the sensors that form a pair, one L_S and one L_R, emit an infrared light towards the graduated circle. The light that reflects off the reflective portion of the circle passes through a slit and is received at the receiving diode part of the sensor. The intensity of the light received depends on the amount reflected, which is related to the position of the reflective material on the circle. Since the circle is rotating at a constant speed the signal received at the sensor is being modulated and this analogue signal is converted to digital and is shown on the right in Figure 2.1 as a square wave. The quantity $\Delta\varphi$ is the phase difference between the two signals obtained from the L_S and L_R sensors. The phase difference is obtained by measuring the passage of time between a graduation passing the L_S sensor and the next graduation passing the L_R sensor.

This procedure is alternated between sensor pairs to obtain a phase difference measurement for each of the 1024 sections, 512 for each sensor pair, through one complete revolution of the circle. Two sensor pairs are used to remove eccentricities in sensor location and the phase difference measurement becomes the mean of all the measured phase differences.

The coarse measurement to determine n is accomplished through the marking of the circles with reference marks which are at a lower frequency than the sections. When one of the sensors recognizes one of the reference marks the remaining sensor in the pair counts the number of full sections that pass by it until it also recognizes a reference mark. This allows the integer number of sections to be determined unambiguously by the processor.

A measurement of the vertical circle is accomplished almost identically with the following slight differences. The receiving diodes use transmitted light instead of reflected

light to carry out the fine measurements. The reason for using transmitted light is to facilitate the process of correcting the vertical circle measurement for instrument mislevelment by passing the light through a liquid compensator. The compensator is a vial filled with a low viscosity silicone oil located between the emitting and receiving diodes of the sensors. In the T2000 only the vertical circle measurement is corrected for mislevelment due to the single axial determination, in line of sight direction, of the residual tilt of the instrument. However, in the latest models, T2002 and T3000, a biaxial method of determining mislevelment is incorporated allowing the horizontal measurement to be corrected as well as the vertical.

The time required to complete a measurement of both the horizontal and vertical circles is approximately 0.9 seconds (s). This can be broken down into 0.3 s for the motors controlling the circles to gain measuring speed, 0.3 s to process the horizontal circle measurements, and an additional 0.3 s to process vertical circle measurements as the same processor is used for both. The least count displayed by the instruments is 0.01 milligons (mgons), however, testing of the T2000 has revealed this value could be 0.05 mgons (Katowski and Salzmann, 1983).

A more detailed treatment of the procedures outlined above as well as some testing results on the T2000 may be obtained from Katowski and Salzmann (1983) and Katowski and Schneider (1987b), which is where most of the above discussion originates.

2.1.2 The Kern Static System

The original measurement system on the early E1 models has undergone some minor changes, mostly involving the use of better electronics, for converting analogue signals to digital. However, on the most part the system has remained unchanged since its inception. As with the Wild system, it requires the measuring of both a coarse and a fine measurement

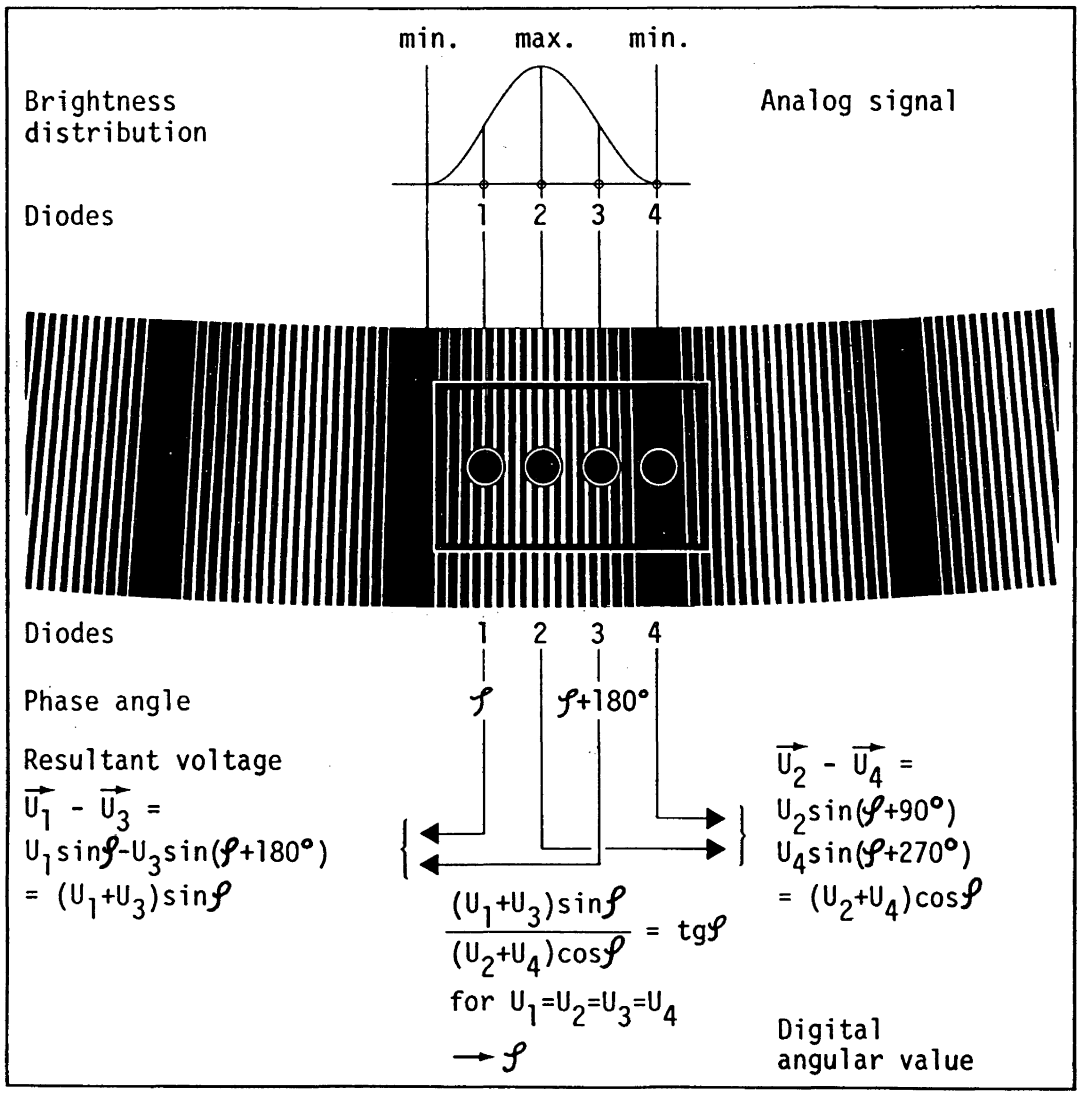

Figure 2.2 The Moiré Pattern of the Kern Static Measuring System (Münch, 1984)

to completely define the observed angle, but is accomplished in a completely different manner.

The glass circles used in the Kern E2 instruments are 70 mm in diameter and are graduated with 20,000 radial marks. Each mark or graduation has a width equal to the spacing between them of 5.5 micrometers (μm), which all together create a grate with a grating constant equal to the combined width of one graduation and space of 11μm or 0.02 gons (Münch, 1984). The E1 instruments have identical circle diameters but there are 25,000 graduation lines creating a grating constant of 0.016 gons (Kern & Co. Ltd., 1981). The reading system incorporates optics which are able to superimpose the graduation marks covering approximately 2 mm on one side of the circle with their diametrical opposites to increase the reading resolution. During the superimposition process the graduations are enlarged in such a way as to create a difference of one in the number of marks superimposed, which has the effect of creating a Moiré pattern as shown in Figure 2.2. This enlargement is further magnified by 2x to double the working length of the area where the measurements are to be performed. The sensors are four photo diodes arranged in this area side by side with a separation equal to one quarter of the created Moiré period, which separates the period into quadrants.

The fine measurement for obtaining $\Delta\varphi$ of equation (2-1) is accomplished statically by locating the position of the current Moiré period, using interpolation, relative to the sensors. A signal is generated by each of the four sensors corresponding to the intensity of the light detected from the pattern. The corresponding signal voltages from the sensors are combined mathematically, as shown in Figure 2.2, to determine the phase offset of the Moiré period, from the first sensor, and the direction of rotation of the alidade (horizontal) or telescope (vertical). The ratio of the phase offset divided by the pattern's period (2π) is multiplied by the expansion factor of 0.01 gons for the E2 and 0.008 gons for the E1, which represents the circle coverage of one Moiré period, to determine the fine measurement value. All four sensors are required to define unambiguosly the phase offset

of the pattern due to each light intensity (except the peak intensity) occurring twice within the period and the differencing between the sensor signals reduces the systematic errors contained in the individual voltages. The fine measurement and the phase offset are both passed to the processor to be combined with the coarse measurement to form the observed angle.

The coarse measurement n of equation (2-1) is obtained quite simply by counting the number of impulses detected by the sensor as the alidade or telescope is rotated. The sensors produce a modulated signal that represents the brightness of the Moiré pattern, which approximates a sinusoid. Various electronic modules are used to create a square signal which has the same zeros as the sinusoid produced by the sensors. Obtaining the number of full periods is done by counting the number of transitions from negative to positive of the square wave. This measurement is also sent to the processor to be combined with the fine measurement.

Once the processor receives the measurements it must determine the direction of rotation of the alidade or telescope to know whether to add or subtract the coarse measurement from the running total that it keeps. As stated previously, this is done by looking at the voltage differences between sensors. An additional task of the processor occurs if the phase of the pattern is close to 0 or 2π. This task is analogous to using a vernier scale where the coarse measurement reference mark is just beyond a full division, but the magnitude of the interpolation scale reading is very large. One full unit must be subtracted, or added if the conditions stated above are reversed, from the coarse value to obtain the proper measurement result. The processor accomplishes this by monitoring the generated square signal and comparing it to the sign of the trigonometric tangent of the measured phase. If the pattern has been counted the sign must be positive and if not counted, negative.

A vertical circle measurement is carried out exactly the same as described above. The only physical difference between the two circles is the initialization. The vertical circle must

be referenced with respect to gravity, in the zenith direction, which requires the counter for the coarse measurement to be zero at a particular inclination of the telescope. This is accomplished by supplying two reference marks, one fixed and one rotating with the telescope, which must be rotated by the fixed mark after power up, to initiate the counter counting. The horizontal counter may be initialized to zero in any orientation. A continuous running count is kept of the number of full periods, maximum of 40,000 for the E2 and 50,000 for the E1 for a full circle revolution, that have passed by the sensors since initialization.

A biaxial and uniaxial liquid compensating system, in the E2 and E1 respectively, is employed separately from the angle measuring components allowing mislevelment corrections to be determined for the vertical circle readings in both the E2 and E1 and horizontal circle readings in the E2. The systems use the reflection of an emitted light off the horizontal surface of a liquid to determine tilts in either the line of sight direction (uniaxial) or the line of sight and the trunnion axis directions (biaxial), which are only applied to the circle readings by the processor when an operator controlled switch is toggled.

If a more detailed representation of the angle measuring system or the liquid compensators are desired the interested reader is referred to Münch (1984) and Kern & Co. Ltd. (1985).

2.2 Electronic and Optical-Mechanical Theodolite Characteristics

The electronic theodolite, like its optical counterpart, is constructed mechanically of three basic assemblies, which are the base, alidade, and telescope. All of the functioning parts of the instrument are housed within these three basic assemblies. The accuracy capable of being achieved by the instrument depends directly on how well each assembly itself has been constructed as well as the overall combining of the assemblies. No feasible

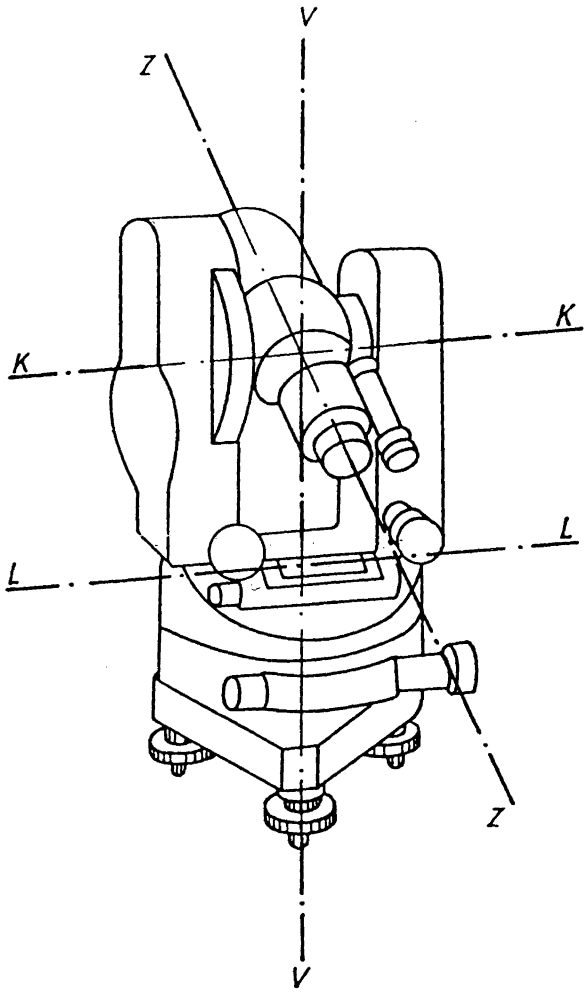

Figure 2.3 Relationship Between the Three Major Axes of a Theodolite (Deumlich, 1982)

amount of electronics can negate the effects of faulty workmanship in these major components.

The comparison between optical-mechanical and electronic theodolites can be divided into two separate categories. The systematic effects that are related to the workmanship in the assembling of the three major components and the random errors that are associated with each instrument and observer pair. Each of these topics will be discussed separately.

2.2.1 The Systematic Errors in Theodolite Construction

The combining of the assemblies forms the three major axes of the instrument, as illustrated in Figure 2.3, which are the collimation (ZZ), horizontal or trunnion (KK), and vertical (VV) axes. It is to these three axes that all angular measurements are referenced making it imperative that they are constructed consistently, even though they are intangible, when assembling the components. Consistently constructed really means that the axes relationships with each other remains constant through the entire working range of the instrument. The individual relationships that must be maintained are listed below :

1. the collimation axis approximately perpendicular to the horizontal axis,
2. the horizontal axis approximately perpendicular to the vertical axis, and
3. the vertical axis coincident with the local gravity vector.

For the first two relationships listed above, the ideal would be to have the axes involved perfectly perpendicular to each other. However, if they are not exactly perpendicular the errors caused may be completely eliminated, if the relationship remains constant, by observing with the telescope in both direct and reverse positions and meaning the two results. The nonperpendicularity of the first relationship yields to the well known collimation axis error, while the nonperpendicularity of the second is labelled in the literature as horizontal axis error.

The third relationship in the list, unlike its predecessors, cannot be removed by observing in both telescope positions, making it imperative to be able to obtain this relationship. The relationship may be realized by either perfectly levelling the instrument or by measuring the amount of residual mislevelment, which is the approach adopted by Kern in their precision instruments. If the amount of vertical axis tilt can be determined in the collimation and horizontal axes directions, both circle readings may be corrected, eliminating this effect. The effect on measurements obtained from the horizontal circle increases with the inclination of the telescope but are nonexistent with the telescope horizontal, while those from the vertical circle are constant for each particular line of sight. This error is known as the vertical axis error or synonymously as the levelling error.

The expected magnitude of the levelling error is related to how well the instrument can be levelled (i.e. sensitivity of the level vial) and the expected inclination of the telescope during observations. The following equation gives a general formula for determining the maximum error in the horizontal circle measurement (σ_L), due to the mislevelment of the instrument (Chrzanowski, 1977).

$$\sigma_L = \varepsilon_L \cot z \qquad (2\text{-}2)$$

where,

ε_L error in levelling the vial
z is the zenith angle.

The value of ε_L, when a spirit level is used, is obtained from how well a bubble may be centered between the graduations of the vial. The levelling error may vary from about 0.02υ to 0.2υ, where υ is the sensitivity of the level vial, depending on the centering technique used. Thus for υ equal to 20" (6.2 mgons), the error of levelling can be between 0.4" (0.12 mgons) and 4" (1.2 mgons). For the liquid biaxial compensator being used on the Kern E2 a σ_L equal to twice the compensator resolution or 0.2 mgon (0.6") irregardless of telescope inclination can be achieved (Münch, 1984). Similar results are expected from

the biaxial compensator now being supplied on the Wild T3000 and T2002 (Wild Heerbrugg Ltd., 1987).

Traditionally, attempts to randomize the effects of the levelling error, by relevelling the instrument between sets of observations, has been the approach. The relevelling of an instrument that has three footscrews (Wild instruments) changes the location of the point of intersection of the primary axes, which is what defines the theodolite's position. For industrial metrology applications this is critical, due to the instruments not being centered over any particular mark, which means that a relevelling would create an entirely different theodolite position.

Another related error, the index error, is caused by misalignment of the vertical axis with the corresponding vertical circle zenith. This error is a constant for each instrument that would have only an affect on the vertical circle measurements, and can be completely eliminated by observing in both telescope positions. However, if the instrument is equipped with a liquid compensator, the index error becomes very sensitive to fluctuations in temperature (Chrzanowski, 1985). Figure 2.4 illustrates the variation in the index error that can be realized with respect to a change in temperature for both the Kern E2 and Wild T2000 electronic theodolites. The change in the index error is the result of the relationship between a variation in the viscosity of the liquid used in the compensators with respect to a fluctuation in temperature.

This means the index error can only be eliminated, or at least reduced, by observing either in a rigorously temperature controlled environment or by using both telescope positions in sighting to the targets at the shortest possible time interval. An industrial environment temperature is rarely constant or consistent, due to the varying amounts of energy released by the large machines involved in a production process, making the second alternative more plausible. If not removed, a 2" variation in the index error creates a 0.1 mm discrepancy at a 10 m sight distance.

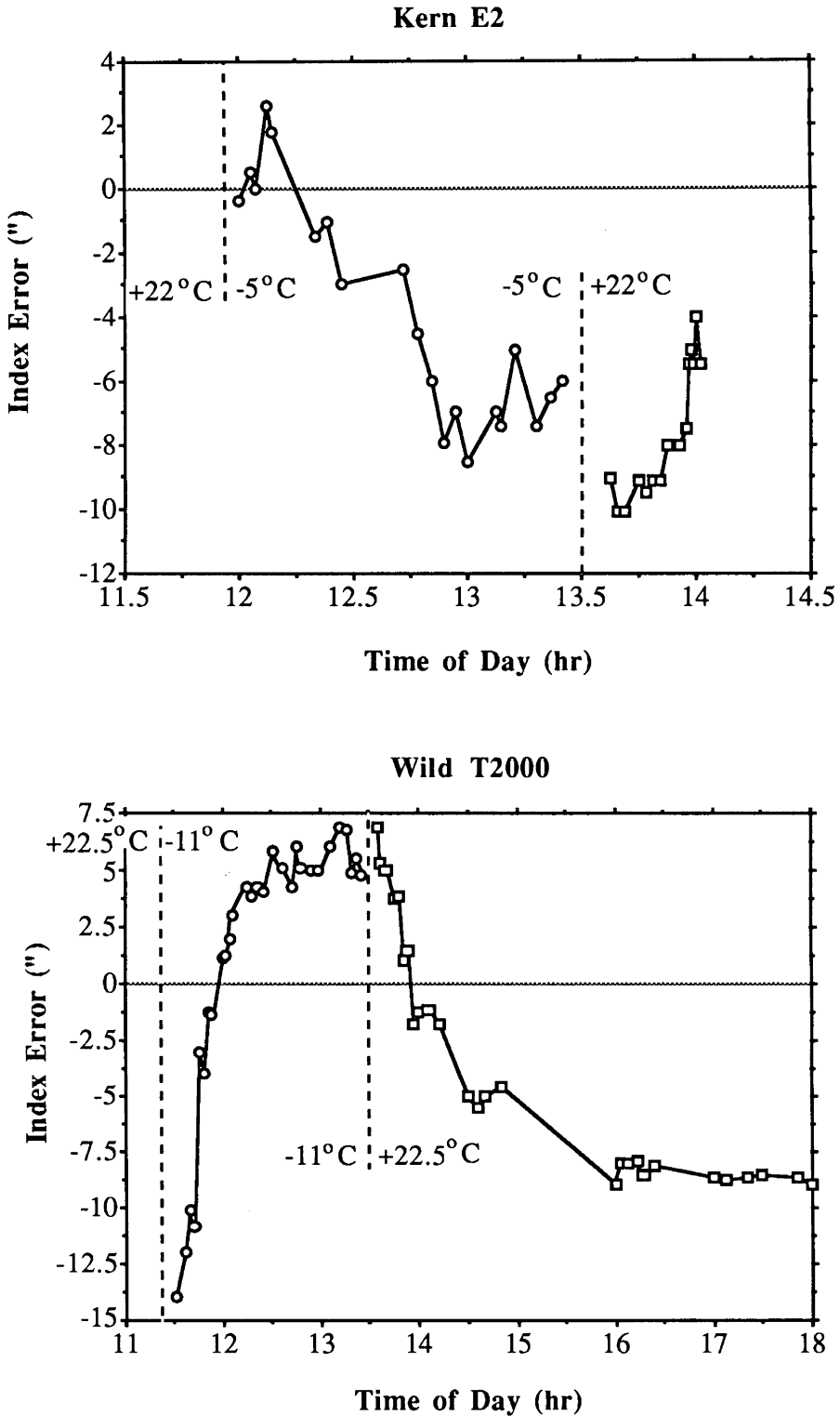

Figure 2.4 Variation of Index Error with Temperature (altered Chrzanowski, 1985)

The above discussion clearly displays a lack of reference to any electronic components indicating that the errors involving the axes are purely mechanical and will occur in any type of theodolite. However, electronic modules make the vertical axis error easier to measure and to apply the proper corrections. Additional errors are inherent in every theodolite involving eccentricities and circle graduation, which is where the electronics are involved.

The eccentric errors are created by the components that must rotate around or intersect with the vertical and horizontal axes of the instrument. For example, a collimation axis eccentricity is created if the three instrument axes do not all intersect at a common point and a graduation eccentricity results if the horizontal circle does not rotate symmetrically around the vertical axis. These eccentric errors may all be completely eliminated by observing with the telescope in both positions and averaging the two results.

In addition, the graduation eccentricities may be removed by observing diametrically opposite sides of the circle while the telescope remains in the same position. Optical theodolites with micrometers accomplish this by using graduation lines from opposite sides of the circle that must coincide to achieve a fine measurement. The Kern electronic theodolite deals with this in a similar fashion by superimposing diametrically opposite sides to create the measurement pattern. Wild in its electronic theodolites has chosen to use sensors located diametrically opposite each other to negate the effects.

The remaining error inherent to theodolite construction is the graduation of the circles involved in the measurements. Due to technological advances the circles being installed today are graduated with a very high absolute accuracy, which is better than the instrument resolution (Münch, 1984; Kern & Co. Ltd., 1985). The graduation errors can be divided into long and short wavelength effects that are caused by the characteristics of the equipment used to graduate the circles (Cooper, 1982).

The Kern system uses the difference of measurements obtained from the graduations contained in two 2 mm sections of the circle, that are located diametrically opposite each

other, to obtain the final measurement result. The use of only 4 mm of the entire circle perimeter (70 mm diameter) makes the Kern system susceptable to the effect of the long period graduation errors, while removing the contributions of the short period errors. In contrast, the Wild system averages the individual measurements taken over the entire circumference of the circle, to obtain the final result. This makes the Wild system free from the effects of both long and short period graduation errors. However, the dynamic approach of the rotating circle creates a constant speed error that is similar in magnitude to the graduation errors. As for the optical instruments, using just two graduations (diametrical opposites) to determine the angular quantity would be a very dangerous practice to rely on. For both the Kern and the optical instruments, the traditional time honoured method of using a different portion of the circle for each set, to randomize the effects of the graduation error, should still be adhered to.

Before closing this section it should be pointed out that there are calibration procedures for determining the magnitudes and correcting the various theodolite errors that have been mentioned. The above discussion points out that if proper observing procedures are followed and the theodolite is mechanically sound, good results will follow, without having to adjust the instrument. However, the one exception to this statement will be caused by the inability to level the instrument to a high degree of accuracy or if applicable, to determine the magnitude of the mislevelment components. If the reader is interested in the various calibration techniques the literature is boundless and to start the reader is directed to Deumlich (1982), Kissam (1962) and Faig (1972)

2.2.2 The Random Theodolite Errors

The only remaining errors to discuss involving the theodolites are the random errors associated with the observer. A determination of the total magnitude of the various random observing errors, gives a priori information on the accuracy capabilities of a theodolite and

observer pair. These errors have been traditionally divided into the categories of reading, pointing, centering, and levelling, of which the last was discussed in the previous section.

The pointing error of an instrument is a function of the magnification of the telescope (M) and a constant related to the length of the sight distances. Other factors such as target design, refraction, and focussing influence the random pointing error (σ_P). In general, the following formula gives a good estimation of σ_P, for short sight distances of a single pointing in stable atmospheric conditions including some residual refraction errors (Chrzanowski, 1977).

$$\sigma_P = 30'' / M \qquad (2\text{-}3)$$

where,

30" = 30 arcseconds.

In most cases, the constant in the above equation can be a little conservative for industrial metrology applications, where there is usually better control of refraction, target design and the sight distance rarely exceeds 20 meters. However, to remove any chance of being overly optimistic this value should be adhered to in computing the expected accuracies, which translates into a σ_P of 0.29 mgons (0.94") for the Kern and Wild precision theodolites, that do not have the panfocal telescope. Both the Wild T2000S and T3000 are equipped with the panfocal telescope, which has the attribute of being able to change magnification with changes in sight distance and still maintain an accurate line of sight (Katowski and Schneider, 1987b; Wild Heerbrugg Instruments Inc. 1987). For these instruments the above σ_P is representative of a 10 metre sight distance.

The random centering error (σ_C) that is normally associated with plumbing the instrument over a station, is completely eliminated in industrial metrology applications where a coordinating system is to be used (see section 3.4.3). This is due to the theodolite stations being located randomly in the work area and tied to the control by redundant observations of wall targets. No observations between instrument stations are required

unless two instruments are being collimated together to form the datum (e.g. Wild RMS 2000), which still requires no centering if the datum has not previously been defined. This unique method removes the large contribution of centering error over very short distances, which normally is a limiting accuracy factor in traditional surveying applications.

The random reading error (σ_R) for an electronic theodolite, like the random centering error, is almost nonexistant because the circles are read with a very high resolution electronically. The operator only has to issue a command, instead of trying to coincide the diametric circle graduations as is the case with an optical instrument. The random error for an optical-mechanical instrument, including the graduation error, is given by equation (2-4) (Chrzanowski, 1977).

$$\sigma_R = 2.5\ d \tag{2-4}$$

where,

d is the smallest division on the micrometer scale.

For the electronic theodolites, assuming that the electronics are capable of reading the circle to an accuracy equal to the instrument least count gives σ_R equal to 0.1, 1.0, and 0.01mgons for the Kern E2, Kern E1, and Wild electronic theodolites, respectively. However, laboratory testing of a T2000 has shown a fine measurement resolution for the Wild system that is 5 times larger, 0.05 mgons (Katowski and Salzmann, 1983), which is due to the constant speed error described previously.

The total expected random error (σ_T) for a direction measured in a single position of the telescope is given by the propagation of the individual random errors, described above, which is illustrated in equation (2-5).

$$\sigma_T^2 = \sigma_L^2 + \sigma_P^2 + \sigma_C^2 + \sigma_R^2 \tag{2-5}$$

Applying equation (2-5) to the various types of Kern and Wild precision theodolites commonly involved in industrial metrology gives the results listed in Table 2.1.

Table 2.1 Total Expected Error for Theodolites
(for a single pointing)

Model	Circle	σ_L[1] (mgons)	σ_P (mgons)	σ_R (mgons)	σ_T (mgons)
Kern					
DKM2-A[2]	H	0.71	0.29	0.78	1.09
	V	0.20	0.29	0.78	0.86
DKM2-AM[2]	H&V	0.20	0.29	0.78	0.86
E1[3]	H&V	0.20	0.29	1.00	1.06
E2	H&V	0.20	0.29	0.10	0.37
Wild					
T2[2]	H	0.71	0.29	0.78	1.09
	V	0.11	0.29	0.78	0.84
T2000[3]	H&V	0.31	0.29	0.05	0.43
T2002	H&V	0.20	0.29	0.05	0.36
T3000[4]	H&V	0.20	0.29	0.05	0.36

1 where applicable a telescope inclination of 30 degrees was used, which is not uncommon in metrology and regularly gets much steeper

2 optical-mechanical theodolites: DKM2-AM has biaxial and DKM2-A has uniaxial compensation, T2 an optically split level vial for removing tilt in line of sight direction, assumes North American version with circles graduated in arcseconds

3 at initialization the T2000 and E1 can be levelled very accurately (1") and (0.2 mgons) respectively using the single axis compensators, but for the rest of the observing session no corrections are made to the horizontal circle readings for any changes in tilt that occur during use

4 the T3000 has a varying magnification, therefore the pointing error will also vary with sight distance. The value given for pointing error represents a 10 m sight distance

In analysing the results contained in Table 2.1 it becomes very apparent that the electronic theodolites add much more to the measurement of a direction then just speed and automation of the data collection. The improvement in the accuracy of a direction is by a factor of 3 when using one of the electronic theodolites, with the exception of the Kern E1, compared with the optical-mechanical single second theodolites. This of course is due to the absence of operator limitations in reading the circles of the electronic theodolites, as the remaining errors, σ_L, σ_P, and σ_C, would be identical for both types of instruments.

Another interesting note is that for one set (a direct and reverse telescope position pointings) of observations the optimum accuracy capable from the electronic instruments would already be achieved, making multiple sets frivolous in terms of improving accuracy for metrology applications (e.g. for the Kern E2, σ_T would be 0.30 and 0.27 mgons for 1 and 2 sets, respectively). However, for the purpose of eliminating blunders and having data quality checks the time honoured practice of turning sets should be adhered to. The interested reader is referred to Chrzanowski (1977), Nickerson (1978), and Blachut et al. (1979) if a more detailed discussion of a priori error analysis in observations is required.

3. General Overview of Traditional Three Dimensional Positioning

The concepts associated with three dimensional geodetic networks have been well known for centuries. However, traditionally networks have been subdivided into separate networks for the horizontal and vertical coordinates. This separation was primarily due to the inability to obtain accurate terrestrial observation data, that contained information on both the horizontal and vertical, that would allow the establishing of a single three dimensional network.

The basic observation for vertical networks has been spirit levelling, which contains no horizontal information and requires the path between adjacent stations to be accessible. In contrast, the observations for horizontal networks of distances, directions, independent angles, and azimuths contain very little vertical information and require intervisibility between adjacent stations. These contrary requirements and characteristics have resulted in the historical practice of establishing vertical benchmarks along roads and railways, while the horizontal stations are located on hilltops and mountains. Until recent decades, the zenith distance (or conversely the vertical angle) was the only observable that contained strong information in all three dimensions, but the inability to eliminate the systematic effects of atmospheric refraction reduced its reliability in merging the horizontal and vertical coordinates.

Since the introduction of EDM in geodetic surveys in the early 50's, making spatial distances easier to observe, the interest in three dimensional network solutions has grown. However, as with the zenith angles, the influence of refraction has not been overcome and still proves to be the limiting factor. In theory, the micronetworks used in industrial metrology, where spatial distances would be much shorter, could be pure trilateration networks.(all observables in the network are distances) The measurement of distances to

the accuracy required to form a trilateration network would be extremely inconvenient, in comparison to the measuring of zenith angles with electronic theodolites.

The three dimensional microtriangulation networks used in industrial metrology rely exclusively on the zenith angle observations for making the connection between the horizontal and vertical components. In these micronetworks sight distances are kept very short and usually are never longer than 20 metres. This reduces the systematic contribution of the refraction effects, however, short sight distances creates reduced observation accuracy due to large instrument centering errors, which must be eliminated if the required accuracies are to be obtained. In addition, the effects of gravity and the earth's geometry have generally been considered negligible in the establishing of most micronetworks. In the context of industrial metrology, where in general the positional accuracy requirements are in the order of 0.1 mm, this statement must be revalidated as to whether all of these effects are still negligible.

3.1 Three Dimensional Coordinate Systems

The introduction of accurate three dimensional data from extraterrestrial positioning techniques (i.e. VLBI, SLR, GPS, and TRANSIT) in the last two decades, has resulted in the reemergence of three dimensional geodetic networks. The principles behind these global networks can be applied to the micronetworks that are used in metrology, but obviously at a much reduced scale. However, in order to carry out a meaningful discussion on these principles, some basic geodetic coordinate systems and parameters must first be defined. The definitions may be obtained from any book describing the coordinate systems used in geodesy, such as Vanicek and Krakiwsky (1986), Krakiwsky and Wells (1971), Torge (1980), and Bomford (1980) and will be reiterated here only for the sake of completeness.

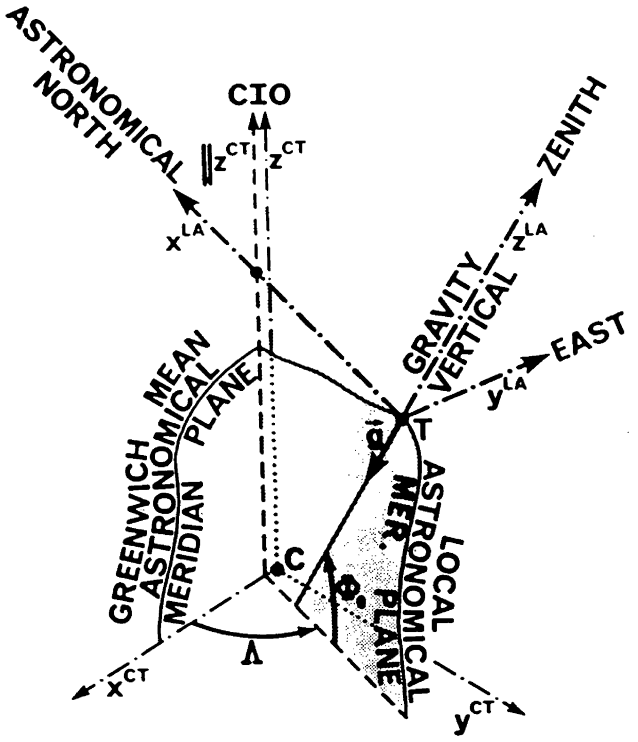

Figure 3.1 The Conventional Terrestrial (CT) Coordinate System
(Vanicek and Krakiwsky, 1986)

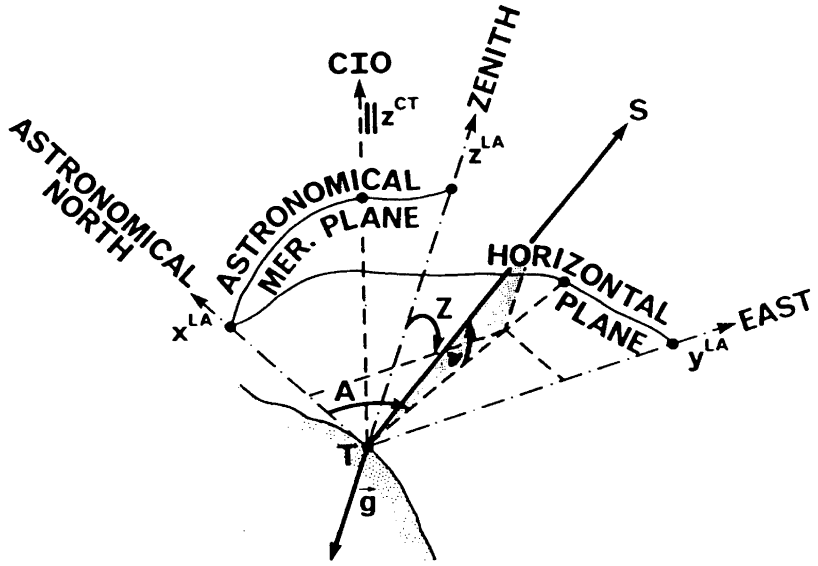

Figure 3.2 The Local Astronomic (LA) Coordinate System
(Vanicek and Krakiwsky, 1986)

The Conventional Terrestrial (CT) is the orthogonal coordinate system that is closest in defining the natural geocentric coordinate system of the earth. The CT system has its origin at the earth's geocentre (centre of earth's mass). The z axis is defined by the Conventional International Origin (CIO), the xz plane contains the mean Greenwich zero meridian (meridian through the Greenwich Observatory) and the y axis is chosen to make a right handed system. A point T may be defined in the CT system by its cartesian coordinate triplet $(x,y,z)_T$ or its direction, by astronomic latitude and longitude Φ_T and Λ_T, respectively. The relationships between the coordinate axes and astronomic latitude and longitude are illustrated in Figure 3.1.

The Local Astronomic (LA) is a topographic coordinate system with its origin located at the position of the observer on the surface of the earth. The z axis, positive outward, is tangent to the local gravity vector at the point defining the station. The positive x axis points toward astronomic north which is defined by the z axis of the CT system (CIO), while the y axis completes the left handed triad. The LA is the coordinate system that the terrestrial observations are actually performed in. The astronomic azimuth (A) and the zenith distance (Z) (or conversely the vertical angle (v)) can both be measured directly and are the parameters that are used to indicate direction in the LA system, to a point of interest, as given by equation (3-1) and illustrated by Figure 3.2.

$$\begin{bmatrix} x \\ y \\ z \end{bmatrix}^{LA} = \begin{bmatrix} \sin Z \cos A \\ \sin Z \sin A \\ \cos Z \end{bmatrix} \qquad (3\text{-}1)$$

The relationship between the LA and the CT systems involve the astronomic latitude and longitude, that have been defined previously, and this relationship is illustrated in Figure 3.2. The transformation equation, between the two systems, is not required for further discussions here, but the interested reader may obtain it from any of the above mentioned literature.

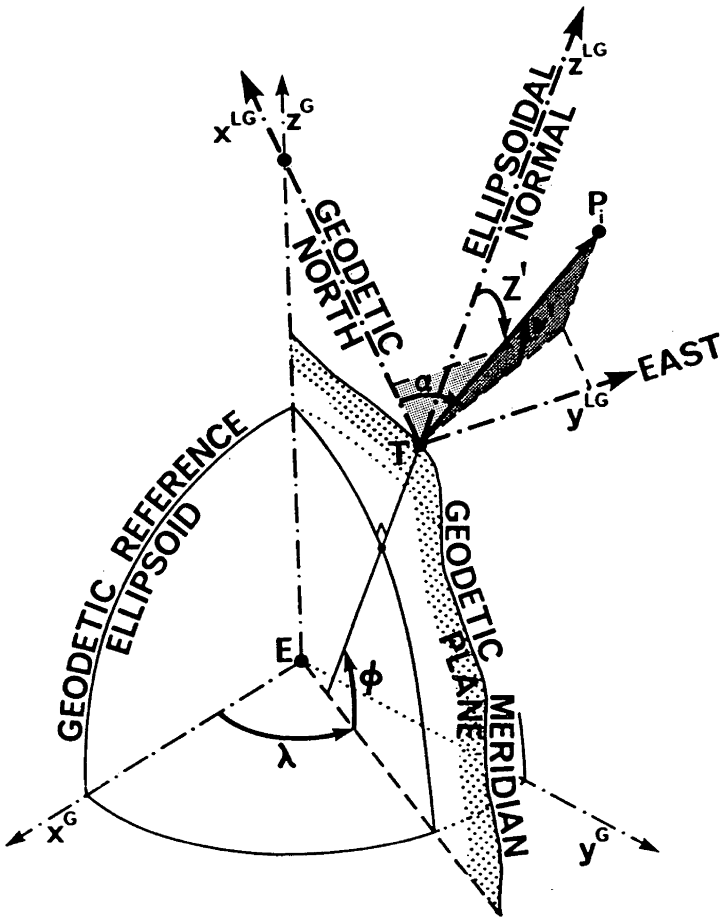

Figure 3.3 The Geodetic (G) and Local Geodetic (LG) Coordinate Systems (Vanicek and Krakiwsky, 1986)

The irregular terrain formulating the surface of the earth is very difficult to describe mathematically, hence, any natural reference surface would also be computationally complex. Therefore, the simpler model of a "best fitting" biaxial ellipsoid is used (Vanicek and Krakiwsky, 1986), which forms the basis of the family of geodetic (G) coordinate systems. The geodetic latitude, longitude and ellipsoidal height, ϕ, λ, and h respectively, are curvilinear coordinates of a biaxial ellipsoid and are illustrated in Figure 3.3. The transformation between the geodetic curvilinear to geodetic cartesian coordinates is given by the following equation (Vanicek and Krakiwsky, 1986):

$$\begin{bmatrix} x \\ y \\ z \end{bmatrix}^{G} = \begin{bmatrix} (N + h) \cos \phi \cos \lambda \\ (N + h) \cos \phi \sin \lambda \\ (N\, b^2/a^2 + h) \sin \phi \end{bmatrix} \tag{3-2}$$

where,

a is the major semi-axis of ellipsoid
b is the minor semi-axis of ellipsoid
$N = a^2 / (a^2 \cos^2 \phi + b^2 \sin^2 \phi)^{1/2}$.

If a geocentric ellipsoid is chosen such that its minor semi-axis is coincident with the z axis of the CT system and all coordinate axes are coincident with their CT complement, than equation (3-2) can be utilized to transform directly between the G curvilinear coordinates and the CT cartesian coordinate differences. For the purposes of this discussion, it will be enough just to enforce the condition of parallelism and not coincidence between the axes of the two systems.

The remaining coordinate system that must be defined is the Local Geodetic (LG), which has a relationship with the G system that is analogous to the relationship the LA has with the CT system. The LG system, like the LA, is a topocentric system with the origin at the observer's location and the z axis, positive outward, coincident with the normal to the biaxial ellipsoid. The positive x axis points toward geodetic north or the z axis of the G system, which coincides with the CIO in this special case, because of the stipulation cited

above for the location of the reference ellipsoid with respect to the CT system. The y axis is such as to make the LG a left handed triad. The parameters that are required to indicate direction in this system are the geodetic azimuth (α) and geodetic zenith angle (Z') (or conversely the geodetic vertical angle (v')), through the following equation and are illustrated in Figure 3.3.

$$\begin{bmatrix} x \\ y \\ z \end{bmatrix}^{LG} = \begin{bmatrix} \sin Z' \cos \alpha \\ \sin Z' \sin \alpha \\ \cos Z' \end{bmatrix} \tag{3-3}$$

The relationship between the LG system and geodetic latitude and longitude are also illustrated in Figure 3.3.

The analogy between the two pairs of coordinate systems described above has already been referred to and the similarities can be seen very clearly in Figures 3.1 and 3.3. In fact, if the ellipsoidal normal coincided with the tangent to the actual gravity vector at the observer's location, the coordinate systems illustrated in Figures 3.1 and 3.3 would be identical. However, this is not very likely to be the case and the deflection of the vertical is defined as the spatial angle created by the intersection of the ellipsoidal normal, which defines the normal gravity vector, and the tangent to the actual gravity vector and is of particular significance in geodesy. The spatial deflection of the vertical can be further reduced into two orthogonal components, the prime vertical (η) and meridian (ξ) components, which are illustrated in Figure 3.4 depicting their relationships to the LA and LG systems. With the condition of axes parallelity fulfilled between the G and CT systems, the simple equations (3-4) and (3-5) are valid in describing the deflection components.

$$\xi = \Phi - \phi \tag{3-4}$$

$$\eta = (\Lambda - \lambda) \cos \phi \tag{3-5}$$

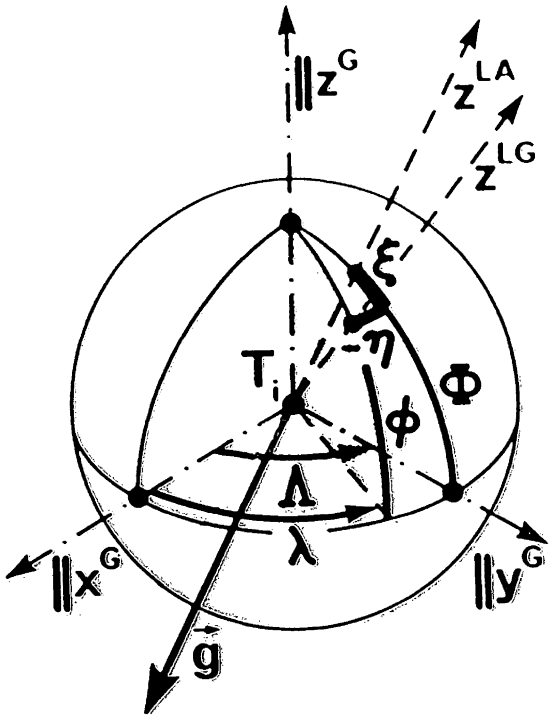

Figure 3.4 The Deflection of the Vertical Components
(altered Vanicek and Krakiwsky, 1986)

An important natural reference surface in geodesy is the geoid, which is described as the equipotential surface of the earth's gravity field that best approximates mean sea level over the entire earth (Vanicek and Krakiwsky,1986). The local shape of the geoid can be characterized with respect to the reference ellipsoid by determining a station's surface deflection components, which approximate the slope of the geoid in the prime vertical and meridian directions. In addition, the geoidal height (or undulation) is used to describe the separation between the geoid and the reference ellipsoid.

3.2 The Terrestrial Observation Equations

As was mentioned previously, the LA system described above is the natural system that the terrestrial observations are actually performed in. A natural extension to this statement would be that the observation equations must be greatly simplified if formulated

in this system and indeed, this is the case. Unfortunately, the North American convention for a coordinate system, in contrast to the previously defined LA system, is right handed with the positive Y axis pointing towards north, which will be introduced as the LA' system.

The relationship between the LA and LA' systems is simply a reflection of the y axis (to make a right handed system) and a rotation around the z axis to switch the locations of the x and y axes. The physical meaning of the LA system is not changed, but only the description of the horizontal coordinate axes. Therefore, to help simplify the discussion and conform with North American convention, the observation equations will be formulated for the LA' system. However, it should be pointed out that they may be formed in any one of the four previously defined coordinate systems by simply accounting for the mathematical relationships that describe the coordinate transformations between systems.

The azimuth, direction, and angle observation equations are all very closely related to each other, hence, will be discussed as a unit. Firstly, the function showing the simple relationship between the cartesian coordinates of the LA' system and an azimuth observation is given by equation (3-6).

$$\tan A_{ij} = (x_j - x_i) / (y_j - y_i) \qquad (3\text{-}6)$$

where,

the subscripts i and j represent the at and to stations, respectively.

A simple rearranging of the terms and the addition of a residual component (r) gives us the observation equation (3-7) that is explicit in terms of the observed quantity, A.

$$r + A_{ij} = \arctan [(x_j - x_i) / (y_j - y_i)] \qquad (3\text{-}7)$$

A direction observation (d) can be considered the same as the azimuth observation above with the addition of a term which defines the orientation of the zero mark on the

instrument's horizontal circle. Therefore, equation (3-8) depicts the observation equation explicit in terms of an observed direction.

$$r + d_{ij} = \arctan [(x_j - x_i) / (y_j - y_i)] - \omega_i \qquad (3\text{-}8)$$

where,

ω is the unknown instrument orientation parameter.

An obvious result of the inclusion of the orientation parameter in the equation is that a minimum of at least two directions must be observed from each instrument set up, to allow for the solution of this added unknown parameter.

The orientation parameter may be eliminated from the above observation equation by simply taking the difference between two direction measurements, to different stations, from the same instrument set up. The result of this difference forms the observation equation, explicit in terms of the observation, for an independent angle (β), which is given in equation (3-9).

$$r + \beta_{ijk} = \arctan [(x_j - x_i) / (y_j - y_i)] - \arctan [(x_k - x_i) / (y_k - y_i)] \qquad (3\text{-}9)$$

where,

the subscripts i, j, and k represent the at, to, and from stations, respectively.

Up to this point it can be seen clearly by analysing the given observation equations, for azimuths, directions, and independent angles, that no information has been introduced concerning the z coordinate (height component in the LA' system). This demonstrates clearly the need for additional observation types , which will link the x,y coordinates above with the z coordinate.

The observation equation for spatial distance can be formulated in any coordinate system simply by forming the expression that gives the defined metric for that coordinate system, which is usually the Euclidean metric. In the three dimensional space defined by the LA' system the Euclidean metric, $\rho(i,j)$, is given by the following equation.

$$\rho(i,j) = [(x_j - x_i)^2 + (y_j - y_i)^2 + (z_j - z_i)^2]^{1/2} \quad (3\text{-}10)$$

The addition of a residual component (r) to (3-10) results in the observation equation for a spatial distance (s) and is given by equation (3-11).

$$r + s_{ij} = [(x_j - x_i)^2 + (y_j - y_i)^2 + (z_j - z_i)^2]^{1/2} \quad (3\text{-}11)$$

where,

i and j subscripts represent the at and to stations, respectively.

The zenith distance observation equation can be formulated in two different ways depending on whether the horizontal or spatial distance between the stations involved, is used. The formulation given here will be based on the spatial distance due to the regularity of the cosine function, when the zenith distance approaches 90 degrees. The functional relationship between the zenith distance and the LA' cartesian coordinates is given by equation (3-12).

$$\cos Z_{ij} = (z_j - z_i) / s_{ij} \quad (3\text{-}12)$$

where,

the subscripts i and j represent the at and to stations, respectively.

By simple rearranging, the addition of a residual term (r), and the replacement of the spatial distance with its cartesian coordinate definition as given by equation (3-11), results in the observation equation for a zenith distance and is given by equation (3-13).

$$r + Z_{ij} = \arccos [(z_j - z_i) / [(x_j - x_i)^2 + (y_j - y_i)^2 + (z_j - z_i)^2]^{1/2}] \quad (3\text{-}13)$$

If alternatively the observation equation for a vertical angle (v) is required, equation (3-13) can be used by replacing the zenith distance term (Z_{ij}) with the expression ($\pi/2$ - v).

Both observation equations (3-11) and (3-13) have added information linking the x,y coordinates with the z coordinate of the LA' system. However, it must be pointed out that the vertical information obtained from a spatial distance is useful only when the lines of

sight are steeply inclined. In addition, in the context of metrology networks only enough distance observations required to alleviate, to a satisfactory degree, the datum scale defect would be used, due to the inability to determine easily spatial distances to the required accuracy. In contrast, the zenith distances are easily obtained to the required accuracy and provide strong vertical information regardless of sight inclination, due to each being a ray emanating from a point. This illustrates the importance of having good systematic error free zenith distance measurements, in order to be able to create a three dimensional network for metrology purposes.

3.3 Variations Between Local Astronomic Coordinate Systems

The review of the observation equations in the previous section was done solely in the LA' coordinate system. This would be fine if only a single theodolite station were to be used in the measurements to determine the coordinates of the network targets. This obviously will not be the case and is even impossible to accomplish, when distance observations are not considered, because a target requires at least two intersecting rays to define its position. However, every network station that is introduced has its own LA coordinate system, with origin at the station and orientation defined by the station's astronomic latitude, longitude, and a tangent to the local gravity vector at the station (see section 3.1).

The traditional approach in micronetworks to alleviate this problem has been to constrain one of the LA systems from moving (or alternatively a fictitious mean system), and to solve for translation components (station coordinates), with respect to this fixed system, for each of the other systems. These constrained methods are quite satisfactory for most small aperature engineering networks, however, the accuracy requirements for these applications are not quite so stringent as in metrological networks. These types of solutions

give no consideration to the nonparallelity of the complement axes of the various LA systems, although some is absorbed in the estimated translation components.

The nonparallelity of the complement axes of the LA systems can be broken down into gravimetric and geometric causes. To obtain an understanding of the magnitude of each's influence on the overall network results, each will be discussed separately.

3.3.1 Gravimetric Reductions

The relationship between gravity and the various coordinate systems has previously been established, in section 3.1, with the development of the definition for the deflection of the vertical. Referring back to Figure 3.4 and the previous discussion on deflection of the vertical, it should be apparent that the only difference between the LG and LA systems as defined in section 3.1, are three small rotations that are caused by the ellipsoidal normal not being coincident with the tangent to the actual gravity vector at the station. These rotations have magnitudes that are equal to the values of the station deflection components, ξ and η, and the difference between the direction of astronomic and geodetic north. The transformation equation between the two systems is given by the relationship contained in equation (3-14) (Vanicek and Krakiwsky, 1986).

$$\begin{bmatrix} x \\ y \\ z \end{bmatrix}^{LG} = \mathbf{R_z}(A - \alpha)\,\mathbf{R_y}(-\xi)\,\mathbf{R_x}(\eta) \begin{bmatrix} x \\ y \\ z \end{bmatrix}^{LA} \qquad (3\text{-}14)$$

where,

$\mathbf{R_x}, \mathbf{R_y}, \mathbf{R_z}$	rotation matrices around the x, y, and z axes, respectively
$A - \alpha$	difference between astronomic and geodetic north
ξ, η	are the station deflection components.

The small angle between astronomic and geodetic north may be obtained using the Laplace equation for azimuths. This relationship is given below as equation (3-15) (Vanicek and Krakiwsky, 1986).

$$A - \alpha = \eta \tan \phi \tag{3-15}$$

where,

ϕ is geodetic latitude.

This simple relationship (3-15) between the two systems only exists because of the initial condition that was enforced when defining the G system, or the biaxial ellipsoid's position, with respect to the CT system (i.e. complement axes parallel).

In the analysis of the above two relationships, (3-14) and (3-15), two characteristics are very apparent:

(i) changes in latitude affect the definition of the rotation angle caused by the different directions for astronomic and geodetic norths,

(ii) if the deflection components remain constant in the area, they affect the transformations from LA to LG identically, excepting point (i) above, for all stations in the network.

The expectation for the small changes in latitude of a metrology network, point (i), to have any affect on the transformation is nonexistant, due to the very short sight distances (usually < 20 metres). However, point (ii) is very interesting, in that it is not the absolute value of the deflections that is important, but the relative changes in these values throughout the network. The obvious approach to determining what error contribution the neglecting of changes in both latitude and the deflection components have, is to compute the differentials for the above transformation with respect to these parameters. It can be appreciated that all three rotations are very small, therefore, making a first order approximation of the total rotation matrix is valid, which gives us equation (3-16) (Vanicek and Krakiwsky, 1986).

$$\begin{bmatrix} x \\ y \\ z \end{bmatrix}^{LG} = \begin{bmatrix} 1 & (A-\alpha) & \xi \\ -(A-\alpha) & 1 & \eta \\ -\xi & -\eta & 1 \end{bmatrix} \begin{bmatrix} x \\ y \\ z \end{bmatrix}^{LA} \qquad (3\text{-}16)$$

where,

A - α, ξ, and η are all in radians.

The derivation of the partial derivatives for all three of the variable parameters is trivial, hence, only the final rearranged differential equations, explicit in terms of the varying parameters, will be given. Equations (3-17) and (3-18) show the partial derivatives explicit in terms of a small change $\partial\phi$ in latitude for x and y, respectively ($\partial z/\partial\phi = 0$).

$$\partial\phi = \partial x \cos^2\phi / \eta\, y \qquad (3\text{-}17)$$
$$\partial\phi = -\partial y \cos^2\phi / \eta\, x \qquad (3\text{-}18)$$

These equations show very clearly that any small change in latitude can be tolerated for networks located anywhere on the earth's surface, for all magnitudes of deflection components, to obtain much less than a tenth of a millimetre for the coordinates involved in the transformation. For example, expecting an accuracy of 0.05 mm on the equator ($\phi = 0^o$) with an x or y coordinate of 30 metres and a deflection component of 10", allows for a change in latitude of almost 2 degrees. This finding is certainly not unexpected and has only been presented for completeness.

The parameters that are of real interest are the deflection components. the two equations (3-19) and (3-20) give the partial derivatives explicit in ξ for the x and z coordinates ($\partial y/\partial\xi=0$), while equations (3-21) to (3-23) are explicit in η, for the x, y, and z coordinates, respectively.

$$\partial\xi = \partial x \,/\, z \qquad (3\text{-}19)$$
$$\partial\xi = \partial z \,/\, -x \qquad (3\text{-}20)$$
$$\partial\eta = \partial x \,/\, y \tan\phi \qquad (3\text{-}21)$$
$$\partial\eta = \partial y \,/\, (z - x \tan\phi) \qquad (3\text{-}22)$$
$$\partial\eta = \partial z \,/\, -y \qquad (3\text{-}23)$$

A network designed for metrological purposes is very likely to be more dominant in either the x or y coordinate (if these are the horizontal components), with a maximum z coordinate almost always less than 10 metres. This results in equation (3-20) showing a more stringent requirement for $\Delta\xi$, while the requirements for $\Delta\eta$ is dependent on network latitude. Figure 3.5 gives an illustration of the maximum allowable deviation for ξ and η (as it varies with latitude), while considering a required accuracy of 0.05 mm in all three coordinates, with a maximum sight distance of 30 metres along either the x or y axis, and a 10 metre z coordinate.

The allowable deviations for both deflection components is in the range between 0.2" to 0.4" (arcseconds). Although this at first seems very stringent, one must bare in mind that these changes must occur over the sight distance of 30 metres. Due to the nature of the geoid, which is considered as a very smooth, always convex surface (Vanicek and Krakiwsky, 1986), this is not very likely to happen. In addition, the case presented is very drastic and is also not very likely to occur, which would allow a little more tolerance for changes in deflection.

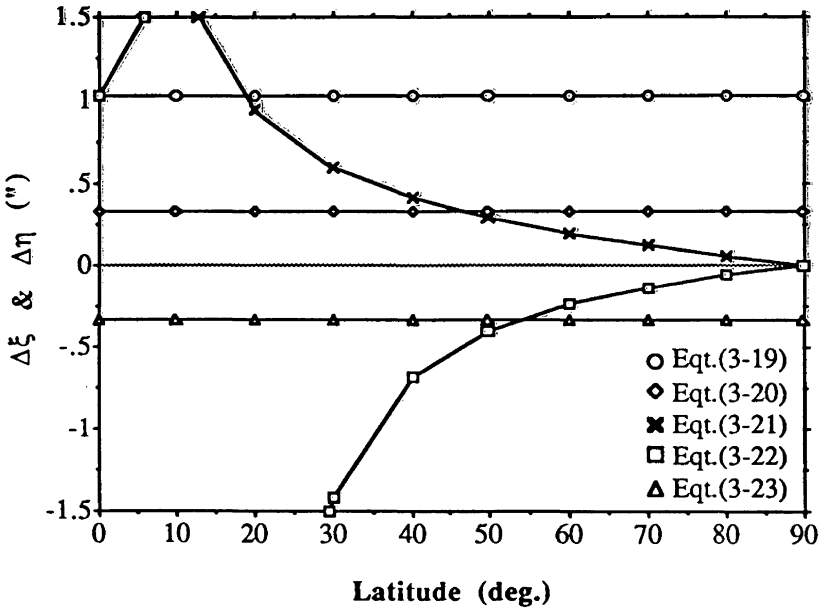

Figure 3.5 Maximum Tolerance for Changes in the Deflection of the Vertical

The relationship between the LA and LG system is more complicated if the axes of the G and CT systems are misaligned. However, the same theory is still applicable, only equations for the deflection components and misalignment of astronomic and geodetic norths are more difficult to obtain. The interested reader is referred to Vanicek and Krakiwsky (1986), Torge (1980), or Bomford (1980) for a more detailed treatment of this situation.

3.3.2 Geometric Reductions

With the effects in the variation of actual gravity removed or neglected (if deemed negligible), the quantity of LA systems forming the network has now been transformed to an analogous network of LG systems. The complement axes of the various LG systems are still not parallel, due to each system's definition of the x axes, changes direction with a change in longitude, and the fact that the systems are located on a curved surface, the reference ellipsoid. However, the mathematical relationships involving this reference surface are very regular and well known, making it a trivial task to determine the effects of neglecting these final reductions.

To simplify the mathematics further a reference sphere will be used in place of the customary ellipsoid. This is a valid simplification due to the very small area and differential rotations that are to be analysed. The minimum (r_{min}) and maximum (r_{max}) radii of curvature of the surface of a biaxial ellipsoid occur at the equator and poles and are given by equations (3-24) and (3-25), respectively (Krakiwsky and Thompson, 1974).

$$r_{min} = a \tag{3-24}$$

$$r_{max} = a / (1-e^2)^{1/2} \tag{3-25}$$

where,

a is the major semi-axis of the reference ellipsoid
$e^2 = (a^2-b^2) / a^2$ is the first eccentricity of the ellipsoid
b is the minor semi-axis of the reference ellipsoid

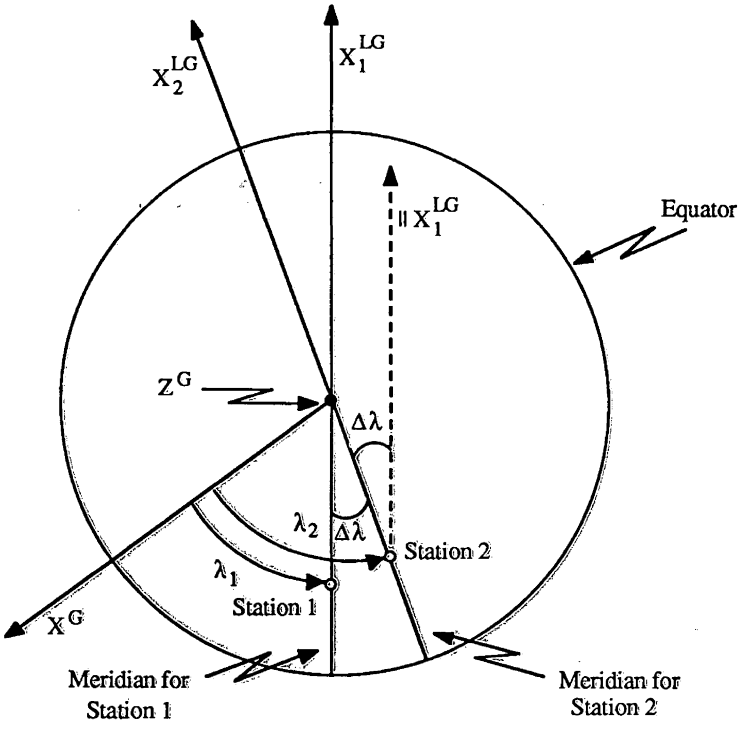

Figure 3.6 Rotation Around the Z axis

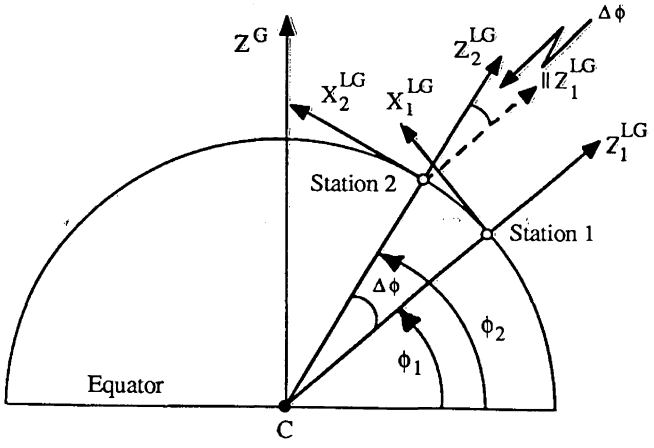

Figure 3.7 Rotation Around the Y Axis

The micronetworks in industrial metrology applications would rarely exceed an aperature of 100 metres. This would translate into an angular variation of only 0.01" between using the maximum and the minimum radii of curvature, using the biaxial ellipsoid parameters for the North American Datum 1984 (NAD 84, a = 6378137.000 m and b = 6356752.314 m). This small variation is negligible when determining the required rotations, hence, a surface with a constant radius (a sphere) is a valid simplification for the computations.

Three small rotation angles can be derived from the two triplets of geodetic curvilinear coordinates (ϕ, λ, h) that define the location of the two LG systems on the ellipsoid. These rotations represent the misalignment of the three coordinate axes of the two systems.

The small rotation required around the z axis of the second system, to make the projection onto a horizontal plane of the remaining two axes parallel to their complements, is simply the difference in longitude between the two stations (see Figure 3.6). The same visualization can be used to determine the small rotation around the y axis of the second system to make the two x axes parallel. This is simply the difference in latitude between the two stations, as illustrated in Figure 3.7. The remaining rotation, around the x axis, to bring the remaining two sets of axes parallel is not as easy to visualize. After the completion of the initial two rotations, the z axis of the second system must be projected into the yz plane of the first system. Figure 3.8 illustrates the cross section of the sphere along the y_1z_1 plane, displaying the simple geometry involving the desired rotation angle (ω), which is given by equation (3-26).

$$\omega = \arctan [d \; / \; (R + h)] \qquad (3\text{-}26)$$

where,

d distance between z axes in the horizontal plane of the fixed LG system
R radius of the reference sphere
h ellipsoidal (spherical) height of the fixed LG system station.

The computed rotation ω is dominated by the magnitude of the sphere's radius, hence, the distance and the height need only be approximate for this computation.

The three rotations when combined form a single total rotation matrix, that can be populated by the first order approximation of its components, due to the rotations being differentially small. Equation (3-27) gives the total transformation relationship, including the origin offsets, that aligns and brings into coincidence, the complement axes between the two LG systems.

$$\begin{bmatrix} x \\ y \\ z \end{bmatrix}^{LG_1} = \begin{bmatrix} 1 & \Delta\lambda & \Delta\phi \\ -\Delta\lambda & 1 & \omega \\ -\Delta\phi & -\omega & 1 \end{bmatrix} \begin{bmatrix} x \\ y \\ z \end{bmatrix}^{LG_2} + \begin{bmatrix} x_o \\ y_o \\ z_o \end{bmatrix} \qquad (3\text{-}27)$$

where,

$\Delta\lambda$, $\Delta\phi$, and ω are all in radians
x_o, y_o, and z_o are offsets of the LG_2 origin in the LG_1 system.

In micronetworks, the above transformation is usually applied implicitly in the formulation of the observation equations. The datum is created, as mentioned previously, by fixing the location of one of the network's LG systems. This fixed coordinate system is translated, maintaining orientation, to the remaining network stations, to obtain offsets describing the origins of each of their systems with respect to the one fixed system. The vectors, describing the observed quantities, are then formulated into observation equations by using the offsets determined for each station's origin, in place of the coordinates defined by the instrument location's LG system.

This procedure completely eliminates the effects of the misrotation ($\Delta\lambda$, $\Delta\phi$, and ω) and horizontal offsets (x_o and y_o) of the various systems, as described in equation (3-27).However, tacitly assumed in the procedure is that all of the stations involved in the network can be described by simple translations. For this assumption to hold, all of the planes formed by the tangents to the earth's surface, at each of the network stations, would have to be parallel. Unfortunately this is not the case, as the network is being

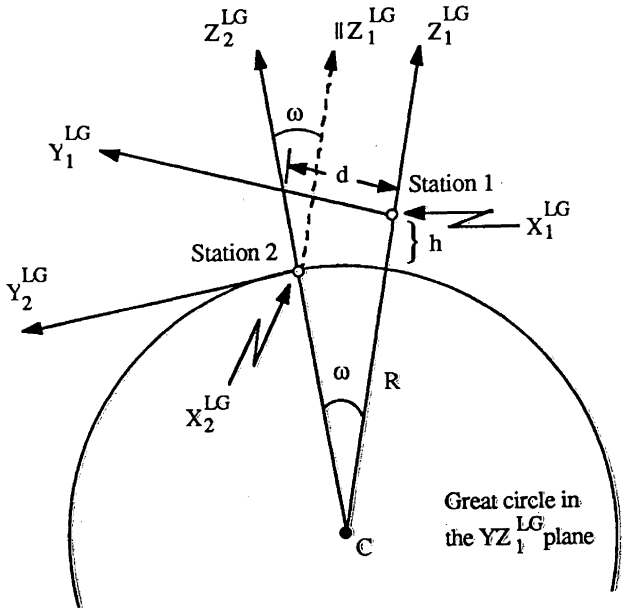

Figure 3.8 Rotation Around the X Axis

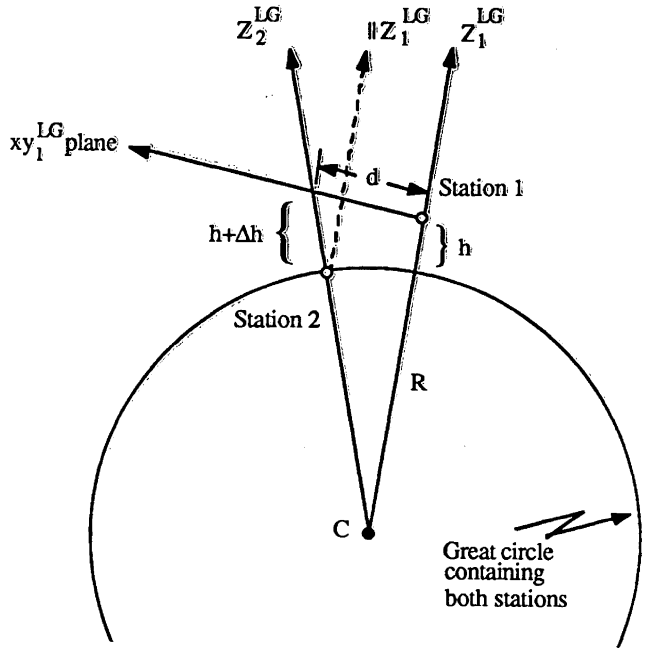

Figure 3.9 The Effect of Neglecting Earth Curvature

formed on a curved surface.

The invalid assumption is reflected in the vertical offset (z_o), of equation (3-27), not being completely eliminated in the formulation of the observation equations. The effect is given in equation (3-28) (Faig, 1972) and illustrated in Figure 3.9, which also show that the magnitude of the expected deviation, will increase with distance away from the fixed LG system.

$$\Delta h = d^2 / 2R \qquad (3\text{-}28)$$

where,

Δh	the error in height caused by neglecting the earth's curvature
d	distance from fixed LG system
R	radius of earth.

A vertical error of 0.1 mm can be introduced, with only a 36 metre distance from the fixed system!

In most metrology applications this probably can be neglected due to the relative smoothness being the more dominant criteria then absolute heights. However, there are some applications that require absolute alignment, in which case this correction must be considered.

3.4 Design Criteria for Metrology Micronetworks

The last topic to discuss concerning three dimensional networks, are the peculiarities that are associated with metrology networks in particular. These networks are of the highest possible order, therefore, need some special considerations in their design as well as measurement. In particular, these considerations are scale, horizontal and vertical refraction, and the removal of the random centering error associated with angular measurements.

3.4.1 Scale Determination

Scale determination in a metrology network is a very interesting problem. Typical engineering networks have a minimum aperature of 1/2 kilometre and are usually larger than this (1 to 2 km). This allows distances to be measured randomly throughout the extent of the network or even possibly to define the entire network (trilateration). There are many portable EODM 's being manufactured that allow distances to be measured, in networks of typical aperature, between 0.5 mm to 3 mm accuracy depending on the type of instrument used. A properly calibrated EODM has proven to be a very successful method of alleviating the scale defect in these networks. However, this same methodology cannot be carried over to metrology networks of a few tens of metres distances, primarily because of the inability to measure the short distances accurately enough (say 0.05 mm) to satisfy the scale requirements.

The only real solution to this problem is the use of calibrated scale bars. The two targets that define the scale bar length can be tied to the network through triangulation, with the known distance between them added as a spatial distance observable. This method eliminates the scale defect in the network, but in doing so creates some additional concerns.

The scale bars themselves must be constructed of some very environmentally stable material, such as invar, to ensure no systematic change in length while being used. The absolute length determination of the bars requires the use of an interferometric comparator, which in practice will only be able to obtain the length to an accuracy of $\pm$ 0.01 mm, due to the difficulties in optical identification of the centres of the attached targets. For a 2 metre scale bar, this already would create a systematic scale error of 5 ppm in the network. This scale error could be reduced by using a longer scale bar, however, this creates logistical problems in transporting and in some cases calibrating, due to the limits of some calibration interferometers.

Of primary importance when using scale bars, is the way in which the scale associated with them is propagated into the network. A chapter can be taken from the geodesists of the past, who created triangulation networks using a single measured baseline for scale (Bomford, 1980). Their techniques were designed for horizontal networks, which is where the concern for scale exists in metrology networks. The height component usually has a much smaller working range, which would probably never exceed a few metres making systematic scale error much less of a problem. However, it is critical to create a reasonable working range in height, not having all stations located in almost the same horizontal plane, to achieve good solutions for this component.

3.4.2 Atmospheric Refraction

The systematic effects of refraction have already been alluded to at the beginning of this chapter. The usual approach to the lessening of the vertical refraction effects, in traditional networks, is by observing simultaneous zenith distances between the two stations. This is not possible to accomplish in metrology networks, where the bulk of the stations are wall targets. In addition, the centering error created by such a procedure would likely overshadow the effects that are to be removed. In addition to vertical refraction, horizontal refraction must also be considered in the confined areas of metrology networks, where the positioning of instrument stations may be dictated by the space available.

The only real solution to the refraction problem is to try to keep the effects to a minimum through the design of the network. If the sight distances are kept very short (< 20 metres) and lines of sight are kept from going close to large bulky apparatus (i.e. large machinery, hanging fixtures, jutting walls, etc.), which may produce heat radiation, most refraction effects can be eliminated. Additional considerations are required for sight directions, if the network is being designed to monitor components involved in a working production process. These processes generally produce a lot of energy which will create a

very inhomogeneous atmosphere. An attempt should be made in the design of the network to eliminate sight directions, if possible, that go over top or close by the sides of any processes that release large irregular quantities of heat energy into the air.

Temperature gradients affect optical light rays by bending them, creating a curved line of sight path. This means that the actual circle readings are with respect to the tangent to the curved path at the instrument station, instead of the required straight line path. The following equation can be used to compute the horizontal error (γ) in the line of sight direction due to lateral refraction (Blachut et al. 1979).

$$\gamma'' = 8.0'' \left[\frac{pS}{T^2}\right] \left[\frac{dT}{dx}\right] \qquad (3\text{-}29)$$

where,

p	is the barometric pressure in millibars
T	is the temperature in kelvin degrees (T = 273.15 + t in ^{o}C)
S	is the sight distance in metres
dT/dx	is the horizontal temperature gradient, perpendicular to the line of sight.

For a 0.1 mm lateral refraction error to occur over a 20 metre sight distance, would require that the tangent to the line of sight at the instrument station deviate in the horizontal plane by 1" from a straight line of sight. From equation (3-29), assuming standard pressure and temperature, a horizontal temperature gradient of 0.5^{o}C/m is all that is required to create this deviation in the line of sight. A gradient of this magnitude can occur if large quantities of heat radiation are being produced.

The temperature gradients could be measured to correct the circle readings for the refraction effects. However, it would be very impractical and difficult (could change many times over a single line of sight) to measure the temperature gradients for various lines of sight. The only real solution to the problem of refraction is to try to minimize the effects by keeping the temperature distribution constant within the work area (i.e. keep doors and windows closed, switch off machinery, etc.).

3.4.3 Centering Error

The remaining consideration for metrology networks is the removal of the random centering error contribution to the observed quantities. This too, has been alluded to at the beginning of this chapter, and also was mentioned previously in section 2.2. In traditional engineering networks this error has been reduced by developing forced centering methods, which reduces the contribution of centering error to $\pm$ 0.1 mm. In addition to not meeting the requirements for metrology, these methods require stationary pillars to be constructed at the network stations. This is obviously not suitable for use in metrology, where instrument locations must be located very close to the components being set out or monitored.

If the datum has not been predefined, the precise physical location of the instruments is immaterial and the actual centering can be ignored. The instruments would not have to be physically centered over a mark, but the precise relative positions between the instruments, in some common coordinate system, would have to be determined. The spatial line connecting the intersection points of the primary axes of each theodolite (see Figure 2.3) can be used to create the reference system. Each instrument can be treated as a combined collimator and telescope, and by using a special technique for sighting on the crosshairs of each instrument (Kissam,1962), the two lines of sight created by each telescope can be brought into coincidence.

Although the above approach solves the relative location between instruments, there are some problems associated with it. The procedure used for the alignment can be quite tedious and time consuming, unless the instruments are specially equipped with targets defining the intersection of the horizontal and vertical axes (e.g. the Wild T2000S). The relative orientation that is established between instruments is determined uniquely, with nopossibility to create any redundancy in the solution. In addition, there are severe limitations for extending the reference system to other theodolite locations, due to the accumulation of error for the collimation techniques. The methodology is very cumbersome

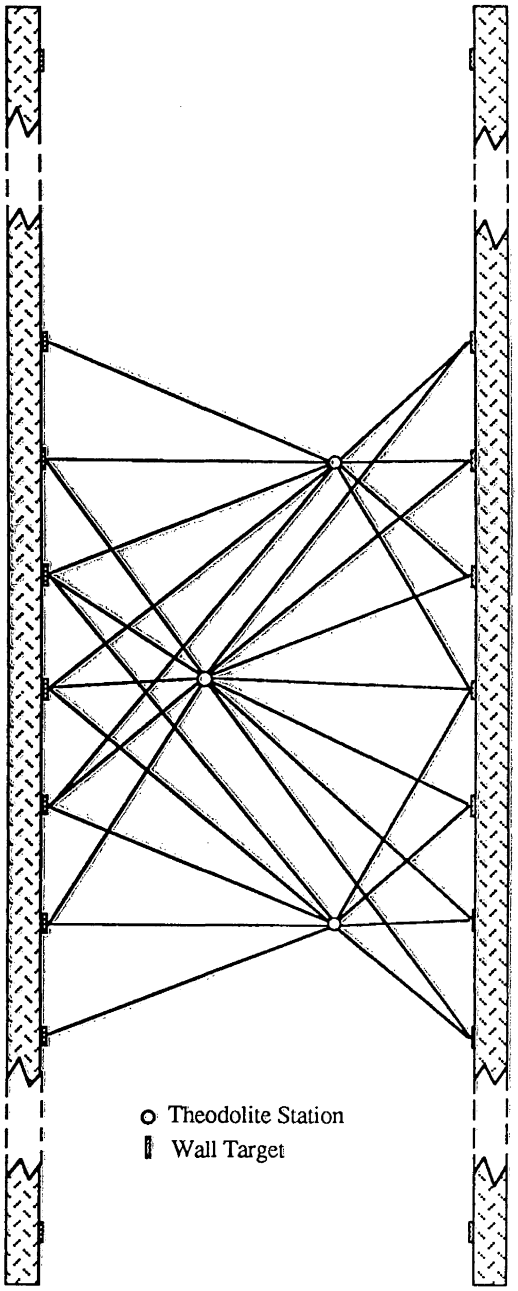

Figure 3.10 The Method of "Free Positioned" Theodolite Stations

to use when the network is being densified or extended, quite possibly making the centering over marks necessary to maintain the datum, which certainly would reduce a coordinating system's accuracy capabilities.

However, the above limitations can be eliminated by using a unique characteristic of metrology networks, that allows the random centering error for each instrument station to be completely removed from the solution. The instrument station locations themselves are not the main concern when establishing the network. It is the locations of the reference wall targets that are the primary objective, with the instrument locations serving only as a link between the different wall targets. This means that the precise physical location of the instrument centre is immaterial as long as it fulfills the designed geometric criteria for the network.

Therefore, if observations between instrument locations are not performed, the instruments can be randomly located in the general vicinity that was designed, with no thought of having to centre over a particular physical mark. The redundancy that is lost by not observing between instrument stations is restored by observing redundant rays to the wall targets. The coordinates of the instrument locations can be thought of as nuisance parameters, which must be added to the network solution in order to obtain the desired quantities, the wall target coordinates. Of course, how well the coordinates of the wall targets are determined is related directly to the accuracy of the linking stations, therefore, great care must still be taken in obtaining good solutions for the instrument coordinates. This approach is analogous to that employed in the bundle method of aerotriangulation (Brown, 1985), where the perspective centres of the different camera locations are determined, only to obtain the link between ground stations. Figure 3.10 shows a typical scheme of direction observations in establishing a reference microtriangulation network using the method of the "free positioned" theodolite stations.

4. Algorithms for Coordinating System Software

The integration of a coordinating system with traditional metrology methods gives the ability to determine coordinates, offset values, corrections, surface coefficients, or whatever is required in virtual real time. This is the major advantage that the system provides, in comparison with the traditional optical-mechanical methods. A disadvantage of the coordinating system is that the parameters needed in the setting out or maintenance surveys are not directly determined, but have to be derived from coordinates. Therefore, as already alluded to in the introduction, it takes a great deal of computer software to give a system the flexibility that is required, for even just a single application of the system.

There are primarily two types of coordinating systems in use in North America, the Wild C.A.T. 2000 and the Kern ECDS2, which together have created a suite of standard algorithms that are being adhered to in industry. In these algorithms, the basic geodetic measurement principles that have prevailed in triangulation for centuries, have been replaced by quicker measuring techniques to lessen the preliminary set up times and to accelerate the obtaining of the required parameters. The loss in accuracy caused by this substitution can be tolerated for some system applications, where the optimum achievable accuracies are not required. However, for any application wanting to use the coordinating systems to their full potential, this becomes a serious limitation as has been shown in section 2.2, where errors inherent in theodolite construction have been discussed.

This chapter is designed to discuss the major aspects of the software that must be considered in order to achieve the optimum accuracies available, with a high degree of certainty in the results. Figure 4.1 illustrates the five main software modules that comprise a coordinating system. The primary considerations for the development of each of the four components surrounding the main program module will be discussed. This will be followed

by a summation of the discussion, presented in the point form of an algorithm. The main program module itself will not be considered as its purpose is simply to coordinate and manage the entire observing and processing effort being performed.

It is these algorithms that have been followed in the author's development of software for the UNB coordinating system (P3DCS). The hardware for the UNB system is comprised of two Kern E2 electronic theodolites interfaced to an Apple Macintosh Plus microcomputer via a Kern ECDS Switch Box and AR1 serial interface.

The surface fitting, contained in the last module, was not required for the aforementioned TASCC project and is being discussed here only to display the entire capability that is required of a coordinating system package. However, the surface fitting has been implemented successfully in a separate project involving the determination of the regularity of a parabolic antenna, which was mentioned in the introduction.

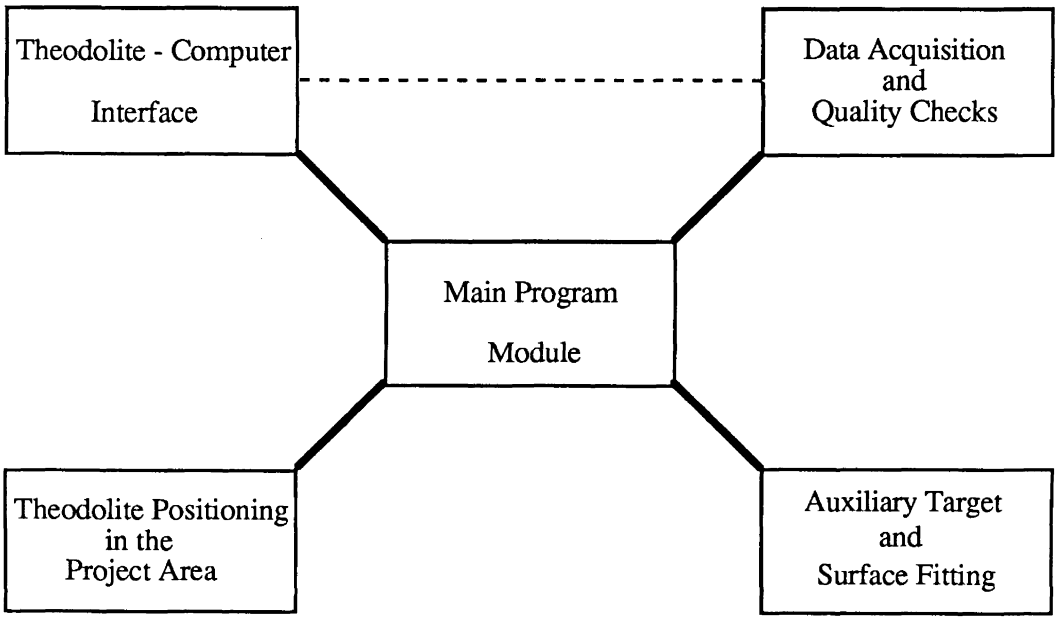

Figure 4.1 The Primary Software Modules of a Coordinating System

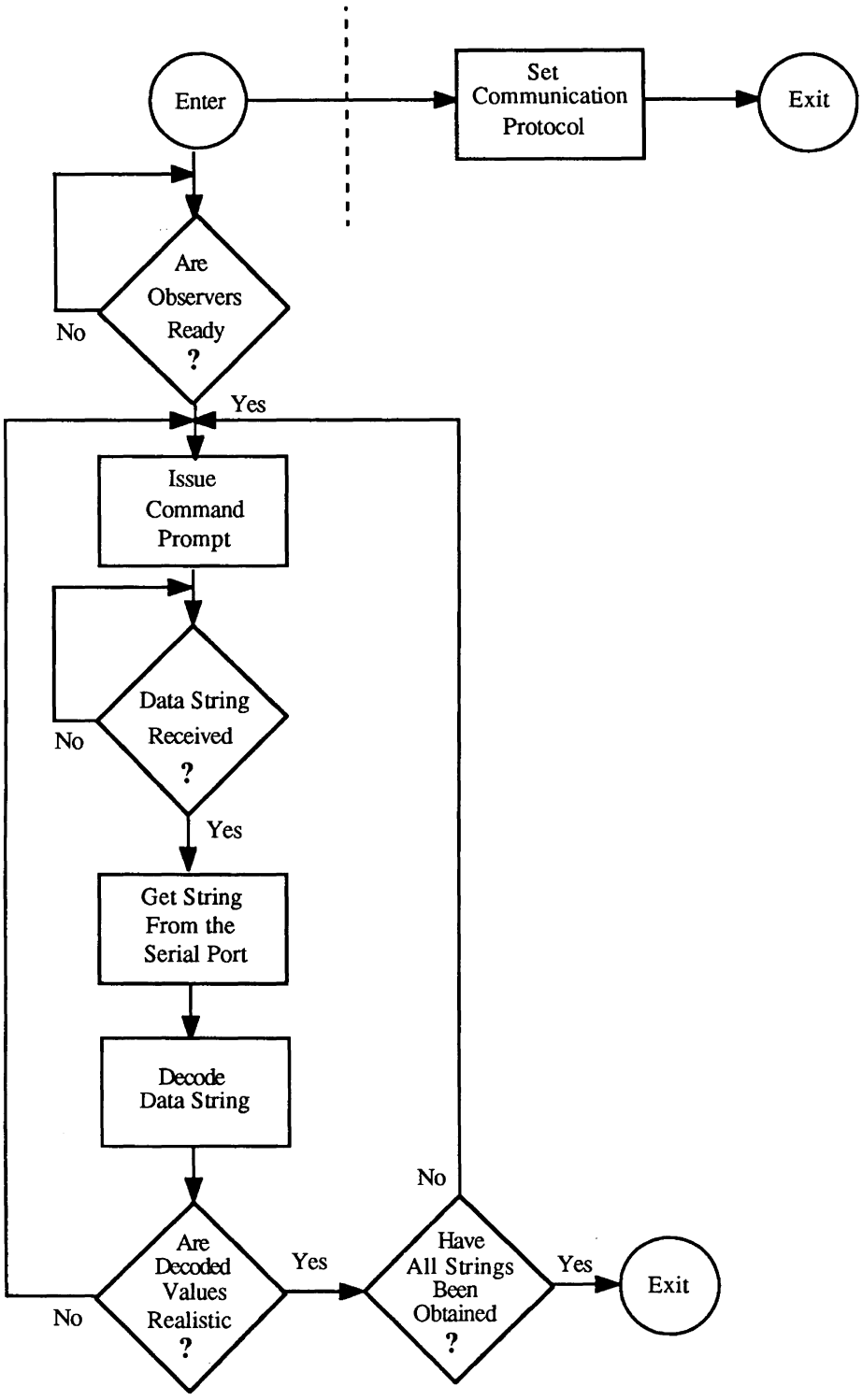

Figure 4.2 Flow Diagram for the Theodolite-Computer Interface

4.1 The Theodolite - Computer Interface

The theodolite-computer interface is the module that controls all of the communication that occurs between the theodolites, computer, and operator issued commands. As such, the tasks that it must perform involve the setting of the serial port communication protocol, prompting theodolites for measurements, receiving the data strings, decoding the data strings, and checking if the decoded values are realistic. No actual data processing is performed by this module as its sole purpose is to supply the observations in a usable form to be processed by the remaining modules.

Figure 4.2 illustrates the flow of events that should occur to obtain successful measurements in one of the telescope positions for all the theodolites involved in the observing of a particular target. From this illustration the task of the interface can be subdivided logically into the setting of the communication protocol and the data decoding.

4.1.1 The Communication Protocol

The first step, setting communication protocol, is a direct result of the mode of communication being serial and obviously is only required to be done once for the entire observing campaign. This accounts for it being segregated in Figure 4.2 by the dashed line. The actual setting of the protocol can be separated into two distinct parts that are hardware and software related.

The hardware component involves the actual physical connection, via cables, between the theodolites and the microcomputer. The connection is usually accomplished using one of the many forms of the RS-232 interface, which is dependent on the interfaces employed by the components being connected, as well as the connector receptacles themselves. The complement pins contained within the interface, in whatever way they are defined, must be properly connected (i.e. data transmit of one component with data receive of the other, etc.)

in order to achieve successful communication between the devices. It is not the author's intent to give a detailed discussion on communication using the RS-232 interface, but only to indicate that it is a critical part of the communication procedure that must not be overlooked. The pin configuration required to complete the interface between the Kern E2 theodolite and the Apple Macintosh Plus and SE computers is illustrated in Figure 4.3. The maximum cable length is usually limited by the transmitting abilities of the DC powered theodolites, but is normally in excess of 100 metres (e.g. the Kern E2 specification is 150 m). The reader interested in obtaining detailed treatment of the pin configuration in the RS-232 interface is referred to Campbell (1984).

The remaining component, software, of the setting of the communication protocol deals entirely with the description of the data being transmitted between the devices. Each device must know what to expect from the other before any meaningful communication can occur. The defining characteristics of a data transmission are the baud rate, bits per character (data bits), number of stop bits, and parity.

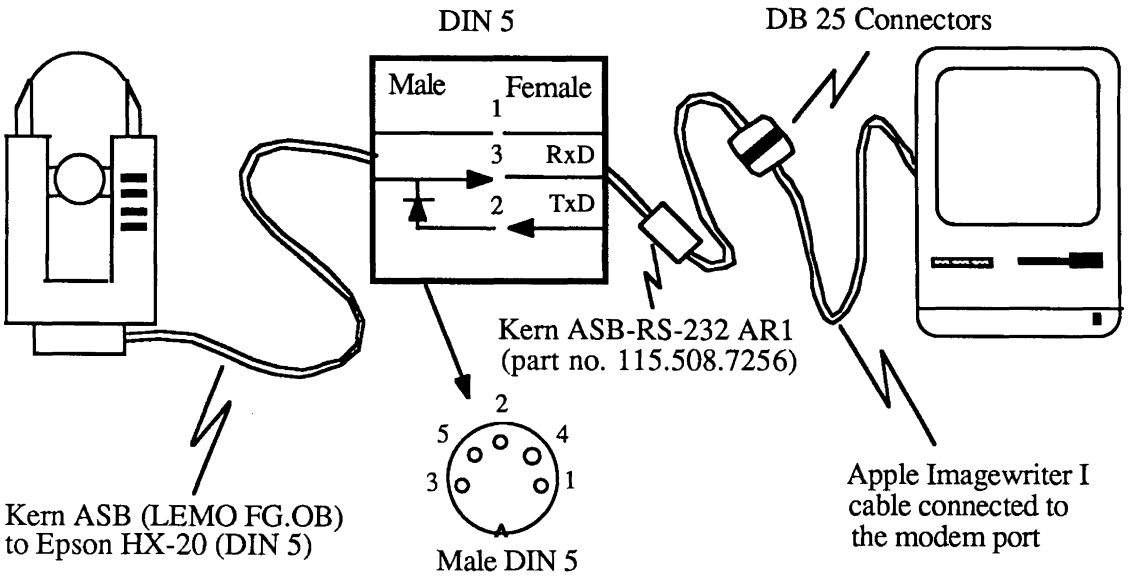

Figure 4.3 The Macintosh Plus/SE - Kern E2 Interface

The theodolites have these parameters fixed at specific values (e.g. Kern E2: 1200 baud, 7 data bits, 2 stop bits, and even parity), which requires that the computer have to conform its serial port to the needs of the instrument. This is accomplished by using software to open the serial port, much like opening a file, with the specified communication parameters. Normally the serial port must be opened twice, once each for input and output, as each is really a separate operation not directly involving the other.

No algorithm will be presented for the software portion of the communication protocol. The approach for software development is dependent on the computer manufacturer's considerations in developing the serial communication port, as well as the type of programming language being used for the software development.

4.1.1 The Data Decoding

Once communication has been established between the theodolites and computer, the primary task of the interface module becomes that of a provider. As such, this portion of the interface is very closely related to the data acquisition module, which is illustrated by the dashed line joining the two in Figure 4.1. The interface must be able to issue the proper measurement commands and provide the observations in a usable form for processing at the data acquisition stage.

A measurement prompt consists of a string of ASCII command characters that are transmitted to the theodolite, which when interpreted begin the electronic measurement of the horizontal and/or vertical circles. As would be expected, each theodolite manufacturer have their own command characters as well as calling sequences. The following string of characters (with hyphens and spaces removed), STX - T - 2 - 1 - 1 - 2 - C_R - L_F, illustrates a command string that would prompt a Kern E2, with I.D. set to 2, to measure and transmit both horizontal and vertical circle readings.

The retrieved transmission from the Kern E2 would be an ASCII variable length record with all trailing and preceding zeros in the circle measurements not being transmitted (e.g. a horizontal circle measurement of 1.2 gons would be transmitted as 11+1.2). The following character string, 11+HHH.HHHH 12+ZZZ.ZZZZ$C_R L_F$, illustrates the format for the maximum length record that would be received using the previously described command string for the Kern E2 theodolite.

Once the data string has been obtained from the serial port the only remaining task of the interface is to decode the string and check if decoded values are realistic, before handing them over to the data acquisition module. The decoding itself is very straight forward, however, different decoding routines are required for the different manufacturer's theodolites due to the variation in data string formats. The check on the decoded values is simply to ensure that either the command or data strings have not been corrupted in the transmitting process by electronic glitches, voltage surges, environmental effects, or whatever. The term realistic simply means that the values decoded are within the measurement range of the instrument (i.e. between 0 and 360^0 for angular measurements). If the values are not deemed realistic the command to measure should be repeated and new values decoded before control is released back to the data acquisition module.

In summarizing the above discussion and referring to Figure 4.2, the following simple algorithm is obtained, which has been conformed to by the author in the development of software for P3DCS.

1. Determine if the operator(s) is/are ready to have the measurements performed.
2. Issue the appropriate measurement prompt string of ASCII command characters.
3. Determine when the input data string has been received at the serial port.
4. Obtain the string from the serial port input buffer and decode it into the separate observables (i.e. horizontal direction and zenith angle).
5. Determine whether the values are realisticly possible (i.e. have not been corrupted). If the values are in doubt, return to step 2.

6. Determine if all the instruments involved in the measurements to this target have been prompted. If not, go back to step 2. and repeat the process for the next instrument. If they have, return to the data acquisition with the results.

Although only examples for the Kern E2 theodolite have been presented, the Wild system is very similar and can be handled in the same way. For more information regarding the two systems, character commands, and instrument response, the interested readers are referred to Kern & Co. Ltd. (1984a) and Wild Heerbrugg Ltd. (1984) for the Kern and Wild electronic theodolites, respectively.

4.2 Data Acquisition and Quality Checks

There is no mystery behind the data acquisition and quality check module, its primary functions are as its name suggests. Its tasks are to acquire the observations complete with station names, perform a station adjustment (if more than one set of observations is made), and provide a reliable filter for quality control. All obvious blunders, mispointings, electronic glitches, and misspelled station names must be eliminated from the data set before control is passed back to the remaining modules. Figure 4.4 illustrates the flow of events that should occur in this module to ensure a reliable data set.

The traditional geodetic methodologies that are normally used in triangulation networks are employed for the data acquisition. This requires that targets be observed in both direct and reverse telescope positions with the well established rules for measuring sets and pointing order within a set being adhered to. The measuring of both telescope positions ensures that the systematic errors inherent in theodolite construction are eliminated, or at least made negligible, from the observations (see section 2.2). This is critical if the coordinating system is being used to obtain the optimum possible accuracies as there cannot be a trade off between accuracy and the speed at which the required parameters are obtained.

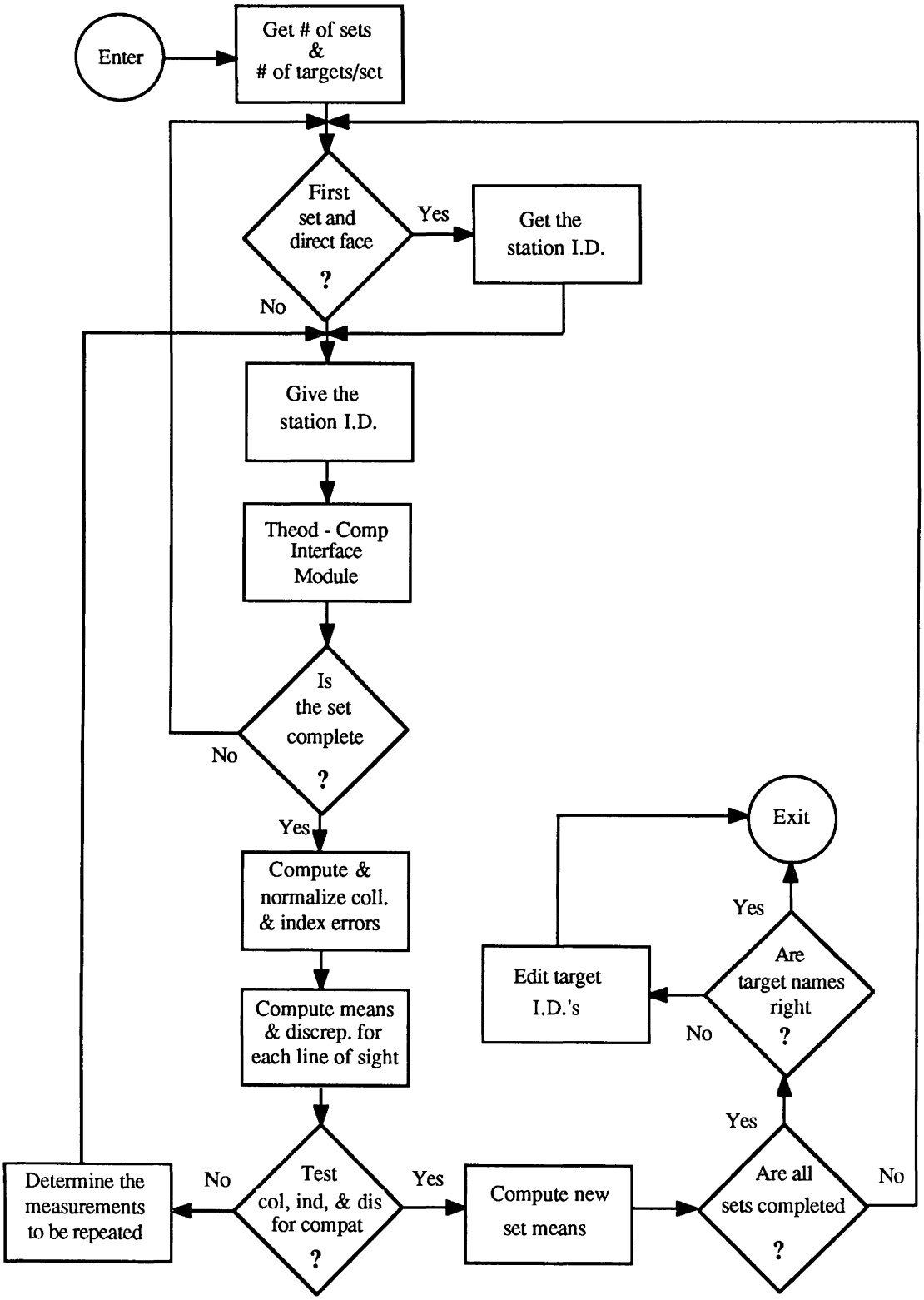

Figure 4.4 Flow Diagram for the Data Acquisition Module

The index error and the true collimation error for each instrument are unique and should remain constant for each set, and as such provide a very good assurance of data quality. The true collimation error can be defined as the angular amount that the collimation axis (optical axis) and the horizontal axis (trunnion axis) deviate from perpendicularity with the instrument telescope having zero inclination. The use of the true collimation error as a consistency check, requires that the derived collimation error from the measurements be modelled for the effects of telescope inclination. The functional relationship to determine the true collimation error (c) from that derived from the measurements (c') and the telescope inclination (γ) is given by equation (4-1) (Cooper, 1982).

$$c = c' / \cos \gamma \qquad (4\text{-}1)$$

The index and true collimation errors are only made available due to the observing of the observations in both telescope positions, which gives even more criteria for following the traditional geodetic approach. In addition, the liquid compensators employed in the instruments are very sensitive to temperature changes (see section 2.2) making the index error very temperature dependent. The index error can change by several arcseconds within a single set of observations, which makes it imperative to monitor changes in its magnitude to detect and remove the possible systematic effects.

The remaining constituent in the quality control filter are the discrepancies that can be computed by redundantly observing targets from the same instrument station. The discrepancy between the mean of the two telescope positions for an observation in the current set and the mean value for the same quantity from all previous sets, can be easily derived. There are two possibilities if a discrepancy is found to be beyond the acceptable limit. If the true collimation or index error, depending on discrepancy observation type, is also found to be unacceptable, a repetition of the current set for that observable is all that is required. Secondly, if the true collimation or index error checks are favorable, all

repetitions of that particular observed quantity would have to be repeated, due to the difficulty in determining which set is the outlying set.

Implicit in the above discussion on quality control is the assumption that there is a known tolerance value. This tolerance value is required in order to determine which measurements are to be considered as outlying quantities. However, it is not so easy to choose a single tolerance value to use for every application of the coordinate system, as it is very project dependent. A project like the setting out of TASCC, with accuracy specifications of 0.1 mm requires a much more stringent tolerance value than if the accuracy requirement was 0.5 mm. Similarly, if the tolerance value is in terms of angular measure, then two projects with specifications requiring the same positional accuracy, would need two different tolerance values if one project has all of its sight distances longer than those in the other project. A single project itself may require different tolerance values if a variety of different sight distances are encountered in the positioning procedures.

Even if a single tolerance could be used in the quality filter, another problem arises when using it to check the computed collimation and index errors for possible outliers. Each of these errors is a constant value that is not necessarily zero, therefore, the actual values of the errors must be known a priori so that they can be used to normalize each computed value from the set of measurements. Once normalized the computed instrument errors can be tested in the identical fashion as the discrepancies, which have been normalized by way of the computational procedure used to obtain them.

If the testing is assumed to be at the 95% confidence level the tolerance value would be equal to 2σ, where σ is equal to the known standard deviation of the sample that the tested quantity has been pulled from. This gives an indication as to how well the actual values of the instrumental errors must be known in regard to the tolerance value that will be used for outlier detection.

This discussion clearly indicates that the operator must be able to supply the actual instrumental errors as well as having some idea of what tolerance value to use. The

instrumental errors can either be known and supplied or an option in the software package can be incorporated to actually measure them on the project site. Both methods are valid, but the operator should be aware for example, of how a varying temperature in the project area may change the expected value of the index error (see section 2.2). If the data checks are done automatically with a preset tolerance value, the operator must have recourse for overriding some remeasurement decisions that may not seem valid for that particular situation.

The beginning of the flow diagram depicts that the number of sets to be observed has been left to the operator's discretion. However, if only a single set is chosen to be observed the effectiveness of the data quality filter is greatly reduced. The filter depends on being able to make comparisons of the discrepancies between sets for all of the observations, as well as monitoring the collimation and index errors for consistency within each set. Some systematic tendencies or even some gross mispointings, that have been repeated in both telescope positions, may be overlooked if only the collimation and index errors are available for scrutinization.

The following algorithm is a summation of the above discussion and the flow diagram illustrated in Figure 4.4. The steps outlined have been implemented by the author in the development of P3DCS.

1. Obtain the number of sets of observations (one set contains a direct and reverse telescope pointing) and the number of targets contained in each set.
2. If it is a direct pointing for the first set, obtain the target identifier. If any other pointing, either direct or reverse, give the identity of the target to sight on.
3. Pass the program control to the theodolite-computer interface module to obtain the decoded observations.
4. Repeat steps 2 and 3 until the entire set is completed.
5. Compute the observed collimation and index errors for each target in the set and correct the observed collimation for telescope inclination, using equation (4-1),

to obtain the true collimation error. Normalize the collimation and index errors (using the apriori actual values that have been determined previously or input directly).

6. Determine the mean values for the direct and reverse pointings and if the set number is greater than one, compute the discrepancies by subtracting these values from the already accumulated means from the previous sets.
7. Test each discrepancy, if available, and each normalized collimation and index error for compatibility with the known means, using the confidence interval given by equation (4-2).

$$- \text{tol} < x_i < \text{tol} \qquad (4\text{-}2)$$

where,

x_i is each individual value to be tested
tol = 2σ for the 95% confidence level ; represents the tolerance criteria.

8. If incompatibilities are found only in the discrepancies, only in the collimation/index errors, or in the discrepancies and in the corresponding collimation/index errors, return to step 2 and repeat the appropriate measurements for all sets, in this set, or in this set, respectively.
9. Update the accumulated observation means with the new set of measurements.
10. If all sets have not been completed, return to step 2 with instrument telescopes in the direct position.
11. If a target identifier is wrong or the name has been misspelled, make the appropriate corrections before leaving the data gathering module.

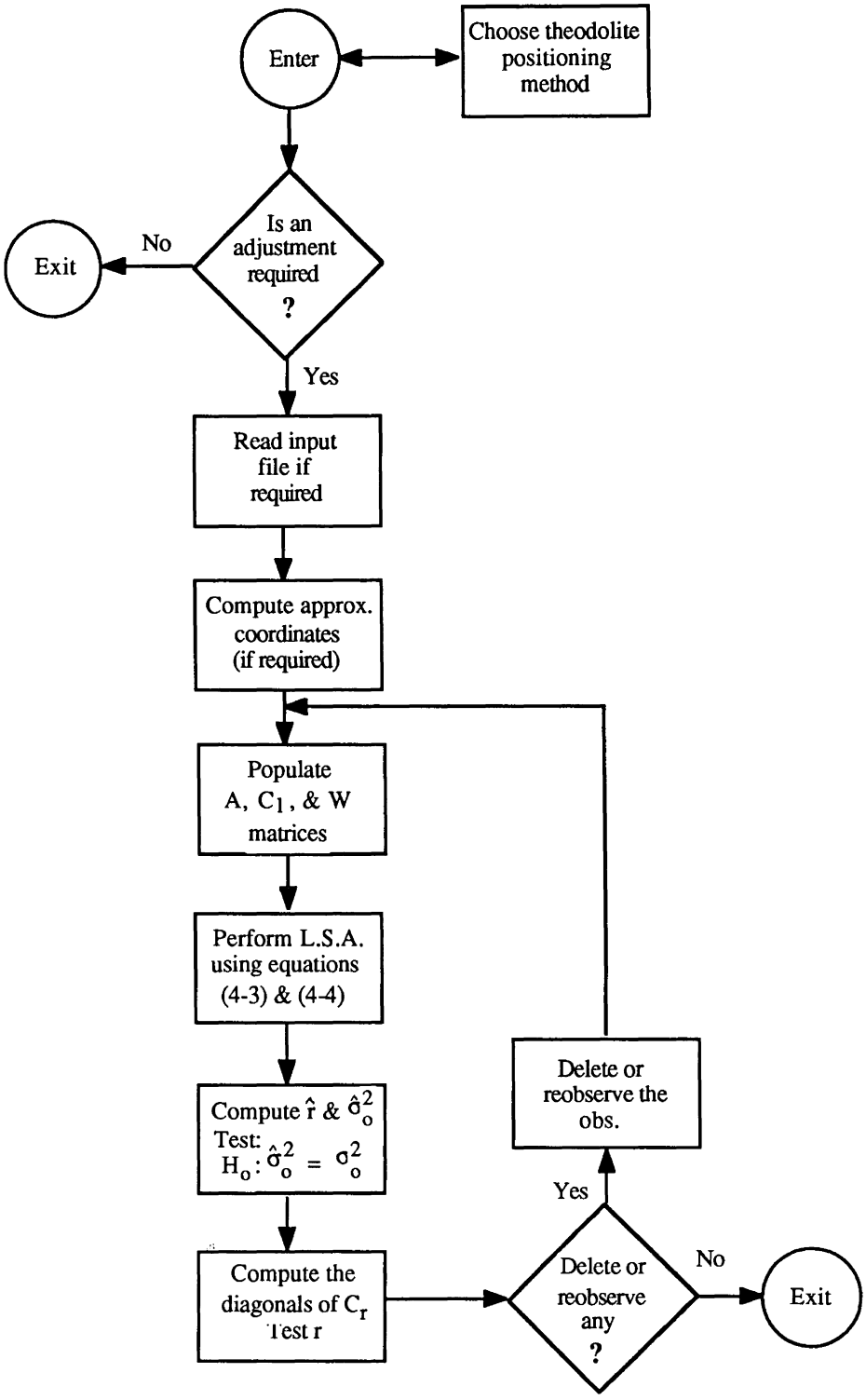

Figure 4.5 Flow Diagram for the Positioning of the Theodolites Module

4.3 Coordinate Determination of the Theodolites in the Project Area

The determination of coordinates for theodolites that are located in the project area must be determined before the coordinates of any object points, which is the usual goal of the entire process, can be computed. The coordinates of the object points are computed using the theodolite positions as fixed locations, therefore, any error in computing the theodolite coordinate triplets is reproduced in the object point triplets. The method for determining the coordinate triplets defining the theodolite locations completely depends on the application at hand, the amount of control distributed throughout the work area, the accuracy of the control, and control point stability. Figure 4.5 illustrates a flow diagram that displays the chain of events for the positioning of the theodolites.

It becomes very apparent that the positioning of the theodolite is extremely critical, but yet is not a trivial task if optimum results are to be obtained. A coordinating system must have the ability to fix, extend, improve, and establish the control in the area of concern. This, of course, means that it must be capable of simply just gathering data, performing resections, carrying out a weighted control adjustment, as well as various combinations of these capacities.

The data gathering option gives the system the ability to obtain a data set, that has passed through the quality filter (see section 4.2), for an auxiliary three dimensional program that is exterior to the coordinating system. This allows the additional flexibility of computing very large or densely targetted networks that are too large to be handled by the coordinating system itself. A file containing the coordinates for the estimated targets with their variance-covariance matrix is all that would be required from the external adjustment by the coordinating system, that would be used as the project control.

In addition, the data gathering option makes it possible to perform all of the available remaining theodolite positioning options, if results are not required in real time. A single

theodolite can be used to perform all the observations at one set up and moved to a second instrument location, to observe all the required targets from this position. The data that has been gathered can be processed together, in the same manner as is normally done in traditional survey practice. However, it must be stressed that results cannot be obtained in real time and once a theodolite is moved, that exact location cannot be reobtained. Even with this limitation, some additional flexibility is added for projects that do not involve having to make adjustments or corrections to observed targets or surfaces.

The list of theodolite positioning options must contain the possibility of executing independent resections to determine the coordinate triplet for any theodolite separately. The separating of the resections gives the operator more flexibility in moving the theodolites around in the work area by only having to redetermine the one position. To be able to carry out resections requires that control have been previously established to a suitable density and accuracy, which depends on the project specifications. The coordinates of target points are assumed to be known with the only unknowns being the horizontal circle orientation parameter (if directions are used as observables) and the theodolite coordinate triplet.

The weighted adjustment option may be used when existing control is available but its accuracy is not suitable enough to treat the control points as fixed and errorless. If the effects of the control errors cannot be negligible (at the levels sought) in the succeeding results or if only a little control exists, then this may be a viable positioning option. Of course, the obvious problem with this technique is the having to handle large fully populated variance-covariance matrices, which not only cause a computational problem but also file management difficulties, especially for very dense micro-networks. Each target used must be sighted simultaneously from at least two theodolite stations to create enough observations to obtain a solution. The benefits of this method are that improved target positions are obtained, the scale would have been previously established, and control may be densified.

A bundle adjustment option involves the positioning of all theodolites and control targets simultaneously. The datum is defined by using a scale bar and each intersection point of the three primary axes of two theodolites (see Figure 2.3). The coordinates of the intersection point of one theodolite and the direction to one of the others are fixed, while directions and zenith angles to each end of a scale bar are measured from at least two theodolite stations. The two remaining coordinates of the second theodolite location used in the datum definition, all remaining theodolite triplets, all control target coordinates, and an orientation parameter for each theodolite location are estimated in a simultaneous adjustment. In order to accomplish this procedure, the restriction that each target used must be sighted by at least two theodolites, yielding unique horizontal determination, must be invoked. If just two theodolites are used the only redundancy in the solution is created by observing two vertical angles to each target, one from each theodolite station. However, in a small area this method of positioning is very plausible, giving extremely good results.

The observation equations that were reviewed in section 3.2 are nonlinear. In order to perform the parametric least squares adjustment the nonlinear equations must be replaced by a linear Taylor's series expansion around initial approximations of the unknown parameters. The least squares solution becomes an iterative procedure of estimating corrections to the unknown parameter values, reformulating the expansion around the updated parameters, and estimating new corrections. The iterations continue until the estimated corrections become negligible. The two equations (4-3) and (4-4) give the expressions used in updating the parameter values and estimating the corrections, respectively (Wells and Krakiwsky, 1971).

$$X^{(i+1)} = X^{(i)} + \hat{\delta}^{(i)} \qquad (4\text{-}3)$$

where,

$X^{(i)}$ are the parameter estimates for the i^{th} iteration

$\hat{\delta}^{(i)}$ estimated corrections for the i^{th} iteration.

$$\hat{\delta} = -(A^T C_l^{-1} A)^{-1} A^T C_l^{-1} W \qquad (4\text{-}4)$$

where,

- A — matrix containing the partial derivatives of the observation equations with respect to the unknown parameters (first design matrix), dimensioned (n x u)
- C_l — variance-covariance matrix representing the accuracies and correlations between the observations, dimensioned (n x n)
- W — vector containing the differences between the observation equations evaluated using the most recent parameter estimates and the actual observed quantities (the misclosure vector), dimensioned (n x 1)
- u — total number of unknown parameters
- n — total number of observation equations.

For the theodolite positioning options where the datum has not been previously established, the required initial approximations may be very hard to compute in real time. Each theodolite's reference mark for measuring horizontal directions is randomly oriented in the project area, dependent on how their horizontal circle has been initialized. The relationships between the reference marks and the datum orientation has to be approximately known before initial estimates can be computed. A plausible solution to this problem, is to set approximately the horizontal zero direction to coincide with what will become the zero azimuth direction of the datum. This would allow the directions obtained from the theodolites to be used directly as approximate azimuths in determining initial values for the unknown parameters, alleviating the orientation problem.

Regardless as to which mode of theodolite positioning is being carried out, the coordinate triplets should be over determined to ensure that reliable blunder free results are obtained. The use of the least squares adjustment criteria not only allows for the solution of the over determined problem, but gives rigorously propagated variances and covariances for all estimated quantities (equation (4-5)) (Wells and Krakiwsky, 1971).

$$C_{\hat{x}} = \sigma_o^2 (A^T C_l^{-1} A)^{-1} \qquad (4\text{-}5)$$

where,

- $C_{\hat{x}}$ — expected variance-covariance matrix of the estimated parameters, dimensioned (u x u)
- σ_o^2 — *a priori* variance factor, scaler quantity

The redundancy itself provides a much improved estimate for the unknown parameters as well as making a post adjustment statistical analysis possible. The *a posteriori* variance factor can be computed, using equation (4-6), which represents the estimated average relative accuracy of the observations from the adjustment process.

$$\hat{\sigma}_o^2 = \hat{r}^T C_l^{-1} \hat{r} / df \qquad (4\text{-}6)$$

where,

$\hat{r}$	the estimated vector of residuals ($\hat{r} = A \hat{\delta} + W$), dimension (n x 1)
df	adjustment degrees of freedom (df = n - u), scaler quantity
$\hat{\sigma}_o^2$	*a posteriori* variance factor, scaler quantity

The χ^2 test on the quadratic form can be performed to test for compatability with the *a priori* value, which represents the expected relative accuracy of the observations before the adjustment process. For the test to be successful the inequality given by equation (4-7) must be satisfied (Vanicek and Krakiwsky, 1986).

$$\frac{df\ \hat{\sigma}_o^2}{\chi^2_{df,1-\alpha/2}} < \sigma_o^2 < \frac{df\ \hat{\sigma}_o^2}{\chi^2_{df,\alpha/2}} \qquad (4\text{-}7)$$

where,

χ^2	value of the Chi- square distribution corresponding to the degrees of freedom and the 1-α/2 or α/2 probability
α	significance level of the test (α = 0.05 corresponds to the 95% confidence level)

The method employed for the testing of the estimated residuals for outlying observations normally depends on the outcome of the above test on the quadratic form. However, in the case of a coordinating system, this global test is used only as a diagnostic tool to determine whether the performing of individual outlier tests are required. The *a priori* variance factor is always assumed to be known, due to the expected accuracies of the target and theodolite coordinates being based on this value. Therefore, the failure of the

global test is used to signify that some of the observations are not as accurate, or in contrast are on average more accurate, than was expected at the beginning of the measurements.

Having observations that are more accurate than expected, quite obviously, does not pose any problem. However, less accurate observations implies the existence of residual outliers whose systematic effects must be removed from the estimated parameters. An iterative strategy has been proposed by Chen et al. (1987) that removes only a single residual from the solution, recomputes the solution, and performs a new set of tests. This is the preferred approach because of the ill effects a residual outlier can have on the remaining residuals, due to the smoothing process of the least squares adjustment.

The statistic that must be computed for the testing is greatly simplified when no correlation between observations exist. A further simplification of the statistic into a standardized residual can be realized, when only the existence of a single residual outlier is being considered. The test has been labelled as the w-test in the literature and is given by the inequality in equation (4-8) (Chen et al. 1987).

$$| \hat{r} / \sigma_{\hat{r}} | \leq N_{1-\alpha/2} \tag{4-8}$$

where,

- N value of the Normal distribution, given a $1-\alpha/2$ probability
- $\sigma_{\hat{r}}$ expected standard deviation of the residual being tested
- α significance level of the test ($\alpha = 0.05$ corresponds to the 95% confidence level)

The residuals that do not satisfy the above inequality are flagged as being possible outliers. However, as only one outlier is being removed at a time, the residual with the largest statistic out of the flagged possibilities, is singled out as the observation to be removed. The computation of the statistic to be tested, requires the diagonal element of the expected variance-covariance matrix for the estimated residual, which may be computed using equation (4-9) (Wells and Krakiwsky, 1971).

$$C_{\hat{f}} = \sigma_0^2 (C_l - A (A^T C_l^{-1} A)^{-1} A^T) \qquad (4\text{-}9)$$

where,

$C_{\hat{f}}$ the expected variance-covariance matrix of the residuals

A successful post adjustment analysis of the residuals and estimated variance factor gives a substantial increase to the reliability of the solution (assuming a reasonable amount of redundancy).

The capabilities of removing and reobserving any outlying observations (residual outliers) should be part of the post adjustment process. Although all of the observations have been subjected to quality control, there still remains the possibility of some systematic effects in a few observations, which will not allow them all to fit together properly. The effects of these systematic errors must be removed from the estimated parameters by either complete removal or reobserving the outlying quantity, if it is a critical observation.

The preceding discussion can be summarized in step fashion, forming an algorithm and a flow diagram, which is illustrated in Figure 4.5. The steps outlined below have been implemented by the author in the development of P3DCS.

1. Choose the method of theodolite positioning to be performed and pass the program control to the data acquisition module (see section 4.2).
2. If only gathering data for an auxiliary adjustment program, return to the main program module.
3. If performing a resection obtain the fixed target coordinates from an auxiliary input file. If the positioning is a weighted adjustment, obtain the weighted target coordinates with the pertinent variance-covariance submatrix from the input file.
4. Compute all required approximate coordinates for the quantities to be estimated. A resection requires initial approximations to be computed for the theodolite coordinates. The weighted adjustment needs approximate coordinates for the theodolite locations and possibly some of the control targets, if densifying the control network. The bundle adjustment option requires initial approximations for

all target and theodolite (except the one being held fixed) positions. Initial approximations for the theodolite horizontal reference marks (ω) are not required, if they have been initialized close to the zero azimuth direction of the datum.

5. Populate the first design matrix (A), the variance-covariance matrix of the observables (C_l), and the misclosure vector (W). The constituents of the C_l matrix can be computed as illustrated in section 2.2, on random theodolite errors.
6. Perform the parametric least squares adjustment by iterating equations (4-3) and (4-4) to get the estimates for all of the unknown quantities.
7. Compute the estimated residuals ($\hat{r}$) from the adjustment using $\hat{r} = A\hat{\delta} + W$.
8. Compute the *a posteriori* variance factor using equation (4-6) and test it against the *a priori* value for compatibility using equation (4-7). If the test passes or fails on the right hand side of the inequality, exit the theodolite positioning module.
9. Compute the $C_{\hat{l}}$ matrix of the estimated residuals using equation (4-9).
10. Test the estimated residuals for outliers using equation (4-8) and flag the one with the largest statistic.
11. Either remove or reobserve the observation (if it is a critical observation) and return to step 5.

4.4 Auxiliary Target Computations and Surface Fitting

After the theodolites have been positioned in the work area, object target coordinates can be determined with a very high accuracy. This is due to the short observing distances combined with the placement of theodolites to optimize the geometry for new target coordinates. The newly computed values can be used to determine corrections, offsets, calibration values (e.g. mapping the movement of a robotic arm (Ackerson and Scott)), or a number of targets can be pooled together to determine surface discrepancies.

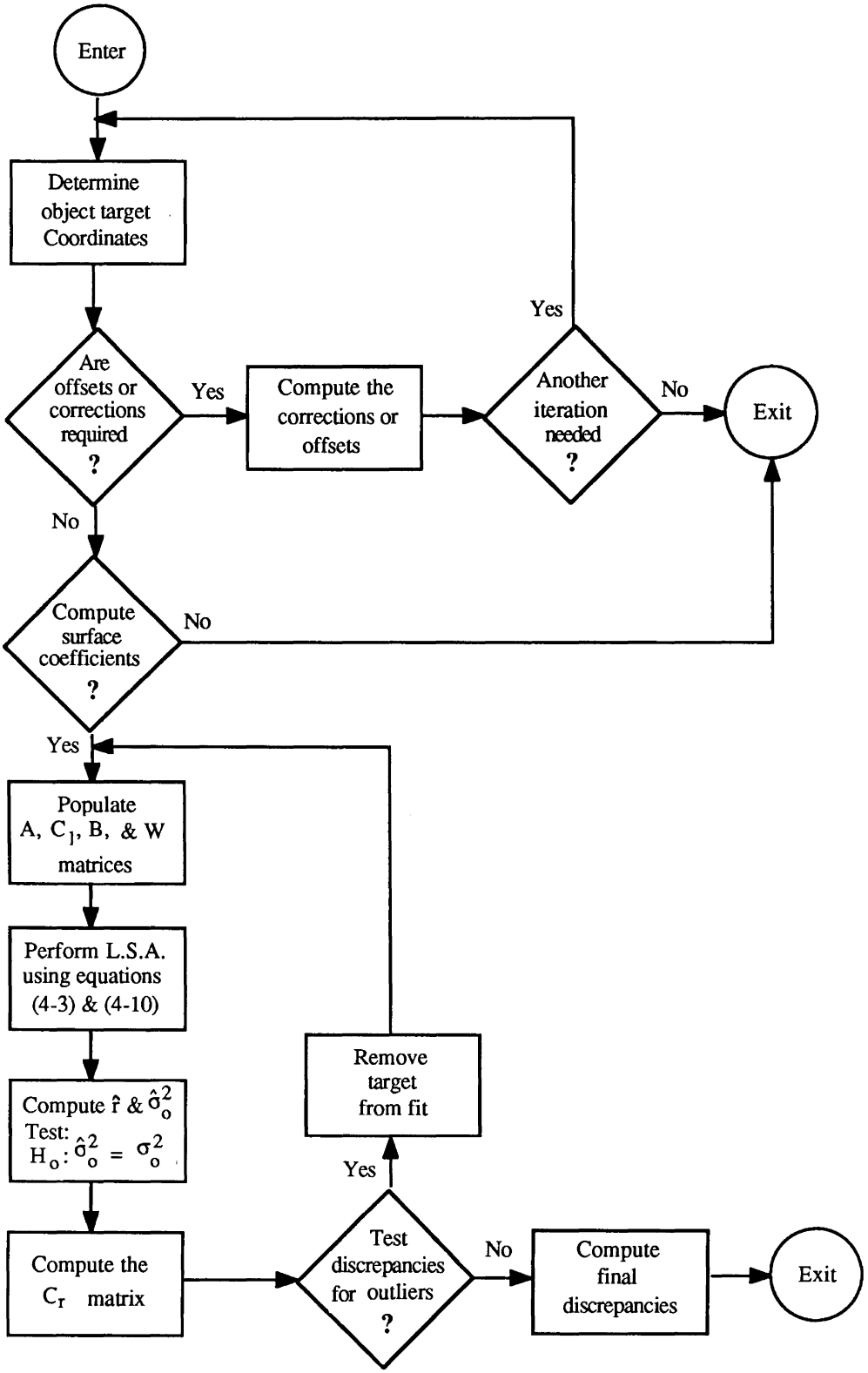

Figure 4.6 Flow Diagram of the Auxiliary Target and Surface Fitting Module

The requirements for this module depend entirely on the application projects. Therefore, it should be constructed with flexibility for interchanging some of the software routines, which would allow for the new needs that will be encountered when engaged in additional projects. A calibration survey is considerably different from a setting out survey and both are distinctly unlike a surface fit determination. However, the common link is that the applications are all based on coordinate values, which is the attribute that can be used to develop the module.

The method used for determining the coordinates is critical if optimum accuracies are to be obtained. Independent angles observed from a fixed control target are required to remove the circle orientation parameters that are inherent with horizontal direction measurements (see section 3.2). If only a single direction is observed (as with the Kern and Wild systems), this implies that the orientation parameter must come from the initialization at the beginning of the set up (i.e. that computed during the independent resections, bundle adjustment, or obtained from the collimation method) This value can change with time over the span of the session and if determined from an adjustment is just a mean value, which can easily have affects into the tenth of a millimetre over short range.

A group of object targets can be determined at one time, which would only require a single extra direction, for each theodolite, to a fixed control target. This would eliminate some of the extra pointings to fixed targets, but creates an additional concern if the object points are to be used in a surface coefficient determination. The correlations between all the coordinates estimated together in the group, would have to be accounted for in the estimation of the fit parameters. This could become very computationally cumbersome for a coordinating system, where as if each object target is determined separately, only the correlations between individual triplets have to be considered.

The determination of the surface fit parameters becomes an iterative procedure, due to the expectation that surface irregularities will exist and be larger than their expected standard deviations. The surface fit parameters and the observations are inseparable, hence,

requires the combined least squares adjustment to obtain estimates for the unknowns. The approach is identical to that described in the previous section for the parametric least squares adjustment, with the equation for computing the corrections to the unknowns ($\hat{\delta}$) (equation (4-4)) being replaced by equation (4-10) (Wells and Krakiwsky, 1971).

$$\hat{\delta} = -(A^T M^{-1} A)^{-1} A^T M^{-1} W \qquad (4\text{-}10)$$

where,

- A — matrix containing the partial derivatives of the observation equations with respect to the unknown parameters (first design or configuration matrix), dimensioned (m x u)
- $M = B\, C_l\, B^T$
- B — matrix containing the partial derivatives of the observation equations with respect to the observations (second design matrix), dimensioned (m x n)
- C_l — variance-covariance matrix formed from the determined accuracies of the object targets, dimensioned (n x n)
- W — vector containing the observation equations evaluated using the most recent parameter estimates and the coordinates of the object targets observed quantities (the misclosure vector), dimensioned (m x 1)
- u — total number of unknown parameters
- n — total number of coordinates (number of object targets x 3)
- m — total number of observation equations.

The observation equations that are used in the adjustment completely depend on the type of surface being analysed. There are no limitations as to what functions can be modelled, as long as enough object targets are available to obtain a good solution, with the geometrical considerations adequately satisfied. However, every different mathematical relationship will require its own separate program module for generating the two design matrices (A and B) and the misclosure vector (W).

The testing of the adjustment results follows the identical procedure as that described in the previous section. The *a posteriori* variance factor is computed using equation (4-6) with the degrees of freedom equal to the number of equations minus the number of unknowns (df = m - u). The expression for computing the estimated residuals ($\hat{r}$) from the combined method is given by equation (4-11) (Wells and Krakiwsky, 1971).

$$\hat{r} = - C_l B^T M^{-1} (A\hat{\delta} + W) \qquad (4\text{-}11)$$

The quadratic form of the residuals is tested using the global test on the variance factor as given by equation (4-7). A failure of the test on the right hand side of the inequality simply means that the object targets have fit together better, than what the expectation from the accuracy of the object target coordinates suggested they would. Conversely, if the global test fails on the left hand side of the equation, statistics are computed for each estimated surface discrepancy (not just individually estimated residuals) with the maximum statistic tested using the w-test for possibly being an outlier. However, the statistic is more complicated to compute due to the estimated discrepancies being tested and the existence of correlations between the coordinate triplets for each target. The estimated discrepancy associated with an object target may be computed from the residuals of its coordinate triplet using equation (4-12).

$$\hat{d}_i = (\hat{r}_x^2 + \hat{r}_y^2 + \hat{r}_z^2)_i^{1/2} \qquad (4\text{-}12)$$

where,

$\hat{d}_i$ is the estimated surface discrepancy for the i^{th} target

$\hat{r}_x$, $\hat{r}_y$, $\hat{r}_z$ the estimated i^{th} target residuals corresponding to the x, y, and z axes,respectively

The w-test when considering a single target being an outlier from uncorrelated target points is given by equation (4-13), where the left hand side of the equation represents the statistic for the estimated discrepancy being tested (Chen et al. 1987).

$$\hat{r}_i^T C_{\hat{r}_i}^{-1} \hat{r}_i \leq \chi^2_{df;1-\alpha} \qquad (4\text{-}13)$$

where,

χ^2 value of the Chi-square distribution, given a 1-α probability

$\hat{r}_i$ a subvector of the residuals containing $(\hat{r}_x, \hat{r}_y, \hat{r}_z)_i$ for the i^{th} target

$C_{\hat{r}_i}$ a submatrix of the estimated residual variance-covariance matrix corresponding to the i^{th} target

α significance level of the test ($\alpha = 0.05$ corresponds to the 95% confidence level)

df number of residuals being tested simultaneously (i.e. 3 for a single target)

i is the target number of the estimated discrepancy being tested

In contrast, if the coordinates of the target points have been determined together in a single group, the correlations between each target must be considered in the computation of the statistic for each discrepancy. The statisitc becomes much more complicated and is given by equation (4-14) (Chen et al. 1987).

$$\hat{r}^T C_l^{-1} E (E^T C_l^{-1} C_{\hat{r}} C_l^{-1} E)^{-1} E^T C_l^{-1} \hat{r} \leq \chi^2_{df;1-\alpha} \qquad (4\text{-}14)$$

where,

χ^2 value of the Chi-square distribution, given a $1-\alpha$ probability

$\hat{r}$ the vector of residuals for all targets

$C_{\hat{r}}$ the estimated residual variance-covariance matrix

C_l variance-covariance matrix for the coordinates of the object targets

E a matrix of 1's and 0's dimensioned (n x df) with each column containing a 1 in the row corresponding to one of the residuals being tested

α significance level of the test ($\alpha = 0.05$ corresponds to the 95% confidence level)

df number of residuals being tested simultaneously (i.e. 3 for a single target)

The variance-covariance matrix of the estimated residuals ($C_{\hat{r}}$) contained in the above statistics may be computed using equation (4-15) (Wells and Krakiwsky, 1971).

$$C_{\hat{r}} = \sigma_o^2 C_l A^T M^{-1} (BC_l - A (A^T M^{-1} A)^{-1} A^T M^{-1} BC_l) \qquad (4\text{-}15)$$

The discrepancy statistics that do not satisfy the inequality of (4-13) or (4-14) are flagged as being possible outliers. However, as only one outlier is being removed at a time, only the target associated with the largest discrepancy statistic is singled out to be removed,

before performing the new surface fit. The possibility does exist that all of the computed statistics will satisfy the inequality of (4-13) or (4-14) even though the global test failed.

The above procedure is repeated until the global test is passed or no individual discrepancy fails. The passing of the global test signifies the estimated parameters are statistically acceptable. In contrast, the failing of the global test with the passing of all discrepancies, means that although each estimated discrepancy is statistically acceptable, their combined effect in the surface fit is less accurate than what was expected.

This iterative approach must be applied to ensure that the best estimate of the true surface fit parameters is obtained, making the final estimated discrepancies give an accurate indication of the magnitude of the surface deviations. The final estimate of surface fit parameters is used to compute the final surface discrepancies for all of the object targets involved (including those that have been removed).

The following algorithm is a summation of the above discussion and the flow diagram illustrated in Figure 4.6. The steps outlined have been implemented by the author in the development of P3DCS. To date only the handling of the surface fitting for a plane and a circular paraboloid has been implemented in the package.

1. Determine the object target coordinates by using an angle measured from a fixed control target as the horizontal measurement.
2. If offset measurements, corrections, or etc. are required compute whatever values are needed. If the object has been moved, return to step 1 to redetermine the new coordinates for the object target or else exit this module.
3. If surface fit coefficients are required, populate the A, B, and C_l matrices and the W vector.
4. Perform the least squares adjustment using equations (4-3) and (4-10).
5. Compute the estimated residuals using equation (4-11) and the *a posteriori* variance factor with equation (4-6). Perform the global test given by equation (4-7).
6. Compute the $C_{\hat{f}}$ matrix for the estimated residuals using equation (4-15).

7. Compute the statistic for each discrepancy as given by the left side of equation (4-13) or (4-14) and test the maximum for being an outlier.
8. If an outlier exists, flag the target for removal from the surface fit and return to step 3.
9. Compute the final discrepancies for all targets using the final estimated surface parameters and return to the main module.

5. Positioning Components of the TASCC Linear Accelerator

5.1 Scope of the Project

In the fall of 1987, the Engineering Surveys Research Group at UNB entered into a research contract agreement to develop a methodology and perform high precision setting-out and alignment surveys, at the Chalk River Nuclear Laboratories of Atomic Energy of Canada Ltd. The project at CRNL involved the so called Phase II construction of their Tandem Accelerator Super Conducting Cyclotron ("TASCC").

The Phase I portion of the project, which had been completed previously with conventional optical tooling methods, involved positioning of the tandem accelerator, a beam path through various bending and focussing magnets, which allowed the charged particle beam to bypass or go through the super conducting cyclotron and finish at the bending magnet BE-1 (see Figure 5.1). Phase II, the subject of the contract agreement, involved the positioning of the residual accelerator components and was further subdivided into Phase IIA and Phase IIB. The Phase IIA was constructed entirely by the UNB team, while Phase IIB was contracted out to Usher Canada Ltd. with consultants from UNB. A schematic illustration of the entire TASCC accelerator is given in Figure 5.1.

The Phase IIA activities were to be carried out during a six month shut down of the accelerator, that when completed would make three new experiment areas available for research. The shut down was scheduled for January to July 1988 with the surveying activities to be performed during the month of February. Table 5.1 lists the elements that are involved in Phase IIA and Figure 5.2 displays their designed locations with respect to BE-1 (the completion of Phase I).

Table 5.1. Components of Phase IIA

QUADRUPOLES							
QE-3	A	B	C	QE-4	A	B	C
QE-5	A	B	C	QE-6	A	B	
QE-7	A	B		QE-8	A	B	
QE-9	A	B		QE-10	A	B	
QE-11	A	B		QE-19	A	B	C
QE-20	A	B	C	QE-21	A		
QE-22	A	B	C	QE-23	A		
QE-24	A	B	C				
DIPOLES							
BE-2				BE-2A			
BE-3				BE-4			
CONES TO ACCOMPANY SLITS							
SE-2				SE-3			
SE-4				SE-7			
SE-8							
FLOOR TARGET LOCATIONS							
T - 1				T - 2			
T - 3				T - 4			
T - 9							

Table 5.2. Components of Phase IIB

QUADRUPOLES							
QE-12	A	B		QE-13	A	B	
QE-14	A	B		QE-15	A	B	
QE-16	A	B	C	QE-17	A	B	C
QE-18	A	B	C	QE-25	A		
QE-26	A	B	C	QE-27	A	B	
QE-28	A	B					
DIPOLES							
BE-6				BE-7			
BE-8							
CONES TO ACCOMPANY SLITS							
SE-6				SE-9			
FLOOR TARGET LOCATIONS							
T - 5				T - 6			
T - 7				T - 8			
T - 9							

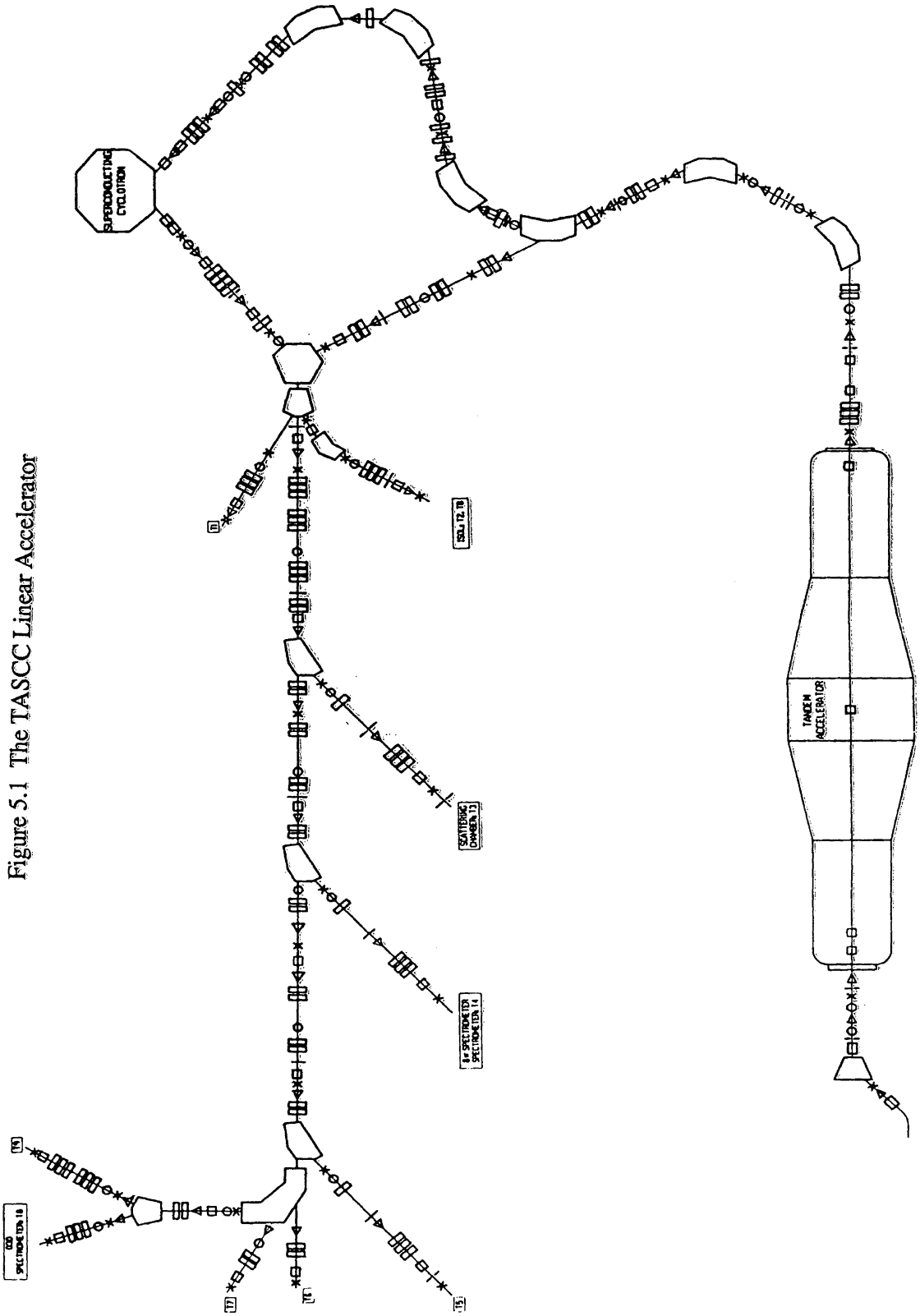

Figure 5.1 The TASCC Linear Accelerator

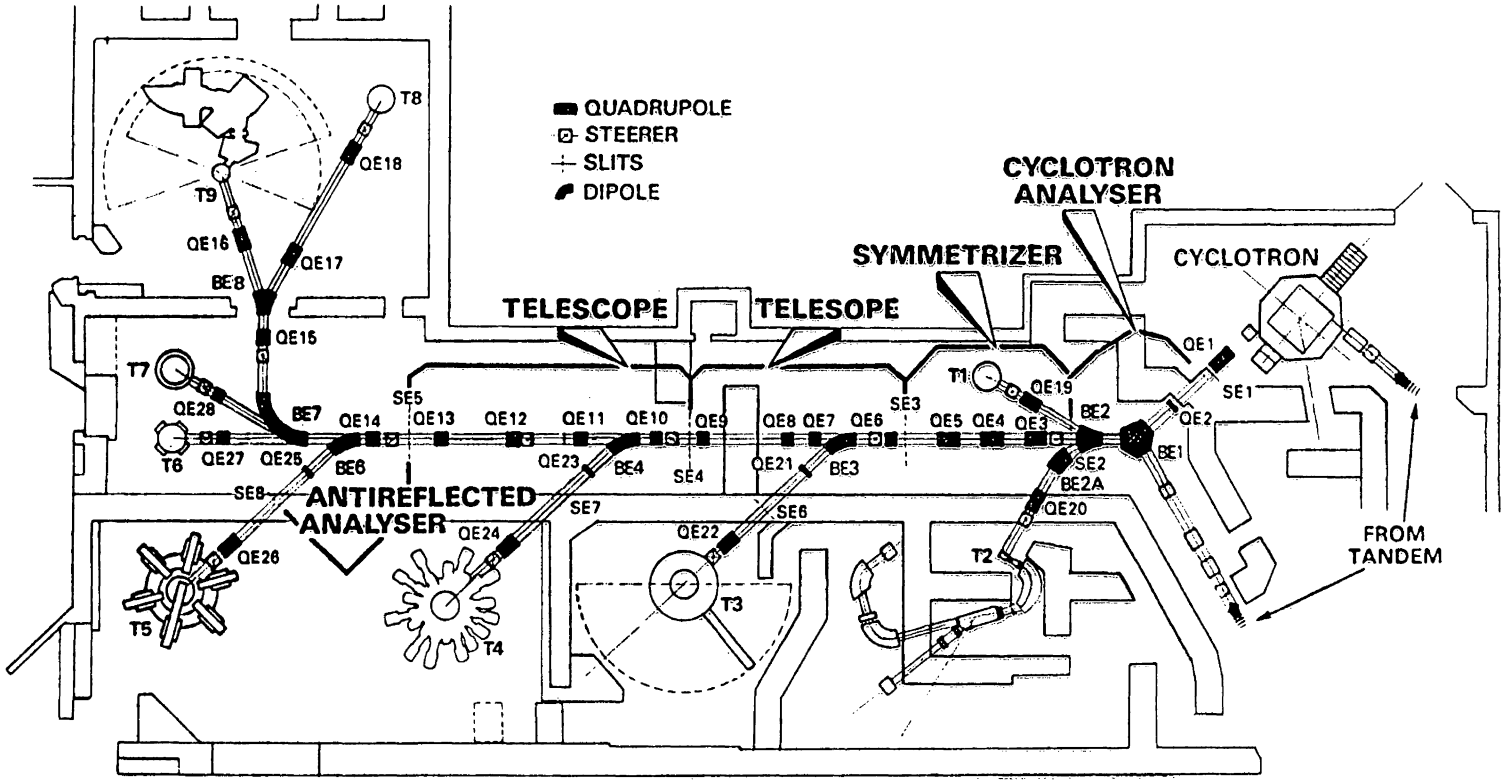

Figure 5.2 A Schematic Diagram of Phase II of TASCC (altered Davies, 1986)

The survey for Phase IIB was to be performed in August 1988 following the reactivation of the beam line at the conclusion of the shut down period, which resulted in a six month time differential between the surveys for the two subphases. The elements involved in the Phase IIB positioning are listed in Table 5.2 with Figure 5.2 illustrating their locations with respect to the focussing doublet QE-11 (the completion of Phase IIA).

The coordinating system ensembled at UNB (P3DCS) has been implemented in the setting out of both subphases of Phase II of the TASCC accelerator. The UNB system enabled the components of the accelerator to be positioned with the highest possible achievable accuracies, while maintaining a real time interaction. This phase of TASCC involved the setting out of 7 bending magnets (dipoles), ranging in mass from a few to almost 16 metric tons, and 60 much smaller focussing magnets (quadrupoles) to extend the primary beam delivery system and create many additional experiment areas.

The main requirement in positioning accelerator components is maintaining a smooth magnetic circuit throughout the entire length of the charged particle path (Gervaise, 1974). The charged particle beam passing through the smooth magnetic circuit created by the magnets or metal lenses is analogous to light rays passing through a series of glass lenses in an optical system. Any misalignment of one of the glass lenses forming the system creates a distorted image or possibly no image at all at the end of the system, but if all the optical lenses were misaligned with respect to their design, yet still retained their relative properties with each other a clear image would be formed. Carrying this over to the metal lenses illustrates that it is not the absolute positioning of each magnet that is important, but the relative accuracy between adjacent elements, especially those forming an operating unit such as a quadrupole doublet or triplet.

The specifications for the alignment of the components comprising Phase II were very stringent, requiring that the geometric centre of each element were positioned to no worse than 0.1 mm in both transverse directions and 0.2 mm in the longitudinal direction. Additional constraints to control the three possible rotations of each component have been

specified at no more than one minute of arc off the beam line design. Compounding the specification requirements was the need to be able to determine the magnitude of misalignment, in terms of the six degrees of freedom, in virtual real time to allow adjustments to be made without any long computational delays. The ability to determine corrections quickly in Phase IIA was imperative due to the time constraint imposed by the time allotted for surveying activities in the shut down schedule. These restrictions were made even more difficult by the realization that the extent of the portion of the accelerator being installed covered a total length of over 40 m and has branch lines extending into four additional enclosed experiment areas (see Figure 5.2).

The traditional methods of optical tooling involving the use of a horizontal alignment telescope, horizontal spirit ("machinists") level with 10" per division sensitivity, and a precision tilting level, were to be integrated with the more modern approach of the coordinating system to satisfy completely the specification criteria listed above. The optical tooling methods allow the magnitudes of the rotations to be determined by comparing measurements of two targets defining the main axis of the element, while the coordinating system can resolve the translations simply by determining coordinates of one of the main axis targets.

5.2 The Establishing of the Reference Geodetic Micro-network

The establishing of the geodetic micro-network was required to satisfy the two following conditions:

1. to create a reference for the design coordinates of the elements in the work area,
2. to facilitate locating the position of a theodolite, randomly set up in the work area, with respect to the design coordinates of the elements.

Both conditions were a direct result of the use of the coordinating system for the project, which applies three dimensional coordinate geometry to position theodolite stations and

object targets. If only traditional optical tooling methodologies were considered there would be no need to create the micro-network, but the translation components of the misalignment would be more difficult to obtain, especially in the longitudinal direction. Additional benefits of creating the micro-network were to obtain a rigorous error estimation of target locations, allow the placing of theodolites where "convenient", and to have a network of reference points for future checking and maintenance surveys.

The micro-network established at CRNL consists of an array of targets adhered to the concrete walls in both the main room housing the primary beam line and the experiment rooms containing the branch lines. In the main room the targets have been installed at approximately 2 m increments on the two walls parallelling the beam line, which are about 7 m apart, along the entire extent of the room. Figure 5.3 and Figure 5.4 give a plan view of the target locations and the actual observation schemes in the main room and the experiment rooms for Phase IIA and Phase IIB, respectively. At each increment an attempt to place two targets, at 3 m and 0.5 m above the floor, was made to guarantee a good working range of values for the height components. The experiment rooms did not have as stringent a control requirement as the main hall, therefore, for each room approximately 12 targets were placed around the experiment area at various heights. However, some consideration had to be given for the placement of a few of the targets, to facilitate the connection of the experiment and main rooms.

The targets themselves were the Wild adhesive type, which have a concentric circle pattern that culminates in a 0.3 mm diameter solid dot at the centre. The concentric circle target pattern was necessary due to the various oblique lines of sight that were used to observe the targets and to facilitate the simultaneous horizontal and vertical pointings that were performed. Brass plaques with a 5 mm thickness and having a surface area suitable to adhere the adhesive target and a name tag, were manufactured at CRNL and installed on the concrete walls at target locations.

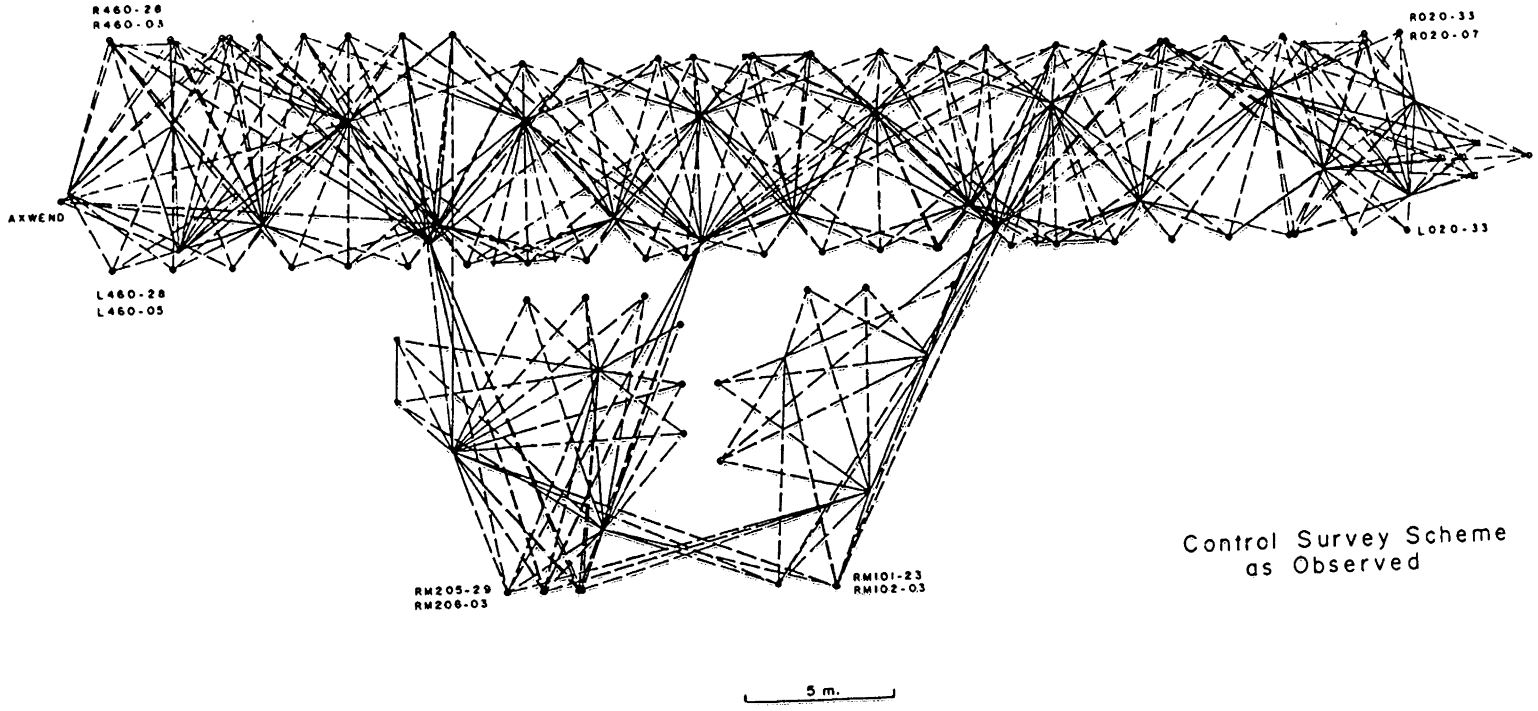

Figure 5.3 Observation Scheme for Phase IIA Control Survey (Secord et al. 1988)

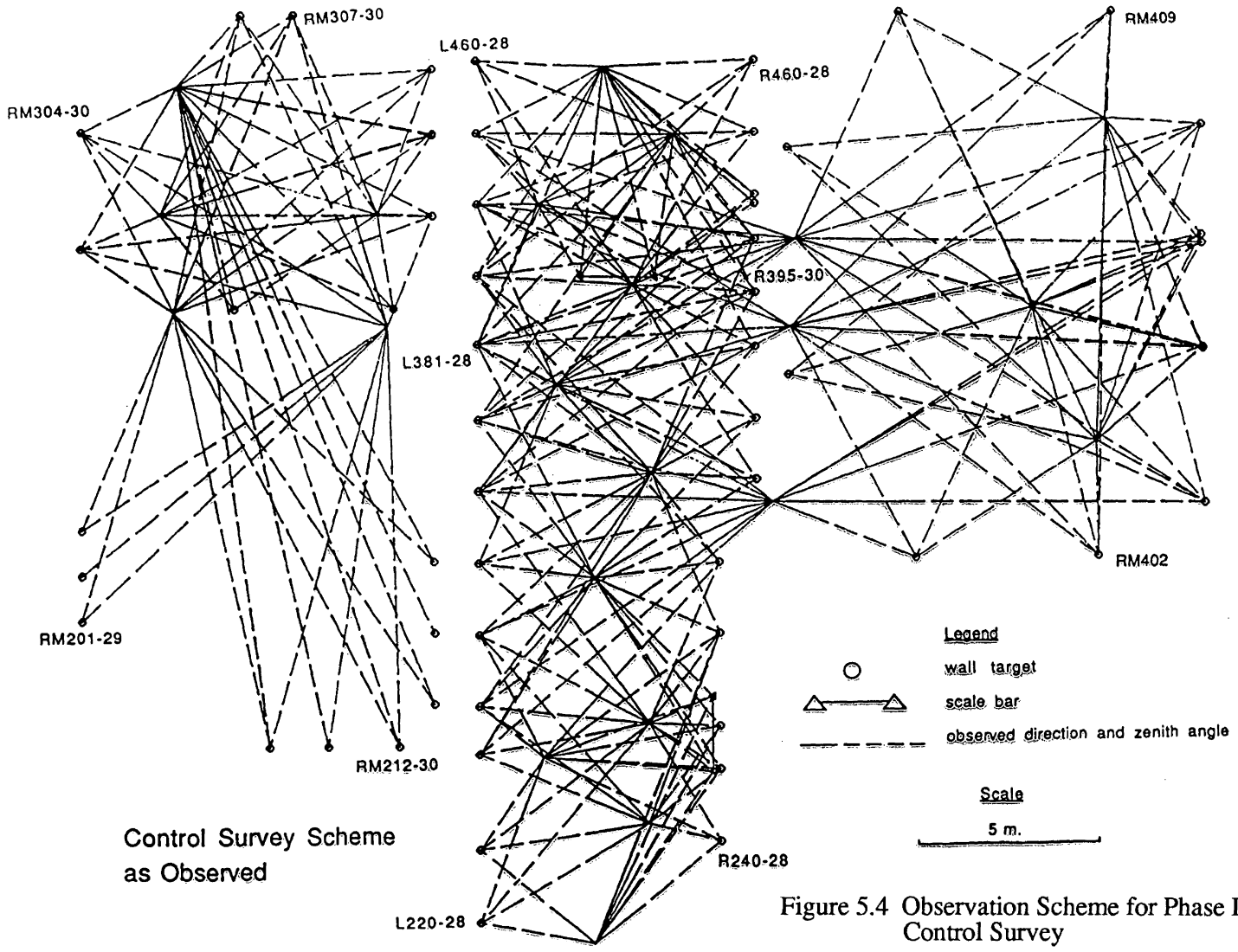

Figure 5.4 Observation Scheme for Phase IIB Control Survey

The definition of the datum for the network, as previously mentioned, was dependent on the definition of the design coordinates of the elements to fulfill the conditions stated above. All of the design coordinate values were with respect to the geometric centre of dipole BE-1 (labelled BE1-C in Figure 5.5 and designating the end of Phase I), which was defined by a dowelled hole in its bottom yoke that could be made accessible for targetting. Therefore, this becomes the logical choice for a fixed station that when the z axis is forced to coincide with the local gravity vector, defines the origin of a horizontal plane at the dictated beam line height (z coordinate) of 1.75260 m (69 inches) above the floor. An existing target ("AXWEND") located at the very end of the main room gave the direction for the designed horizontal path for the main delivery beam. This made that target very suitable to be used to create orientation in the horizontal plane of the micro-network by defining the x,z plane as the vertical plane passing through the geometric centre of BE-1 and the target AXWEND. The remaining y,z plane was defined as being perpendicular to both the horizontal and x,z planes to create a right handed cartesian system. Figure 5.5 illustrates the relationship between the coordinate axes and the primary beam line.

Describing the coordinate axes in this fashion creates one irregularity concerning the assumption of the gravity vector being straight and parallel throughout the CRNL facility. This will obviously not be the case as the extent of the main beam line covers an area of about 40 m in length. Neglecting this creates a maximum systematic deviation of 0.12 mm, at the extrema of the main beam line, between a spatial line and the equipotential surface defined by the level vials of the surveying instruments (see section 3.3.2). This deviation systematically accumulates with progression along the beam line, but had no affect on the relative smoothness between successive elements, which was the most important criteria for consenting to the neglect of this effect.

The only remaining datum defect in the triangulation micro-network is the lack of scale definition. The scale component was achieved by measuring directions and zenith angles to the targetted ends of two calibrated scale bars, designed and manufactured at

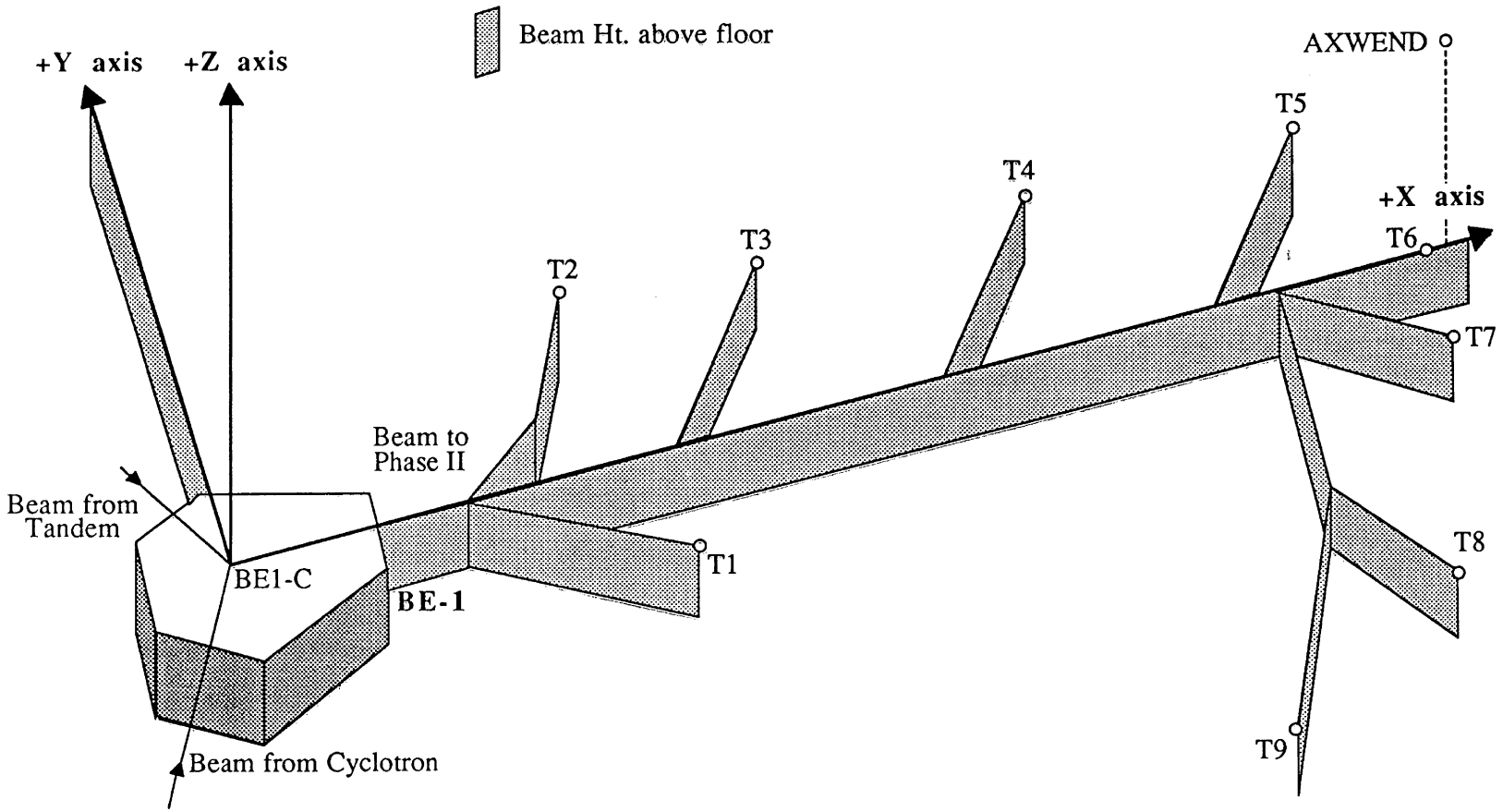

Figure 5.5 Datum Definition of the Control Network

UNB, that had been situated in different locations throughout the network. The lengths of the scale bars were treated as spatial distance observations with the targetted ends of the scale bars (for each location) observed in the same ways as the wall targets, with their coordinate triplets being estimated in the adjustment process. Each scale bar was approximately 2 m in length and made from 6 mm invar rod with targets, the same design as the Wild adhesive targets, attached to each end. The actual distance between a target pair on a scale bar was measured to a standard deviation of ± 0.01 mm, using an HeNe laser interferometer, by the Laboratoire de Métrologie, Département des Sciences Géodésiques et Télédétection, Université de Laval.

The error of ± 0.01 mm involved in the calibration of the 2 m scale bars transformed into a possible 5 parts per million (ppm) scale error in the coordinate determinations of the micro-network. This error would have a systematic effect proportionally increasing with distance away from the origin of the network (BE1-C), reaching a maximum value of 0.2 mm for the x coordinates in the far end of the main room. However, similar to the effects of the nonparallelity of the gravity vector, the relative accuracies between adjacent units would remain very high. This allows the smoothness between elements to be maintained, which again is the most important characteristic.

The observing of directions and zenith angles to the wall and scale bar targets was facilitated by the UNB coordinating system, using the data gathering mode, which has been described in section 4.3. This allowed data quality checks and station adjustments to be performed, in real time, to determine beforing leaving a particular set up as to whether all the data gathered was acceptable. The observing procedure and data quality checks used have been fully described in section 4.2. The method of triangulation without sighting between instrument stations, as described in section 3.4.3, was followed throughout the measurements to achieve the highest possible quality of angular measurements.

Table 5.3 Statistical Summary of Phase IIA Control Survey

Observables
- 591 Horizontal Directions (± 1")
- 591 Zenith Angles (± 1")
- 12 Spatial Distances (± 0.001 mm, artificial constraint*)
- 1 Azimuth (± 0.01", artificial constraint)

Unknown Parameters
- 477 Coordinates
- 51 Orientation (nuisance, associated with direction rounds)

667 Degrees of Freedom

The value 1.11 was estimated as the variance factor *a posteriori* and was found to be compatible at the 95% level of confidence with the value of 1.00 assumed *a priori.*

* The error of ±0.01 mm in the calibration of a scale bar has been considered as systematic and was not included in the error propagation of the adjustment.

Table 5.4 Statistical Summary of Phase IIB Control Survey

Observables
- 245 Horizontal Directions (± 1")
- 245 Zenith Angles (± 1")
- 4 Spatial Distances (± 0.001 mm, artificial constraint*)
- 1 Azimuth (± 0.01", artificial constraint)

Unknown Parameters
- 201 Coordinates
- 17 Orientation (nuisance, associated with direction rounds)

277 Degrees of Freedom

The value 0.563 was estimated as the variance factor *a posteriori* and was found to be not compatible at the 95% level of confidence with the value of 1.00 assumed *a priori,* which showed the observations on average were more accurate than 1 arcsecond.

* The error of ±0.01 mm in the calibration of a scale bar has been considered as systematic and was not included in the error propagation of the adjustment.

All of the observations were combined to perform a single simultaneous least squares adjustment to obtain estimates of the wall target triplets to be used in the setting out of the elements and subsequently in their maintenance. The standard deviation of ± 1" used for the directions and zenith angles was computed while taking a pessimistic view of the *a priori* error considerations discussed in section 2.2.2, to ensure that the propagated errors of the wall targets were realistic. The estimated coordinate triplets of the theodolite stations, scale bar targets, and orientation parameter for each round of observations are all considered nuisance parameters and may be mathematically removed from the estimation process if desired. A statistical summary for each of the two adjustments performed, Phase IIA and Phase IIB, are contained in Table 5.3 and Table 5.4, respectively.

5.3 The Setting Out of the Components

The procedures used for the setting out of the accelerator components was identical for both Phase IIA and Phase IIB. The coordinating system was integrated with traditional metrological methodologies to create redundancy, while hastening the set out times. The setting out can be broken down into targetting requirements, offset determinations, the coarse alignment, the fine alignment, and future maintenance considerations. A discussion of each of these topics is required to gain an understanding of how the project requirements were met.

5.3.1 Targetting of the Component Axes

A very complex targetting problem was involved in defining the primary axis of the quadrupoles to be positioned, which was the axis that had to be aligned with the designed beam path. For a quadrupole this was an intangible axis and was defined as being the geometric centre created by the 4 magnetic poles. Figure 5.6 shows the configuration of the

magnetic poles of a quadrupole and illustrates the complexity of the targetting problem. However, the magnetic poles have been machined to very high tolerances, which means this intangible axis could be created by machining an apparatus with the proper aperature to fit snugly against the poles. A nylon collar, manufactured by CRNL for this purpose, was equipped with a nylon disc containing the Kern burnished concentric circle target design. The centre of the Kern target was placed to coincide with the machined centre of the machined disc using a microscope. Again, the concentric design of the targets was required because of viewing from oblique lines of sight. This targetting system allowed the tangible targetting of the intangible axis, which when tested for centricity, deviated by no more than 0.02 mm.

The targetting problem was much simpler for the dipoles, as the referencing of the axes was considered and marked during the construction of each unit. The horizontal axes (bending magnet has at least 2 horizontal axes) were defined by 3 mm diameter dowel holes that have been drilled with a specification of ±0.1 mm maximum deviation from the true axes. The holes were located along the axes in the bottom yoke of the magnet, of which the centre of the beam path was to travel over by exactly 18 mm. Therefore, an omnidirectional conical target, according to UNB's design, was precision machined by CRNL to fit in the dowel holes. This defined a vertical reference plane of 18 mm, which fulfilled the requirements for determining the primary axes of the dipoles. Figure 5.7 shows the design of the conical target.

5.3.2 The Offset Measurements for the Quadrupoles

The offset determinations were required for the quadrupoles to obtain the relationship, in the design reference system, between two axial targets (see section 5.3.1) inserted tightly against the front and back faces of the poles. The knowledge of this relationship enabled the designed coordinates of the geometrical centres of the quadupoles

to be transferred to either of the two targets located on the outside face of the poles, by knowing the designed orientation of the quadrupole. However, this required the assumption that the geometric centre of the quadrupole was actually the midpoint between the two axial targets.

A quadrupole located on the main beam line had only one offset, which was in the along beam direction (x axis of the control network). The amount of the offset was equal to half the magnitude of the vector between the two axial targets inserted in either side of the quadrupole. A quadrupole located on a branch line required that this offset value be resolved into two orthogonal components, corresponding with the x and y axes of the control network. The resolution into components was controlled by the angle that the branch beam line made with the main beam line.

The determination of the magnitude of the vector was performed separately in a two stage process. Firstly, by resecting two theodolites in the work area to the wall targets and subsequently determining coordinates for the front axial target of a quadrupole by intersections. Secondly, the theodolites were repositioned on the back side of the quadrupole, where coordinates for the back axial target could be obtained by intersection, without disturbing the quadrupole. Figure 5.8 illustrates all four theodolite locations required to determine the offsets for a single quadrupole. Offsets for 5 or 6 quadrupoles could be determined at one time, when the process was performed using a stable support so the magnets would not move during the entire procedure. The magnitude of the vector joining the geometric centre with one of the axial targets ranged between $\pm$ 0.2 mm, from the overall mean value, for all the quadrupoles with most being less than $\pm$ 0.1 mm.

In addition to the vector joining the axial targets, the coordinates to an omnidirectional conical target, with the same design as that used for defining the dipole axes, inserted in a dowel hole in the front top plate of the quadrupole (see Figure 5.6) were determined. These coordinate values were reduced to offsets with respect to the geometric

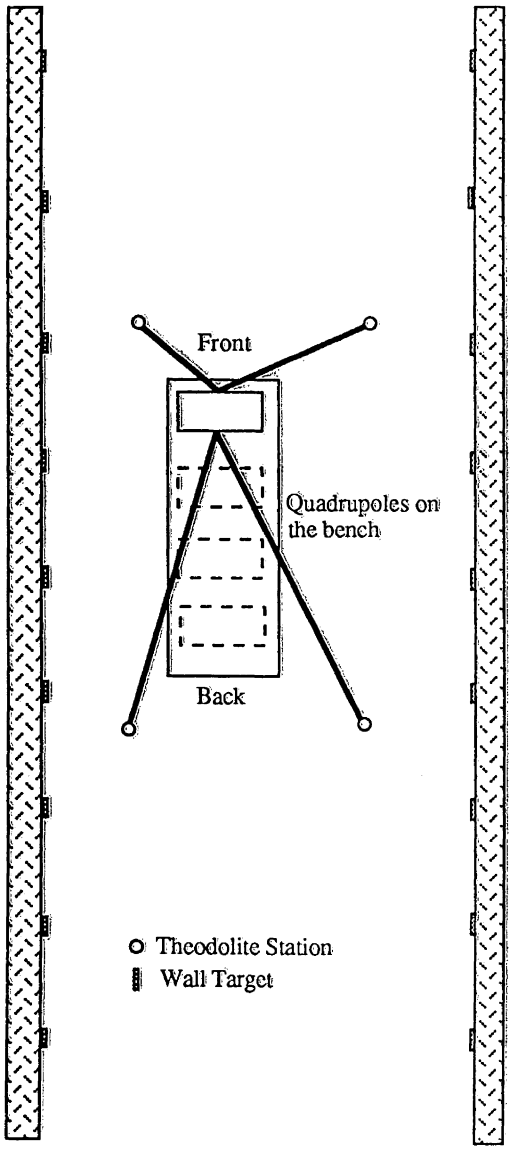

Figure 5.8 Theodolite Locations for Quadrupole Offset Determinations

centre of the quadrupole, which will be used in the future maintenance of the TASCC system (see section 5.3.5).

5.3.3 The Coarse Alignment

When the magnets were positioned to within the specifications of their nominal locations the quadrupoles were supported on stands and the dipoles on concrete pedestals. This implies that a coarse alignment had to be performed, which simply involved setting out of the supports to within the working range of the fine adjustment mechanisms (± 5 mm), for both the quadrupoles and the dipoles.

The quadrupole support stands were manufactured in the CRNL shops from special pressure treated steel to ensure that no load deformation in the location of the positioned elements would occur, once in place. The stands themselves were scribed in the machine shop with reference lines enabling them to be properly oriented and set to within the specified distance along the beam line very easily. The procedure simply involved an alignment telescope for horizontal orientation, tilting level for the vertical orientation, and a steel tape for the distance along the beam line. Once aligned, the stands were bolted to the floor, their alignment rechecked, and if found satisfactory they were grouted in place for stability.

The dipoles required concrete pedestals for stability due to their enormous bulk and critical locations (the bending points of the beam line). The coarse alignment consisted of positioning the forms for the poured concrete and the anchor bolts, for securing the tubular steel support base for the dipole. A steel plate, the same shape as the pedestal, was scribed with lines representing the beam axes and had holes drilled in it describing the required bolt pattern with respect to the beam axes. The plate was aligned with respect to the designed location of the beam axes, which gave the positions of the pedestals and the appropriate

bolt pattern orientation. This portion of the coarse alignment was considered part of the construction and was performed by CRNL with their own staff on site.

5.3.4 The Fine Alignment

The fine adjustment was very similar for both the quadrupoles and dipoles, incorporating an iterative procedure to converge to within the specifications for their nominal locations. The instrumentation used for the traditional metrology procedures employed a Kern DKM2-A single second optical mechanical theodolite with a parallel plate micrometer, a Wild N3 precision tilting level, and a machinist's horizontal spirit level with 10"/division sensitivity. As previously described, the coordinating system was comprised of two Kern E2 electronic theodolites interfaced to a Macintosh Plus microcomputer.

For the coordinating system, the electronic theodolites were located around the element to be set out in a way that optimized the intersection geometry and created average sight distances of approximately 5 metres. A typical instrument set up showing the redundant resections and the locations of the electronic theodolites with respect to the element is shown in Figure 5.9. Two sets of direction measurements to 8 to 10 control targets were performed for each resection, in an attempt to randomize the effects of the control target errors.

For the traditional methods, the DKM2-A was used as a horizontal alignment telescope, which required it to be located in the vertical x,z plane defined by the designed beam line. For the main beam line, this was accomplished using an iterative measurement of the included angle (near 180 degrees) procedure (Chrzanowski, 1983). This method could be utilized because of the accessibility of the end targets at BE1-C and AXWEND, which defined the extremes of the beam line as well as the datum for the control network (see section 5.2). For the branch lines, the beam line was defined by the targets inserted in the dowel holes that were located in the bottom yoke of the relevant dipole, that had already

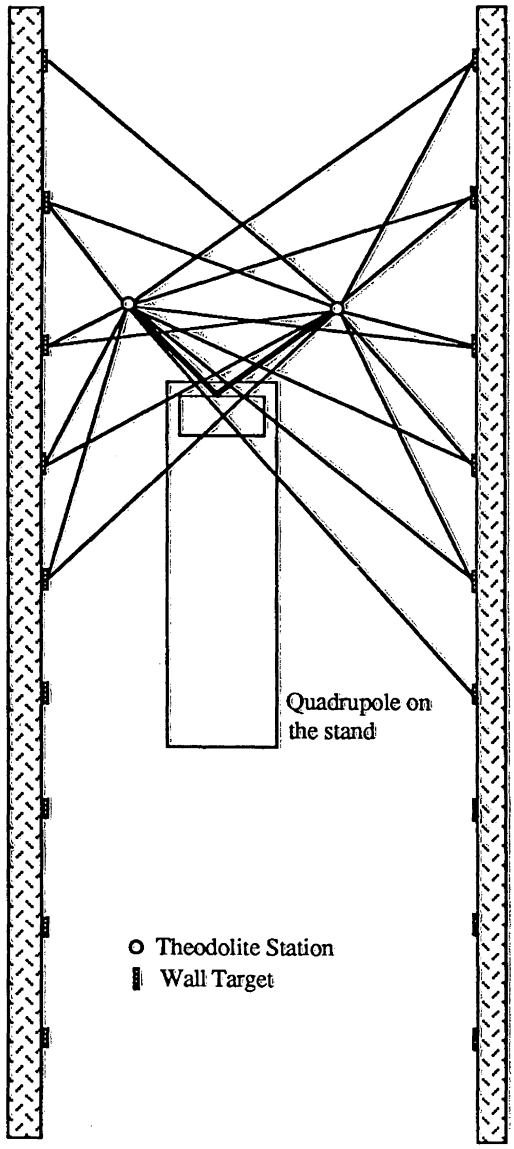

Figure 5.8 Typical Theodolite Locations for the Setting Out Survey

been set out on the main line. Therefore, the DKM2-A had to be brought on line by an iterative extrapolation of the direction given by the inserted targets.

For both the dipoles and quadrupoles, the design of the fine adjustment mechanisms were conducive to allowing the horizontal and vertical adjustments to be segregated in the setting out procedures. The four vertical adjustment bolts (a ball and cup assembly) for a quadrupole, were located in the centre of each side of the base plate. The bolts were machined with a ball at one end, which fit into a cup that was fastened securely to the quadrupole stand. The quadrupole could be raised or lowered, rotated around the beam line, and rotated along the beam line, simply by threading the appropriate bolts in/out of the base plate. The five horizontal adjustments were located beside the vertical bolts for the front and both sides, while the back contained two horizontal adjustment screws located outwardly towards the sides of the base plate. The horizontal adjustment mechanism is the same as that for the vertical, except that the screws are threaded through a block of metal that has been fixed to the top of the base plate into cups that are no longer stationary, but push against the quadrupole. The remaining three degrees of freedom could be adjusted by backing off the adjustments on one side while tightening the appropriate ones on the opposite side.

For the dipoles, the tubular supports securely bolted to the pedestals contained all of the adjustment mechanisms for adjusting them. The dipole itself rested on three small brass plaques, whose heights could be controlled by large diameter finely threaded bolts, machined with a ball on one end, that were attached to the tubular supports. The dipole could be raised or lowered, rotated around the beam line, and rotated along the beam line, simply by threading the appropriate bolts in/out of the tubular support. Two square brackets, located on either end of the support, were used for the horizontal adjustments. Each bracket contained four screws that were positioned perpendicular to each other in the horizontal plane, which were oriented to allow movement in the transverse and longitudinal incoming beam line directions. The remaining three degrees of freedom could easily be

removed by pushing the screws against metal blocks that were securely fastened to the dipole and fit into the square brackets.

Each quadrupole was guided into its nominal location by integrating the traditional optical tooling methods with the coordinating system and following the procedure listed below.

1. Removal of rotation about the beam axis (x axis) by the horizontal machinist's (spirit) level placed on the forward horizontal top plate of the quadrupole (see Figure 5.6). A special adaptor and rotatable mirror assembly was designed by UNB to allow the placing of the level on the front plate and to facilitate the viewing of the vial.
2. Removal of the forward/backward rotation (y axis) by sighting the two axis targets using the Wild N3 (reference plane is created by initially sighting a conical target inserted in a dowel hole of an already set out dipole).
3. Removal of the z translation by paired intersections to one of the axis targets from the two resected Kern E2 theodolites.

Steps 1, 2, and 3 were repeated until all three discrepancies were eliminated.

4. Removal of the along beam line translation, which is along the x axis on the main beam line, by paired intersections to one of the axis targets from the two resected E2 theodolites, with the required offsets applied (see section 5.3.2).
5. Removal of the rotation about the z axis through horizontal transverse alignment using the Kern DKM2-A, which has been brought on line using one of the appropriate methods, as discussed above.
6. Removal of the translation transverse to the beam line, which is the y translation on the main beam line, by paired intersections to one of the axis targets from the two resected E2 theodolites. The branch lines required an offset to be applied to remove the y translation(see section 5.3.2).

Steps 4, 5, and 6 affect the results of steps 1, 2, and 3. Hence, all six steps were repeated until all six discrepancies were negligible.

For the setting out of the dipoles, steps 1, 2, and 3 above can be replaced with the following:

1.& 2. Removal of the rotation about the beam axis (x axis) and along the beam axis (y axis) by the horizontal spirit level positioned on the bottom yoke, to use the three height adjustment screws in the same fashion as leveling the vial of a theodolite.

3. Removal of z translation by paired intersections to an omnidirectional conical target placed in an on axis dowel hole on the bottom yoke.

A final set of intersections were made to the axis targets and derived discrepancies were compared with those obtained from the optical tooling instrumentation. Excessive differences were investigated until they could be resolved. Any further adjustments led to additional intersections until all discrepancies and differences were negligible.

The coordinating system itself was capable of determining the coordinate triplets of the axial targets, however, the Wild N3 and Kern DKM2-A provided redundancy for the z and y translations respectively, ensuring reliable results. Appendix I contains the computed discrepancies between the designed coordinates and those determined by the coordinating system in the setting out, for both Phase IIA and Phase IIB. Figure 5.11 illustrates a portion of the already aligned beam line after all of the hardware has been installed.

5.3.5 The Maintenance of the System

Once the TASCC accelerator components had been positioned to their nominal locations, a system had to be devised to permit the checking and relocating of the element positions in the future. The poles forming both the quadrupoles and dipoles will no longer be accessible for targetting once the beam line is commissioned, primarily due to the

insertion of vacuum tubes that are required for the beam. In addition, the centre element of a quadrupole triplet has both its axial targets blocked from view, for the oblique lines of sight required by the coordinating system, by the two remaining members of the triplet.

The inaccessibility problem could be overcome by placing accessible targets on the side walls of each individual element and determining their vector relationship with respect to the element's geometric centre. For a quadrupole, two Wild self adhesive targets were adhered to opposite sides of the frame (see Figure 5.6), to create as long a baseline as could be observed using the coordinating system. The targets, called "wing targets", were tied to the reference control network using triangulation, which gave their position with respect to the already set out position of the element (see section 5.3.4). The same procedure was used for a dipole with a third adhesive target replacing the conical target. The "wing targets" combined with the vertical offset of the conical target previously determined, can be used to eliminate all the degrees of freedom involved in the repositioning of an element.

The "wing targets" combined with the array of wall targets forms the maintenance system that can be used to check and reposition any element in the TASCC system in the future. However, as the setting out was done using coordinate determinations the maintenance scheme itself is centered around being able to redetermine the "wing target" values. This could be a very time consuming process for a routine inspection of all the elements or if a group of elements are suspect to deformation.

The placement of the "wing targets" on the quadrupoles was done with particular attention being taken to ensure that the targets were located at the same height on each element, at least within the working range of a precision level's micrometer (10 mm). This enables a quick relative check to be performed, independent of the wall targets, utilizing the height differences between the "wing targets" determined initially. In addition, during the setting out procedure, the front top plate of each quadrupole was levelled, in the direction transverse to the beam line, using a precision machinist's level. This creates another

independent check as to whether an element has moved nonuniformly in the vertical, simply by monitoring the amount of mislevelment of this plate.

If the position of an element is to change, it is highly unlikely that it would occur in only the horizontal location without affecting the vertical component. Therefore, the above independent checks can be relied on very heavily to detect or confirm any changes that may be occurring in element positions. However, because the quick check methods rely solely on vertical changes, they are limited to being able to detect movements and cannot be used by themselves for readjusting an element. The use of the coordinating system is the only recourse for repositioning an element once it has been detected as being unstable or is being reinstated after repairs. The quick checks can be used to provide a degree of redundancy for the vertical in the repositioning.

5.4 The Stability of the Micro-Network

The stability of the micro-network for both the short and long terms is very important. The short term stability was imperative to maintain the same reference datum for all of the setting out procedures ensuring that the relative smoothness of the entire system is maintained. The long term stability is required to allow future monitoring of the element positions as well as removal and reinstallation without sacrificing any of the relative smoothness obtained in the initial installation.

The main frame of the portion of the building housing the TASCC accelerator was constructed in the 1940's. Canadian specifications for nuclear facilities are very stringent requiring very thick poured concrete walls and floors, with reinforcing steel and without dilatation gaps. This creates a very sound structure with some of the interior and exterior walls approaching a thickness of 4 feet, and such are the walls where the targets forming the micro-network have been installed.

The expectation was that the short term stability would be guaranteed due to the enormous bulk of the structure. However, an attempt to improve wall target triplets and enhance their accuracies by combining network and set out observations, carried out over a time span of a month, into a single simultaneous adjustment for Phase IIA results in discrepancies between estimated results from the initial and combined adjustments. The discrepancies, contained in Appendix II, show a systematic decrease with accumulated distance from the origin for the two horizontal coordinates for each target. The changes are up to a maximum of 0.32 and 0.06 mm for the x and y axes respectively, which transforms into a suggested scale change of -7 ppm.

The scale bars themselves were only introduced to determine scale during the original network survey, therefore, any scale error contribution by them could not possibly be seen in the results of the combined adjustment. Assuming the above discrepancies are scale related and elimination of the scale bars as the reason, leaves the only other possibility that the wall targets themselves have moved. The systematic contraction of an entire wall to duplicate a scale change points to the suspicion of the walls being affected by thermal expansion, which is further substantiated because no dilatation gaps exist.

The coefficient of thermal expansion for concrete is given as $1x10^{-5}/C^{o}$ which means to create a -7 ppm scale change the walls would only have to undergo an average change in temperature of -0.7 C^{o}. During the setting out survey, which was performed during the on going construction, the outside and inside temperatures differed by 10's of C^{o} resulting in large temperature fluctuations when construction materials were brought inside, by opening the entrance from outside. On numerous occasions the setting out had to be halted to allow the temperature to stabilize as it affected both instrumentation (compensators in theodolites) and lines of sight (refraction). The long term effect on the concrete walls of these short term temperature fluctuations is difficult to determine, but clearly with such large temperature differences the effect cannot be considered negligible. The long term effects of the continually large outside and inside temperature differential will

Table 5.5 Displacements and Error Ellipses (95%) for XY Plane

Station	Dx (mm)	Dy (mm)	Total Disp (mm)	Az of Disp (deg.)	a (mm)	b (mm)	Az of a (deg)	To Ellipse Periphery (mm)	
L220-28	-.20	.17	.26	310.6347	.36	.19	296.5963	.34	*
L240-28	-.10	.19	.22	332.1854	.32	.17	298.2210	.24	*
L266-28	-.09	.22	.23	338.4848	.28	.12	306.2388	.19	**
L280-28	-.05	.14	.15	339.4244	.25	.11	308.8037	.18	*
L300-28	-.02	.04	.04	332.4126	.22	.11	319.0799	.20	
L320-28	.03	.04	.05	31.0427	.21	.10	331.4671	.11	*
L340-28	.03	.06	.07	27.8510	.20	.08	343.3551	.11	*
L360-28	.00	-.02	.02	171.3245	.21	.08	358.6058	.20	
L381-28	.02	-.10	.11	170.1925	.21	.09	16.8148	.15	*
L400-28	-.03	-.11	.12	195.4373	.22	.10	30.0315	.19	*
L420-28	.06	-.13	.14	156.0500	.25	.11	42.8898	.12	**
L440-28	.05	-.13	.14	158.9996	.28	.12	51.7062	.13	**
L460-28	.05	-.01	.05	98.7221	.33	.14	57.1745	.19	
R240-28	-.20	.00	.20	270.8940	.27	.07	87.9290	.27	*
R260-28	-.14	-.12	.19	228.8983	.23	.09	84.4119	.14	**
R260-03	-.13	-.01	.13	266.8372	.24	.08	83.4635	.24	*
R272-28	-.10	-.13	.17	218.0738	.21	.09	84.1698	.11	**
R300-28	-.07	-.19	.20	199.7154	.17	.09	71.8490	.11	**
R300-03	-.04	-.06	.07	212.3871	.17	.11	73.1472	.13	*
R320-28	.00	-.20	.20	180.9340	.14	.09	38.3084	.12	**
R343-28	-.04	-.09	.10	202.6107	.18	.08	8.4508	.16	*
R343-03	.05	-.07	.09	144.4088	.18	.08	8.4345	.11	*
R360-28	.01	-.05	.05	166.9789	.17	.08	354.7478	.16	
R380-03	.11	.02	.11	78.3442	.17	.09	342.0523	.09	**
R395-30	-.04	.05	.06	322.8777	.18	.10	326.0013	.18	
R410-30	.03	.05	.06	29.8312	.18	.10	303.8460	.10	*
R422-03	.07	.01	.07	85.9098	.19	.10	288.6139	.17	*
R422-28	.01	.05	.05	15.8400	.20	.11	291.0354	.11	*
R440-28	.04	.08	.09	22.8851	.24	.12	285.8424	.12	*
R460-28	.02	.08	.08	11.7912	.30	.13	283.1263	.13	*
R460-03	.06	.00	.06	89.2711	.30	.06	278.8944	.24	

Table 5.6 Displacements and Error Ellipses (95%) for XZ Plane

Station	Dx (mm)	Dz (mm)	Total Disp (mm)	Az of Disp (deg.)	a (mm)	b (mm)	Az of a (deg)	To Ellipse Periphery (mm)	
L220-28	-.20	.01	.20	272.5277	.33	.07	273.1297	.33	*
L240-28	-.10	.01	.10	274.2765	.29	.06	272.7677	.29	
L266-28	-.09	.00	.09	269.0327	.24	.04	274.5027	.20	*
L280-28	-.05	-.08	.09	214.8248	.21	.06	276.3756	.07	**
L300-28	-.02	-.10	.10	192.2721	.17	.06	276.2105	.06	**
L320-28	.03	-.09	.09	163.8526	.13	.06	281.2370	.07	**
L340-28	.03	-.06	.07	153.4526	.10	.06	287.5015	.07	*
L360-28	.00	-.03	.03	174.1309	.08	.06	297.1403	.06	*
L381-28	.02	-.02	.03	135.5085	.10	.06	270.2117	.07	
L400-28	-.03	.05	.06	327.9714	.14	.07	87.2375	.08	*
L420-28	.06	.11	.12	27.2908	.19	.08	85.4002	.09	**
L440-28	.05	.12	.13	21.9207	.24	.08	86.1432	.09	**
L460-28	.05	.18	.19	16.1323	.29	.09	84.8182	.10	**
R240-28	-.20	.09	.22	294.3081	.27	.07	276.1988	.18	**
R260-28	-.14	.10	.17	306.7311	.23	.07	275.5686	.12	**
R260-03	-.13	.00	.13	269.2616	.24	.03	83.6689	.19	*
R272-28	-.10	.13	.17	321.0372	.21	.07	274.2831	.09	**
R300-28	-.07	.16	.17	336.9482	.16	.06	275.9801	.07	**
R300-03	-.04	.02	.04	295.6190	.17	.06	77.7170	.09	*
R320-28	.00	.23	.23	359.1860	.12	.06	279.7472	.06	**
R343-28	-.04	-.01	.04	252.4809	.08	.07	278.9265	.08	*
R343-03	.05	-.14	.15	159.4006	.10	.07	36.0527	.08	**
R360-28	.01	-.04	.05	165.0424	.08	.06	71.1321	.06	*
R380-03	.11	-.10	.15	132.2967	.11	.08	310.5613	.11	**
R395-30	-.04	-.10	.11	199.5862	.13	.06	81.1802	.07	**
R410-30	.03	-.06	.06	153.3566	.16	.05	85.5805	.06	**
R422-03	.07	-.06	.09	127.5564	.20	.08	288.2726	.16	*
R422-28	.01	-.02	.02	141.2909	.19	.05	88.6579	.07	
R440-28	.04	.00	.04	83.3748	.24	.03	88.9969	.20	
R460-28	.02	.10	.10	9.2210	.30	.07	87.7585	.07	**
R460-03	.06	.04	.07	56.4980	.31	.07	285.5449	.09	*

Table 5.7 Displacements and Error Ellipses (95%) for YZ Plane

Station	Dy (mm)	Dz (mm)	Total Disp (mm)	Az of Disp (deg.)	a (mm)	b (mm)	Az of a (deg)	To Ellipse Periphery (mm)	
L220-28	.17	.01	.17	87.0552	.24	.06	81.5810	.22	*
L240-28	.19	.01	.19	87.7408	.22	.05	81.4741	.20	*
L266-28	.22	.00	.22	90.3813	.19	.04	84.6648	.17	**
L280-28	.14	-.08	.16	118.3520	.18	.06	80.8877	.09	**
L300-28	.04	-.10	.10	157.3974	.18	.06	82.5569	.06	**
L320-28	.04	-.09	.10	154.3102	.19	.06	82.7692	.06	**
L340-28	.06	-.06	.08	136.6028	.19	.06	83.0202	.07	**
L360-28	-.02	-.03	.04	213.9678	.21	.06	81.7430	.08	*
L381-28	-.10	-.02	.11	260.0203	.20	.06	82.8429	.20	*
L400-28	-.11	.05	.12	293.8184	.20	.06	80.6185	.10	**
L420-28	-.13	.11	.17	310.7261	.20	.07	77.5866	.08	**
L440-28	-.13	.12	.18	313.6488	.20	.07	78.8976	.09	**
L460-28	-.01	.18	.18	357.4592	.22	.08	77.1679	.09	**
R240-28	.00	.09	.09	1.9787	.08	.07	327.4296	.08	**
R260-28	-.12	.10	.16	310.5423	.10	.06	299.9482	.10	**
R260-03	-.01	.00	.01	256.8704	.09	.03	74.0669	.09	
R272-28	-.13	.13	.18	314.0878	.10	.06	297.6023	.09	**
R300-28	-.19	.16	.24	310.1013	.11	.06	286.6102	.09	**
R300-03	-.06	.02	.06	286.9180	.12	.06	70.8029	.09	*
R320-28	-.20	.23	.31	318.9266	.13	.06	284.5569	.08	**
R343-28	-.09	-.01	.09	262.5104	.18	.06	280.2000	.14	*
R343-03	-.07	-.14	.15	207.7071	.19	.07	70.0523	.10	**
R360-28	-.05	-.04	.07	229.1199	.17	.06	278.5514	.07	*
R380-03	.02	-.10	.10	167.2253	.17	.07	67.5462	.08	**
R395-30	.05	-.10	.11	154.8222	.16	.06	279.6568	.07	**
R410-30	.05	-.06	.08	138.8164	.13	.05	277.8847	.07	**
R422-03	.01	-.06	.06	174.6866	.13	.07	54.8932	.08	*
R422-28	.05	-.02	.05	109.4956	.12	.05	277.1114	.11	*
R440-28	.08	.00	.08	87.1932	.13	.03	276.0560	.11	*
R460-28	.08	.10	.13	37.8714	.14	.06	282.7947	.07	**
R460-03	.00	.04	.04	1.1011	.12	.05	30.9208	.08	*

certainly create some thermal expansion in the outside walls, which form part of the reference network.

It is the above findings that became the criteria in deciding to resurvey a portion of the main micro-network, described in section 5.2, that would be involved in the Phase IIB setting out. A by-product of this completely independent survey is the ability to determine the displacement vector for each target between the two epochs of survey. The displacements are determined with rigorous error estimations by removing the datum biases created by the adjustment minimal constraints, using the weighted projection methodology (iterative weighted s-transformation), which is part of the generalized approach developed at UNB for modelling deformations (Chrzanowski et al. 1982; Chen, 1983; Secord, 1985; Chrzanowski, 1986). The displacements for the targets involved are projected onto the three coordinate planes with Tables 5.5, 5.6, and 5.7 giving the components with error ellipses for the (x,y), (x,z), and (y,z) planes, respectively. The figures contained in Appendix III illustrate the magnitudes of the projected displacements with respect to their corresponding 95% confidence level error ellipses in the (x,y), (x,z), and (y,z) planes, respectively. The projected displacements for the (y,z) plane are illustrated in a series of cross sections, for reasons of clarity, because their projected locations are almost identical in this plane.

It can be clearly seen from the illustrations that even over just a 6 month period the movement of some of the targets is significant (up to 0.31 mm in the y,z plane) and there are some systematic trends to the changes. This unfortunately poses some serious doubts on the ability of the micro-network to remain stable in the long term. However, if the displacements detected here have been temperature induced then rigorous environmental controls may be the answer to the longevity of the micro-network.

Continuing on this line, the setting out survey for Phase IIB had a similar time span as that for Phase IIA. However, the inside temperature was kept constant at 17 ^{o}C throughout, with the magnitude of the inside outside temperature differential only a few

degrees for the entire setting out. In addition, this same temperature differential had been occurring at least two months previous to the Phase IIB setting out survey. The same procedure of combining the set out observations with the repeated network observations and performing a simultaneous adjustment was repeated for Phase IIB. The result was that the original expectation was achieved, namely, improved target triplets with only slight changes in values between adjustments. This result further substantiates the theory of long term thermal expansion of the concrete walls and gives a little more credibility to environmental controls.

6. Conclusions and Recommendations

The objective of this thesis was to give some insight and lift some of the mystique surrounding the new technology of coordinating systems for use in industrial metrology. To accomplish this, discussions were required describing the working components of the systems, primarily the theodolites. With interfacing to a microcomputer and using the well established geodetic surveying procedures, accuracies of a few hundredths of a mm are possible over short distances. An additional objective was to show that traditional optical tooling methods should not be replaced by coordinating systems, but the two should complement each other and they should be integrated to allow optimum accuracies to be achieved, with strong reliabilities, and minimal observational effort. Each methodology has assets over its counterpart that cannot be taken away.

The comparison of electronic theodolites with their optical-mechanical versions showed conclusively that the circle reading and automation of data collection are the only differences between the two. The newer electronic instruments still require the same basic solid mechanical structure, and once given this, are capable of achieving angular measurements with an expected accuracy improvement of a factor of 3 over their 1" optical predecessors mainly due to the improved accuracy of the electronic circle reading. In addition, electronic instruments with biaxial compensators are able to maintain this improvement, both horizontally and vertically, for long durations of time. Instruments equipped with uniaxial compensators allow the instruments to be levelled very precisely initially, but have no way of correcting the horizontal circle readings for level drift during use. Stability of instrument set ups over long periods of time are the norm in industrial metrology, which means an electronic theodolite with a biaxial compensator must be made

the standard instrument in coordinating systems, to maintain reliability throughout an observing session.

The accurate determination of network scale has been a problem facing geodesists since the beginning of triangulation and now for the confined areas of industrial metrology seems to be the limiting factor as well. The maximum length of a precisely calibrated scale bar, due to the logistics of calibration and transportation, is 2 to 3 m. If the bar can only be calibrated to ± 0.01 mm this results in a 3 to 5 ppm systematic scale error in the project area. If it is a small confined project, like the antenna experiment, then this isn't a problem, however , the TASCC project covered over 40 m which introduced a maximum systematic error of up to 0.2 mm in that direction! Fortunately, for this project the systematic scale error was not a major concern, but it does illustrate the problems associated with the determination of network scale that must be overcome to advance the capabilities of the coordinating systems.

The traditional methods of triangulation prove to be reliable for the establishing of geodetic micro-networks. The merit in the incorporation of the unique method of triangulation with the "free positioned" theodolites without sighting between theodolite stations, to increase angular accuracy, has been displayed by the adjustment results of TASCC Phase IIB, where the internal room temperature was kept constant. If the a posteriori variance factor (0.56) is used to scale the observation variance-covariance matrix then the expected accuracies discussed in section 2.2 for the Kern E2 are obtained.

The stability of geodetic micro-networks is critical in industrial applications where measurements are performed periodically to check alignment, calibrate a robotic arm, or determine the shape of an assembled surface. Based on the results from TASCC, it can be appreciated that the influences of long term thermal expansion could easily produce biased results at the level of accuracy usually sought in these applications. In addition, the bulk of the effect is due to inside outside temperature differentials, which are not easily removed or modelled. Inside environmental controls can be implemented, as was the case at TASCC,

but they will only help the observing consistency and will do very little for long term thermal expansion, due to the inside outside temperature differential.

The observation reductions for the effects of gravity, in most cases, may be ignored due to the small areas of interest creating negligible changes in the deflections of the vertical and direction of the gravity vector. However, there may be instances where nonparallelity of the gravity vector throughout the project area may have to be considered to achieve results at the few hundredths of a mm level. Again, the TASCC project illustrates this by showing the possible maximum deviation of 0.12 mm between a spacial line and an equipotential surface.

The algorithms developed in chapter 4 have been implemented with great success in the TASCC project. The data used in the least squares adjustments, for both Phase IIA and B, to determine the micro-network target triplets combined together very favorably as shown by the statistical testing summaries contained in section 5.2. Observational blunders, mispointings, and electronic glitches had all been removed or reobserved during the data acquisition process using the data quality check algorithm. A visual inspection of the collimation error, index error, and discrepancies between the observed set of angular quantities and their mean values is procedure enough to ensure that only data of adequate quality is maintained and used in coordinate determinations. The data checks are imperative when locating theodolites in the work area, where the observations are used in real time to obtain theodolite station as well as object target triplets. However, collimation and index errors are obtained to be analysed only if observations are performed in both positions of the theodolite telescope, which is a requirement for coordinating systems as shown by the discussions in sections 2.2 and 3.4. All errors inherent in theodolite construction, with the exception of vertical axis error, may be removed by observing a direction in both positions of the telescope. Manufacturers attempt to eliminate the errors as best they can during the assembling of the components, but not all errors behave consistently (i.e. collimation and index errors) as shown in section 2.2.

The least square adjustment algorithms made it possible to obtain the theodolite station triplets by redundant resections. This enabled a number of wall targets to be observed for each theodolite set up, randomizing their effects on the overall result and creating very well defined theodolite locations. The same algorithms also made it possible to relocate each theodolite independently in the work area which created a great deal of flexibility and allowed some time to be saved in the setting out process.

The TASCC project has proven to be a very adequate environment for testing the practicability of the developed algorithms, establishing micro-network methodology, and integrating traditional optical tooling with a coordinating system. An indication of the quality of the alignment results can be obtained with the realization that, for Phase IIA, only a few hours were required to commission the beam at the conclusion of the construction. Unfortunately, results for Phase IIB are not yet available as the supporting hardware (i.e. vacuum tubes, beam line monitors, slit assemblies, etc.) is still being installed.

References

Ackerson, D. Scott. "Uses of WILD C.A.T. 2000 Electronic Theodolites with Robots and Robot Workcells." Paper commissioned by Wild Heerbrugg Instruments, Inc., Farmingdale, New York, 9 pp.

Bauke, Walter E. (1983). "Adaption of Precision Surveying for Alignment of the Antares Laser Inertial Fusion System." The Proceedings of the American Congress of Surveying and Mapping, Annual Meeting, Washington D.C., Mar., pp 676-685.

Bauke, Walter, David A. Clark, Peter B. Trujillo (1985). "Surveying and Optical Tooling Technologies Combined to Align a Skewed Beam Line at the Lampf Accelerator." The Proceedings of the American Congress of Surveying and Mapping, Annual Meeting, Washington D.C., Mar., pp 311-320.

Bethel, James, John Sedej (1986). "Submarine Hull Mapping and Fixture Set-Out: An Application of the ECDS System." The Proceedings of the American Congress of Surveying and Mapping, Annual Meeting, Washington D.C., Mar., pp 92-96.

Blachut, T. J., A. Chrzanowski, J. H. Saastamoinen (1979). Urban Surveying and Mapping. Springer-Verlag New York Inc., New York, USA, 372 pp.

Bomford, G. (1980). Geodesy. 4th Edition, Oxford University Press, 855 pp.

Brown, Duane C. (1985). "Adaptation of the Bundle Method for Triangulation of Observations Made by Digital Theodolites." Proceedings of the Conference of South African Surveyors, Paper No. 43, 18 pp.

Campbell, Joe (1984). The RS-232 Solution. SYBEX Computer Books, Berkeley, Ca, USA, 194 pp.

Chen, Yong-qi (1983). Analysis of Deformation Surveys - A Generalized Method, Dept. of Surveying Engineering Technical Report 94, University of New Brunswick, Fredericton, N.B., Canada, 262 pp.

Chen, Y.Q., M. Kavouras, A. Chrzanowski (1987). "A Strategy For Detection of Outlying Observations in Measurements of High Precision." The Canadian Surveyor, Vol. 41, No. 4, winter, pp 529-540.

Chrzanowski, A. (1977). Design and Error Analysis of Surveying Projects, Dept. of Surveying Engineering Lecture Notes 47, University of New Brunswick, Fredericton, N.B., Canada, ??? pp.

Chrzanowski, A., Y.Q. Chen, J.M. Secord (1982). "On the Analysis of Deformation Surveys." Proceedings of the 4th Canadian Symposium on Mining Surveying and Deformation Measurements, Banff, Alberta, June, pp 431-452.

Chrzanowski, A. (1983). Selected Topics in Engineering Surveys Part III - Alignment Surveys, Dept. of Surveying Engineering draft lecture notes and supplementary reading material, University of New Brunswick, Fredericton, N.B., Canada, 153 pp.

Chrzanowski, A. (1985). "Implementation of Trigonometric Height Traversing in Geodetic Levelling of High Precision." Contract Report. 85-006, Geodetic Survey of Canada, 93 pp.

Chrzanowski, A., Y.Q. Chen, J.M. Secord (1986). "Geometrical Analysis of Deformation Surveys." Proceedings of the Deformation Measurements Workshop, Modern Methodology in Precise Engineering and Deformation Surveys-II, Massachusettes Institute of Technology, October, pp 170-206.

Cooper, M.A.R. (1982). Modern Theodolites and Levels. Granada Publishing Ltd, London, 258 pp.

Curtis, C., W. Oren, R. Ruland (1986). "The Use of Intersecting Lasers in the Alignment of the New Electron-Positron Collider at the Stanford Linear Accelerator Center." The Proceedings of the American Congress of Surveying and Mapping, Annual Meeting, Washington D.C., Mar., pp 61-69.

Davies, W. G. (1986). "Design of the Extraction Beam Lines for the Chalk River Superconducting Cyclotron." The Proceedings of the XI International Conference on Cyclotrons and their Applications, Tokyo, Japan, Oct. 13-17.

Deumlich, Fritz (1982). Surveying Instruments. Walter de Gruyter, Berlin / New York, 316 pp.

Faig, Wolfgang (1972). Advanced Surveying I, Dept. of Surveying Engineering Lecture Notes 26, University of New Brunswick, Fredericton, N.B., Canada, 225 pp.

Friedsam, H., W. Oren, M. Pietryka, R. Pitthan, R. Ruland (1985). "The Alignment of Stanford's New Electron-Positron Collider." The Proceedings of the American Congress of Surveying and Mapping, Annual Meeting, Washington D.C., Mar., pp 321-329.

Gervaise, J. (1974). "High-Precision Survey and Alignment Techniques in Accelerator Construction." Proceedings of the Meeting on Technology Arising From High-Energy Physics, Cern, Geneva, April, Vol. 1, pp 46-66.

Gervaise, J. (1976). "Geodesy and Metrology at CERN: A source of Economy for the SPS Programme." Cern 76-19, Super Proton Synchrotron Division, Geneva, November, 19 pp.

Greve, A. (1981). "Metrology of the Effelsburg 100 Meter Radio Reflector." Zeitschrift für Vermessungswesen, Vol. 106, No. 6, pp 308-315.

Hedquist, Bruce E. (1981). "Structural Alignment by 3-D Space Intersection." The Proceedings of the American Congress of Surveying and Mapping, Fall Meeting, San Francisco, Sept., pp 218-231.

Heilimo, Eric (1983). "Optical Tooling Applications Part I." The Ontario Land Surveyor, Spring, pp 10-15.

Heilimo, Eric (1983). "Optical Tooling Applications Part II." The Ontario Land Surveyor, Summer, pp 16-20.

Katowski, O. and W. Salzmann (1983). "The Angle-measurement System in the Wild THEOMAT T2000.", Wild Heerbrugg Ltd., Precision Engineering, Optics, Electronics, Heerbrugg, Switzerland, 9 pp.

Katowski, Olaf (1987a). "Automation of Electronic Angle-Measuring Instruments." Wild Heerbrugg Ltd., Precision Engineering, Optics, Electronics, Heerbrugg, Switzerland.

Katowski, O. and A. Schneider (1987b). "Industrial Surveying.", Wild Heerbrugg Ltd., Precision Engineering, Optics, Electronics, Heerbrugg, Switzerland.

Kern & Co. Ltd. (1980). "DKM2-A One-Second Theodolite with Automatic Vertical Indexing." Kern & Co. Ltd., Mechanical, Optical and Electronic Precision Instruments, Aarau, Switzerland.

Kern & Co. Ltd. (1981). "E1 Electronic Theodolite." Kern & Co. Ltd., Mechanical, Optical and Electronic Precision Instruments, Aarau, Switzerland.

Kern & Co. Ltd. (1983). "DKM2-AM One-Second Theodolite with Trunnion Axis Micrometer." Kern & Co. Ltd., Mechanical, Optical and Electronic Precision Instruments, Aarau, Switzerland.

Kern & Co. Ltd. (1984a). "Kern ASCII Single-Bus (ASB) System." Kern & Co. Ltd., Mechanical, Optical and Electronic Precision Instruments, Aarau, Switzerland, 7 pp.

Kern & Co. Ltd. (1984b). "Instruction Manual Electronic One-Second Theodolite E2." Kern & Co. Ltd., Mechanical, Optical and Electronic Precision Instruments, Aarau, Switzerland, 30 pp.

Kern & Co. Ltd. (1985). "Kern E2: Accuracy Analysis of the Graduated Circle." Kern & Co. Ltd., Mechanical, Optical and Electronic Precision Instruments, Aarau, Switzerland, Kern Bulletin No. 37, pp 3-6.

Kern & Co. Ltd. (1987). "The Mobile 3D Measuring System ECDS 2: Taking Measure!." Kern & Co. Ltd., Mechanical, Optical and Electronic Precision Instruments, Aarau, Switzerland.

Kern Instruments, Inc. (1986). Instruction Manual for the Kern ECDS-PC Software. Kern Instruments, Inc., Brewster, N.Y., 150 pp.

Kissam, Philip (1962). Optical Tooling. McGraw Hill Book Company, Inc., New York, 272 pp.

Krakiwsky, E.J., D.E. Wells (1971). Coordinate Systems in Geodesy, Dept. of Surveying Engineering Lecture Notes 16, University of New Brunswick, Fredericton, N.B., Canada, ?? pp.

Lardelli, A. (1985). "ECDS 1 - An Electronic Coordinate Determination System for Industrial Applications." Kern & Co. Ltd., Mechanical, Optical and Electronic Precision Instruments, Aarau, Switzerland, 11 pp.

Mikhail, Edward M. (1976). Observations and Least Squares. Harper & Row, Publishers, Inc., New York, 492 pp.

Münch, K.H. (1984). "The Kern E2 Electronic Precision Theodolite." Kern & Co. Ltd., Mechanical, Optical, and Electronic Precision Instruments, Aarau, Switzerland, 22 pp.

Nickerson, B.G. (1978). A Priori Estimation of Variance For Surveying Observables, Dept. of Surveying Engineering Technical Report No. 57, University of New Brunswick, Fredericton, N.B., Canada, 52 pp.

Oren, William, Robert Ruland (1985). "Survey Computation Problems Associated with Multi-Planer Electron-Positron Colliders." The Proceedings of the American Congress of Surveying and Mapping, Annual Meeting, Washington D.C., Mar., pp 338-347.

Oren, William, Robert Pushor, Robert Ruland (1987). "Incorporation of the Kern-PC Software Into a Project Oriented Software Environment." The Proceedings of the American Congress of Surveying and Mapping, Annual Meeting, Baltimore, Mar., pp 88-94.

Ruze, John (1966). "Antenna Tolerance Theory - A Review." Proceedings of the IEEE, Vol. 54, No. 4, pp 633-640.

Sah, R.C. (1981). "The Recent High Precision Surveys at PEP." Proceedings of the American Congress of Surveying and Mapping, Annual Meeting, Washington D.C., Feb., pp 155-164.

Secord, James M. (1985). Implementation of a Generalized Method for the Analysis of Deformation Surveys, Dept. of Surveying Engineering Technical Report 117, University of New Brunswick, Fredericton, N.B., Canada, 161 pp.

Secord, J.M., A. Chrzanowski, M.W. Rohde, and F. Wilkins (1988). "TASCC Phase II Control and Setting Out Surveys at the Chalk River Nuclear Laboratories." Final Report for Atomic Energy of Canada Limited, Chalk River, Ontario, Canada, 84 pp.

Torge, Wolfgang (1980). Geodesy. Walter de Gruyter, Berlin / New York, 254 pp.

Vanicek, P.; E.J. Krakiwsky (1986). Geodesy: The Concepts. North-Holland Pub. Co., Amsterdam, 697 pp.

Wells, D.E., E.J. Krakiwsky (1971). The Method of Least Squares, Dept. of Surveying Engineering Lecture Notes 18, University of New Brunswick, Fredericton, N.B., Canada, 180 pp.

Wild Heerbrugg Instruments Inc. "The Portable C.A.T. 2000 Coordinate Measurement System." Wild Heerbrugg Instruments, Inc., Industrial Measurement Systems, Atlanta, Georgia, USA.

Wild Heerbrugg Instruments Inc.(1987). "Wild THEOMAT T3000." Wild Heerbrugg Ltd., Precision Engineering, Optics, Electronics, Heerbrugg, Switzerland, Product information.

Wild Heerbrugg Ltd. (1984). "Informatic Theodolite THEOMAT Wild T2000 Operator's Manual", Wild Heerbrugg Ltd., Heerbrugg, Switzerland.

Wilkins, Fred, A. Chrzanowski, M. Rohde, H. Schmeing, J. Secord (1988). "A Three Dimensional High Precision Coordinating System." Proceedings of the 5th International Symposium on Deformation Measurements and the 5th Canadian Symposium on Mining Surveying and Rock Deformation Measurements, Fredericton, N.B., June, pp 580-592.

Wolf, Paul R. (1974). Elements of Photogrammetry. McGraw-Hill Book Company, New York, U.S.A., 562 pp.

Appendix I

(Design versus Set-out Coordinates)

The nominal or designed values (N), the set out or installed values (S), and their differences (N-S) for both Phase IIA and Phase IIB are given below. The x' and y' values for the differences are the components along and transverse to a branch beam line, respectively.

Phase IIA

Dipole	Axis	Nominal (N [m])	Set Out (S [m])	Difference (N-S [mm])
BE-1 1	X	0.72090	0.72094	-0.04
	Y	0.00000	0.00004	-0.04
	Z	1.75260	1.75260	0.00
BE-1 2	X	-0.50950	-0.50957	0.07
	Y	-0.47180	-0.47174	-0.06
	Z	1.75260	1.75259	0.01
BE-1 3	X	-0.36813	-0.36826	0.13
	Y	0.63761	0.63787	-0.26
	Z	1.75260	1.75261	-0.01
BE-1 C	X	0.00000	0.00000	0.00
	Y	0.00000	0.00000	0.00
	Z	1.75260	1.75260	0.00
BE-2 1	X	1.55859	1.55859	0.00
	Y	0.00000	0.00000	0.00
	Z	1.75260	1.75268	-0.08
BE-2 2	X	2.50348	2.50348	0.00
	Y	0.00000	0.00003	-0.03
	Z	1.75260	1.75266	-0.06
BE-2 3	X	2.44661	2.44657	0.04
	Y	0.23792	0.23799	-0.07
	Z	1.75260	1.75261	-0.01
BE-2 4	X	2.44658	2.44661	-0.03
	Y	-0.23791	-0.23787	-0.04
	Z	1.75260	1.75263	-0.03
BE-2 C	X	2.03440	2.03445	-0.05
	Y	0.00000	0.00005	-0.05
	Z	1.75260	1.75263	-0.03
BE-2A 1	X	3.30291	3.30298	-0.07
	Y	0.73213	0.73201	0.12
	Z	1.75260	1.75255	0.05
BE-2A 2	X	3.95310	3.95317	-0.07
	Y	1.38206	1.38202	0.04
	Z	1.75260	1.75253	0.07

BE-2A C	X	3.71504	3.71504	0.00
	Y	0.96998	0.96998	0.00
	Z	1.75260	1.75250	0.10
BE-3 1	X	13.04986	13.04975	0.11
	Y	0.00000	-0.00007	0.07
	Z	1.75260	1.75257	0.03
BE-3 2	X	13.34982	13.34971	0.11
	Y	0.00000	0.00001	-0.01
	Z	1.75260	1.75260	0.00
BE-3 3	X	13.92836	13.92836	0.00
	Y	0.22678	0.22678	0.00
	Z	1.75260	1.75263	-0.03
BE-3 4	X	14.14847	14.14847	0.00
	Y	0.43053	0.43054	-0.01
	Z	1.75260	1.75265	-0.05
BE-3 C	X	13.68360	13.68349	0.11
	Y	0.00000	0.00010	-0.10
	Z	1.75260	1.75261	-0.01
BE-4 1	X	22.57348	22.57327	0.21
	Y	0.00000	-0.00008	0.08
	Z	1.75260	1.75263	-0.03
BE-4 2	X	22.87329	22.87308	0.21
	Y	0.00000	-0.00004	0.04
	Z	1.75260	1.75261	-0.01
BE-4 3	X	23.45166	23.45166	0.00
	Y	0.22681	0.22681	0.00
	Z	1.75260	1.75262	-0.02
BE-4 4	X	23.67182	23.67182	0.00
	Y	0.43070	0.43071	-0.01
	Z	1.75260	1.75259	0.01
BE-4 C	X	23.20697	23.20676	0.21
	Y	0.00000	0.00000	0.00
	Z	1.75260	1.75261	-0.01

Quadrupole	Axis	Nominal (N [m])	Set Out (N [m])	Difference (N-S [mm])
QE-3 A	X	4.56640	4.56627	0.13
	Y	0.00000	0.00002	-0.02
	Z	1.75260	1.75252	0.08
QE-3 B	X	4.97890	4.97898	-0.08
	Y	0.00000	0.00002	-0.02
	Z	1.75260	1.75250	0.10

QE-3 C	X	5.39140	5.39144	-0.04
	Y	0.00000	0.00003	-0.03
	Z	1.75260	1.75251	0.09
QE-4 A	X	6.42930	6.42929	0.01
	Y	0.00000	0.00006	-0.06
	Z	1.75260	1.75256	0.04
QE-4 B	X	6.84180	6.84188	-0.08
	Y	0.00000	-0.00001	-0.01
	Z	1.75260	1.75255	0.05
QE-4 C	X	7.25430	7.25436	-0.06
	Y	0.00000	-0.00003	0.03
	Z	1.75260	1.75256	0.04
QE-5 A	X	8.29220	8.29212	0.08
	Y	0.00000	0.00003	-0.03
	Z	1.75260	1.75257	0.03
QE-5 B	X	8.70470	8.70481	-0.11
	Y	0.00000	0.00003	-0.03
	Z	1.75260	1.75261	-0.01
QE-5 C	X	9.11720	9.11726	-0.06
	Y	0.00000	0.00005	-0.05
	Z	1.75260	1.75259	0.01
QE-6 A	X	11.05505	11.05498	0.07
	Y	0.00000	0.00001	-0.01
	Z	1.75260	1.75259	0.01
QE-6 B	X	11.39255	11.39251	0.04
	Y	0.00000	0.00007	-0.07
	Z	1.75260	1.75257	0.03
QE-7 A	X	14.64249	14.64248	0.01
	Y	0.00000	0.00001	-0.01
	Z	1.75260	1.75264	-0.04
QE-7 B	X	14.97999	14.97998	0.01
	Y	0.00000	0.00006	-0.06
	Z	1.75260	1.75256	0.04
QE-8 A	X	15.95499	15.95497	0.02
	Y	0.00000	0.00000	0.00
	Z	1.75260	1.75263	-0.03
QE-8 B	X	16.29249	16.29248	0.01
	Y	0.00000	-0.00002	0.02
	Z	1.75260	1.75262	-0.02

QE-9 A	X	19.26588	19.26586	0.02
	Y	0.00000	0.00004	-0.04
	Z	1.75260	1.75260	0.00
QE-9 B	X	19.60338	19.60338	0.00
	Y	0.00000	0.00001	-0.01
	Z	1.75260	1.75261	-0.01
QE-10 A	X	21.42838	21.42843	-0.05
	Y	0.00000	0.00005	-0.05
	Z	1.75260	1.75259	0.01
QE-10 B	X	21.76588	21.76582	0.06
	Y	0.00000	0.00007	-0.07
	Z	1.75260	1.75265	-0.05
QE-11 A	X	25.01591	25.01594	-0.03
	Y	0.00000	-0.00001	0.01
	Z	1.75260	1.75263	-0.03
QE-11 B	X	25.35341	25.35347	-0.06
	Y	0.00000	0.00003	-0.03
	Z	1.75260	1.75262	-0.02
QE-19 A	X	4.70825	4.70814	0.11
	X '			0.12
	Y	-1.54378	-1.54372	-0.06
	Y '			0.00
	Z	1.75260	1.75259	0.01
QE-19 B	X	5.06548	5.06540	0.08
	X '			0.08
	Y	-1.75005	-1.75002	-0.03
	Y '			0.01
	Z	1.75260	1.75258	0.02
QE-19 C	X	5.42271	5.42276	-0.05
	X '			-0.04
	Y	-1.95631	-1.95631	0.00
	Y '			-0.02
	Z	1.75260	1.75260	0.00
QE-20 A	X	4.52131	4.52137	-0.06
	X '			-0.01
	Y	2.36563	2.36561	0.02
	Y '			0.06
	Z	1.75260	1.75262	-0.02
QE-20 B	X	4.72765	4.72760	0.05
	X '			0.10
	Y	2.72281	2.72271	0.10
	Y '			0.06
	Z	1.75260	1.75263	-0.03

QE-20 C	X	4.93400	4.93394	0.06
	X '			-0.05
	Y	3.07999	3.08008	-0.09
	Y '			-0.10
	Z	1.75260	1.75259	0.01
QE-21	X	15.31974	15.31987	-0.13
	X '			-0.26
	Y	1.51477	1.51495	-0.24
	Y '			-0.09
	Z	1.75260	1.75263	-0.03
QE-22 A	X	18.36946	18.36948	-0.02
	X '			-0.06
	Y	4.33788	4.33794	-0.06
	Y '			-0.03
	Z	1.75260	1.75261	-0.01
QE-22 B	X	18.67217	18.67211	0.06
	X '			0.04
	Y	4.61810	4.61811	-0.01
	Y '			-0.05
	Z	1.75260	1.75258	0.02
QE-22 C	X	18.97488	18.97494	-0.06
	X '			0.00
	Y	4.89832	4.89826	0.06
	Y '			0.08
	Z	1.75260	1.75256	0.04
QE-23	X	24.84267	24.84292	-0.25
	X '			-0.24
	Y	1.51505	1.51514	-0.09
	Y '			0.10
	Z	1.75260	1.75260	0.00
QE-24 A	X	28.25858	28.25863	-0.05
	X '			-0.08
	Y	4.67859	4.67866	-0.07
	Y '			-0.02
	Z	1.75260	1.75260	0.00
QE-24 B	X	28.56123	28.56112	0.11
	X '			0.15
	Y	4.95888	4.95878	0.10
	Y '			0.00
	Z	1.75260	1.75263	-0.03
QE-24 C	X	28.86388	28.86392	-0.04
	X '			-0.04
	Y	5.23916	5.23917	-0.01
	Y '			0.02
	Z	1.75260	1.75262	-0.02

Phase IIB

Dipole	Axis	Nominal (N [m])	Set Out (N [m])	Difference (N-S [mm])
BE-6 1	X	35.77147	35.77146	0.01
	Y	0.0	0.00009	-0.09
	Z	1.75260	1.75256	0.04
BE-6 2	X	36.07145	36.07144	0.01
	Y	0.0	0.00007	-0.07
	Z	1.75260	1.75256	0.04
BE-6 3	X	36.64967	36.64966	0.01
	Y	0.22659	0.22664	-0.05
	Z	1.75260	1.75256	0.04
BE-6 4	X	36.86980	36.86978	0.02
	Y	0.43041	0.43048	-0.07
	Z	1.75260	1.75258	0.02
BE-7 1	X	-	37.70843	-
	Y	0.0	0.00000	-0.00
	Z	1.75260	1.75263	-0.03
BE-7 3	X	-	-	-
	Y	-	-	-
	Z	1.75260	1.75260	0.00
BE-7 6	X	39.65817	39.65821	-0.04
	Y	-	-1.95024	-
	Z	1.75260	1.75257	0.03
BE-8 1	X	39.65817	39.65821	-0.04
	Y	-	-5.74551	-
	Z	1.75260	1.75260	0.00
BE-8 C	X	39.65817	39.65822	-0.05
	Y	-6.22140	-6.22143	0.03
	Z	1.75260	1.75259	0.01

Quadrupole	Axis	Nominal (N [m])	Set Out (N [m])	Difference (N-S [mm])
QE-12 A	X	28.02847	28.02838	0.09
	Y	0.0	0.00002	-0.02
	Z	1.75260	1.75259	0.01
QE-12 B	X	28.36597	28.36601	-0.04
	Y	0.0	-0.00004	0.04
	Z	1.75260	1.75258	0.02
QE-13 A	X	31.61597	31.61604	-0.07
	Y	0.0	-0.00001	0.01
	Z	1.75260	1.75266	-0.06

QE-13 B	X	31.95347	31.95341	0.06
	Y	0.0	-0.00007	0.07
	Z	1.75260	1.75261	-0.01
QE-14 A	X	34.65822	34.65821	0.01
	Y	0.0	0.00003	-0.03
	Z	1.75260	1.75260	0.00
QE-14 B	X	35.14572	35.14586	-0.14
	Y	0.0	0.00006	-0.06
	Z	1.75260	1.75262	-0.02
QE-15 A	X	39.65817	39.65811	0.06
	Y	-4.51245	-4.51241	-0.04
	Z	1.75260	1.75264	-0.04
QE-15 B	X	39.65817	39.65813	0.04
	Y	-4.99995	-4.99992	-0.03
	Z	1.75260	1.75258	0.02
QE-16 A	X	40.64537	40.64538	-0.01
	X'			-0.09
	Y	-9.16613	-9.16622	0.09
	Y'			0.02
	Z	1.75260	1.75256	0.04
QE-16 B	X	40.77649	40.77651	-0.02
	X'			-0.04
	Y	-9.55724	-9.55728	0.04
	Y'			-0.01
	Z	1.75260	1.75260	0.00
QE-16 C	X	40.90760	40.90758	0.02
	X'			0.12
	Y	-9.94834	-9.94822	-0.12
	Y'			-0.02
	Z	1.75260	1.75256	0.04
QE-17 A	X	38.51739	38.51748	-0.09
	X'			0.02
	Y	-8.19941	-8.19944	0.03
	Y'			-0.09
	Z	1.75260	1.75261	-0.01
QE-17 B	X	38.31130	38.31142	-0.12
	X'			0.07
	Y	-8.55674	-8.55673	-0.01
	Y'			-0.10
	Z	1.75260	1.75258	0.02

QE-17 C	X	38.10522	38.10528	-0.06
	X'			0.04
	Y	-8.91407	-8.91406	-0.01
	Y'			-0.05
	Z	1.75260	1.75260	0.00
QE-18 A	X	35.75960	35.75954	0.06
	X'			0.01
	Y	-12.98115	-12.98110	-0.05
	Y'			0.08
	Z	1.75260	1.75260	0.00
QE-18 B	X	35.55352	35.55347	0.05
	X'			0.02
	Y	-13.33848	-13.33843	-0.05
	Y'			0.07
	Z	1.75260	1.75264	-0.04
QE-18 C	X	35.34743	35.34734	0.09
	X'			-0.03
	Y	-13.69581	-13.69579	-0.02
	Y'			0.09
	Z	1.75260	1.75259	0.01
QE-25	X	38.04101	38.04092	0.09
	X'			0.07
	Y	1.51495	1.51494	0.01
	Y'			0.05
	Z	1.75260	1.75261	-0.01
QE-26 A	X	41.45718	41.45719	-0.01
	X'			-0.01
	Y	4.67816	4.67817	-0.01
	Y'			0.00
	Z	1.75260	1.75258	0.02
QE-26 B	X	41.75986	41.75990	-0.04
	X'			-0.06
	Y	4.95843	4.95847	-0.04
	Y'			0.00
	Z	1.75260	1.75261	-0.01
QE-26 C	X	42.06253	42.06258	-0.05
	X'			-0.06
	Y	5.23869	5.23873	-0.04
	Y'			0.00
	Z	1.75260	1.75263	-0.03
QE-27 A	X	41.41442	41.41448	-0.06
	Y	0.0	-0.00003	0.03
	Z	1.75260	1.75256	0.04

QE-27 B	X	41.90192	41.90196	-0.04
	Y	0.0	-0.00002	0.02
	Z	1.75260	1.75264	-0.04
QE-28 A	X	41.57749	41.57738	0.11
	X'			0.12
	Y	-1.85666	-1.85662	-0.04
	Y'			0.02
	Z	1.75260	1.75259	0.01
QE-28 B	X	41.99966	41.99963	0.03
	X'			0.05
	Y	-2.10043	-2.10038	-0.05
	Y'			0.03
	Z	1.75260	1.75257	0.03

Appendix II

(Difference in Coordinates Between Original Control and the Combined Adjustments for Phase IIA)

The coordinate differences between the original control network survey adjustment (X_o, Y_o, and Z_o) and those determined from the simultaneous adjustment (X_c, Y_c, and Z_c) containing the combined original control, setting out, and the "wing target" observations.

Station	X_o-X_c (mm)	Y_o-Y_c (mm)	Z_o-Z_c (mm)
BE1-1	-0.009	-0.005	0.018
BE1-2	0.017	0.006	-0.001
BE1-3	0.005	-0.006	0.001
L020-33	-0.020	-0.002	-0.012
L038-33	-0.025	0.003	-0.009
L060-33	-0.030	0.005	-0.019
L060-05	-0.011	0.049	-0.023
L080-20	0.000	0.069	-0.008
L100-26	0.071	0.078	0.000
L100-05	0.064	0.092	-0.030
L120-28	0.096	0.085	0.017
L140-28	0.114	0.079	0.029
L140-05	0.107	0.090	-0.013
L154-28	0.123	0.084	0.041
L180-28	0.150	0.051	0.017
L180-05	0.138	0.054	0.011
L200-28	0.147	0.056	0.019
L220-28	0.159	0.070	0.016
L220-05	0.164	0.060	0.040
L240-28	0.192	0.083	0.024
L266-28	0.200	0.076	0.015
L266-05	0.205	0.069	-0.009
L280-28	0.212	0.072	0.011
L300-28	0.227	0.064	0.007
L300-05	0.227	0.062	-0.002
L320-28	0.243	0.059	0.008
L340-28	0.258	0.050	0.011
L340-05	0.259	0.050	-0.007
L360-28	0.272	0.039	0.010
L381-28	0.286	0.032	0.009
L381-05	0.285	0.032	-0.005
L400-28	0.298	0.025	0.008
L420-28	0.306	0.020	0.007
L420-05	0.306	0.020	-0.002
L440-28	0.314	0.015	0.007
L460-28	0.321	0.010	0.007
L460-05	0.321	0.011	-0.001
R020-33	-0.045	0.062	-0.032
R020-07	-0.017	0.057	0.005
R032-20	-0.032	0.078	-0.038
R060-33	-0.064	0.122	-0.018
R060-05	-0.040	0.123	-0.024
R080-28	-0.055	0.126	0.028
R100-28	0.018	0.119	0.032
R100-03	0.008	0.086	-0.024
R120-28	0.068	0.125	0.037
R136-28	0.091	0.112	0.024

R136-11	0.093	0.111	-0.011
R160-28	0.115	0.081	0.024
R177-28	0.128	0.080	0.018
R177-03	0.120	0.067	-0.011
R196-26	0.121	0.065	0.005
R220-28	0.111	0.004	0.026
R220-03	0.128	0.018	0.000
R240-28	0.127	-0.018	0.033
R260-28	0.165	-0.006	0.026
R260-03	0.163	0.019	-0.017
R272-28	0.176	-0.021	0.034
R300-28	0.216	0.001	0.014
R300-03	0.206	-0.012	-0.017
R320-28	0.231	-0.006	0.009
R343-28	0.246	-0.015	0.011
R343-03	0.246	-0.012	-0.007
R360-28	0.258	-0.014	0.011
R380-03	0.273	-0.013	-0.006
R395-30	0.281	-0.013	0.010
R410-30	0.288	-0.011	0.009
R420-03	0.291	-0.011	-0.003
R422-28	0.292	-0.012	0.008
R440-28	0.300	-0.012	0.007
R460-28	0.305	-0.013	0.006
R460-03	0.304	-0.014	-0.001
AXW35	0.075	-0.008	-0.007
AXWEND	0.325	0.000	0.015
FLAX1	-0.049	0.045	0.030
FLAX2	0.146	0.054	0.006
FLAX3	0.182	0.054	-0.011
FLAX5	0.246	0.033	-0.010
FLAX6	0.283	0.018	-0.006
FLAX7	0.304	0.008	-0.005
RM101-23	0.323	0.027	-0.009
RM102-03	0.335	0.035	0.020
RM103-24	0.331	0.027	0.006
RM104-03	0.331	0.027	0.015
RM105-30	0.297	0.012	-0.004
RM106-03	0.292	0.014	-0.004
RM107-30	0.277	0.020	0.003
RM108-03	0.262	0.013	0.001
RM109-29	0.236	0.036	0.025
RM110-03	0.238	0.040	0.011
RM111-29	0.228	0.065	0.028
RM112-03	0.235	0.063	0.008
RM113-29	0.197	0.061	0.079
RM201-29	0.285	0.037	0.008
RM202-03	0.284	0.035	0.008
RM203-29	0.281	0.032	0.007
RM204-03	0.283	0.033	0.008
RM205-29	0.278	0.029	-0.002
RM206-03	0.281	0.030	0.009
RM207-30	0.279	0.035	0.000
RM208-05	0.261	0.030	0.007

RM209-30	0.264	0.042	0.009
RM210-05	0.264	0.042	0.004
RM211-30	0.249	0.016	0.022
RM212-30	0.290	0.098	0.006
RM213-30	0.281	0.055	0.002
RM214-05	0.288	0.037	0.017
RM215-30	0.287	0.061	-0.009
BE1-C	0.000	0.000	0.000

Appendix III

(Plots of Displacements and their 95% Error Ellipses

Between Phase IIA and Phase IIB)

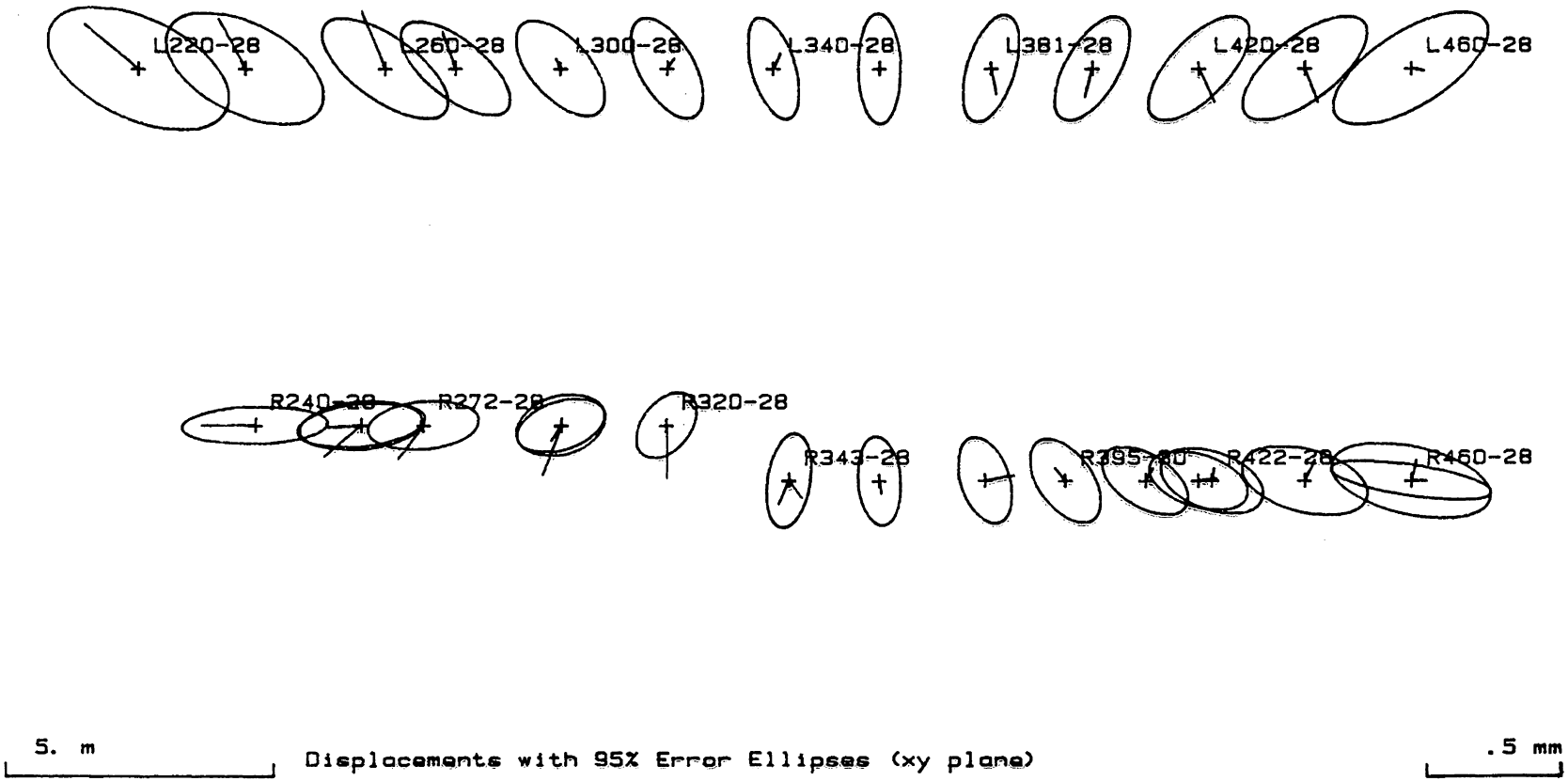
L220-28
L260-28
L300-28
L340-28
L381-28
L420-28
L460-28
R240-28
R272-28
R320-28
R343-28
R395-28
R422-28
R460-28
5. m
Displacements with 95% Error Ellipses (xy plane)
.5 mm

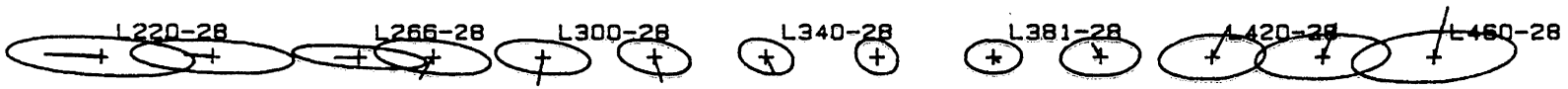

5. m

Displacements with 95% Error Ellipses (xz plane left wall)

.5 mm

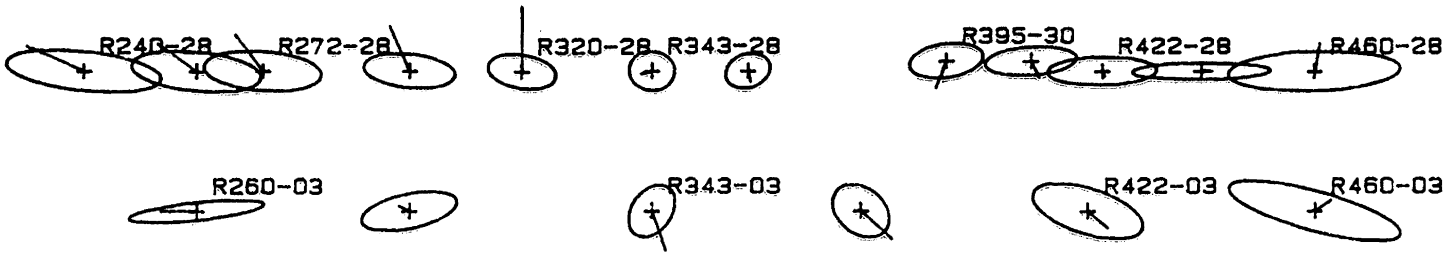

5. m

Displacements with 95% Error Ellipses (xz plane right wall)

.5 mm

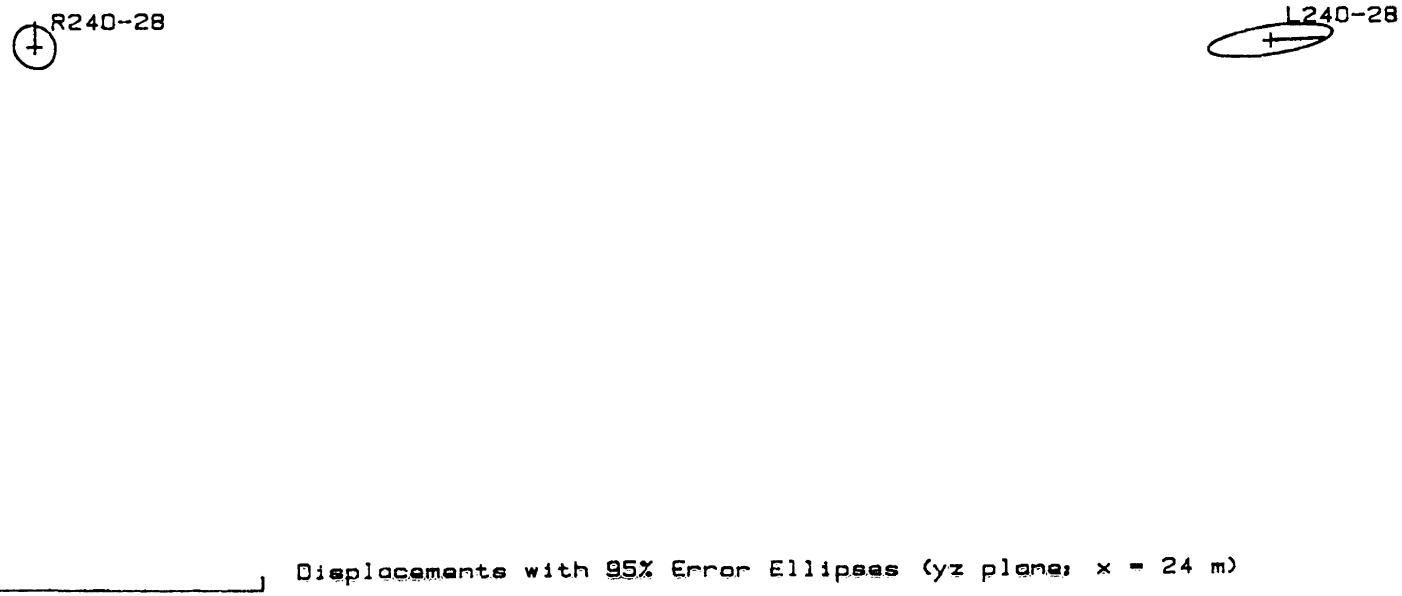
R240-28
L240-28
2. m
Displacements with 95% Error Ellipses (yz plane: x = 24 m)
.5 mm

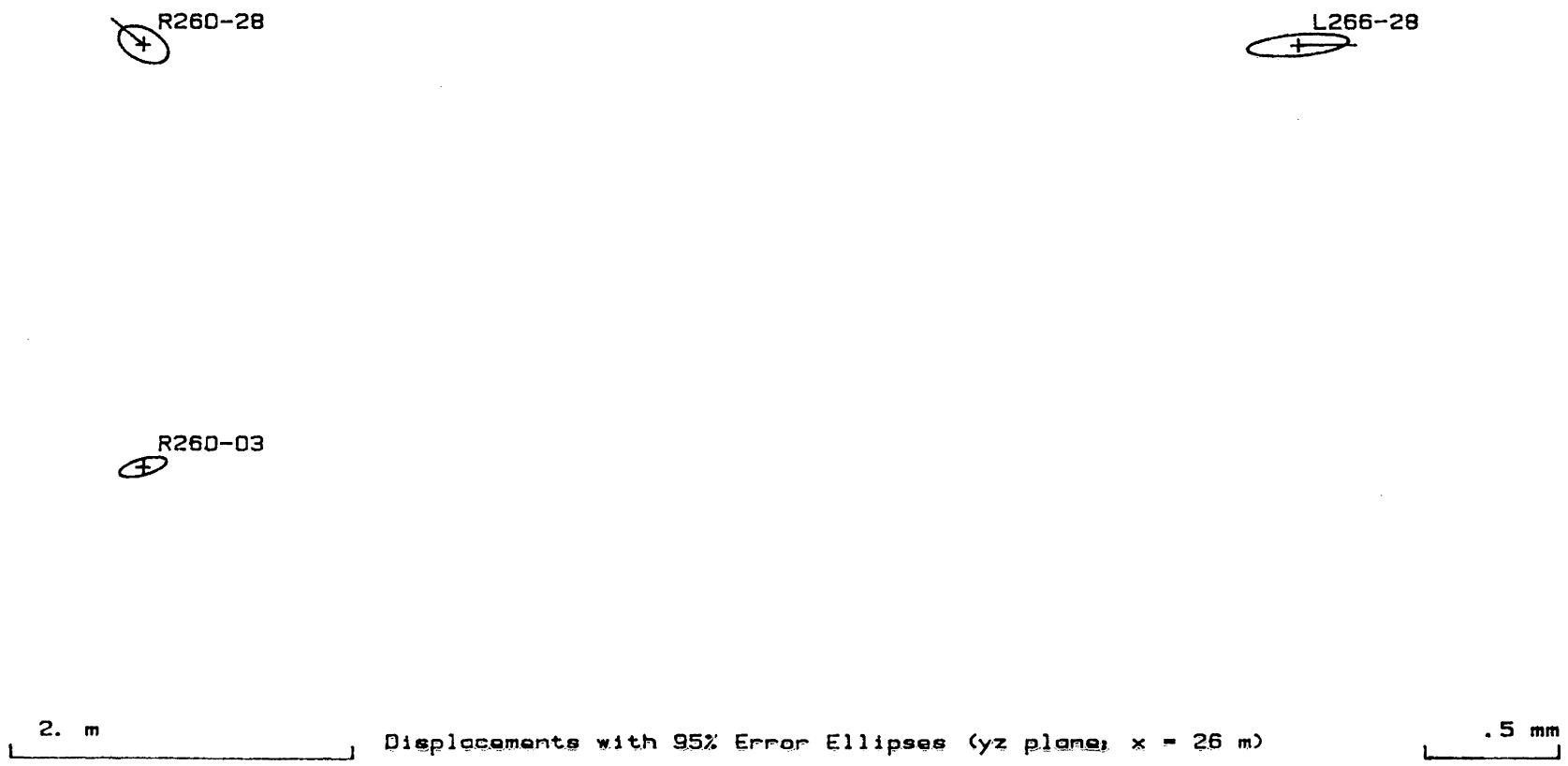
R260-28
L266-28
R260-03
2. m
Displacements with 95% Error Ellipses (yz plane; x = 26 m)
.5 mm

2. m

Displacements with 95% Error Ellipses (yz plane: x = 28 m)

.5 mm

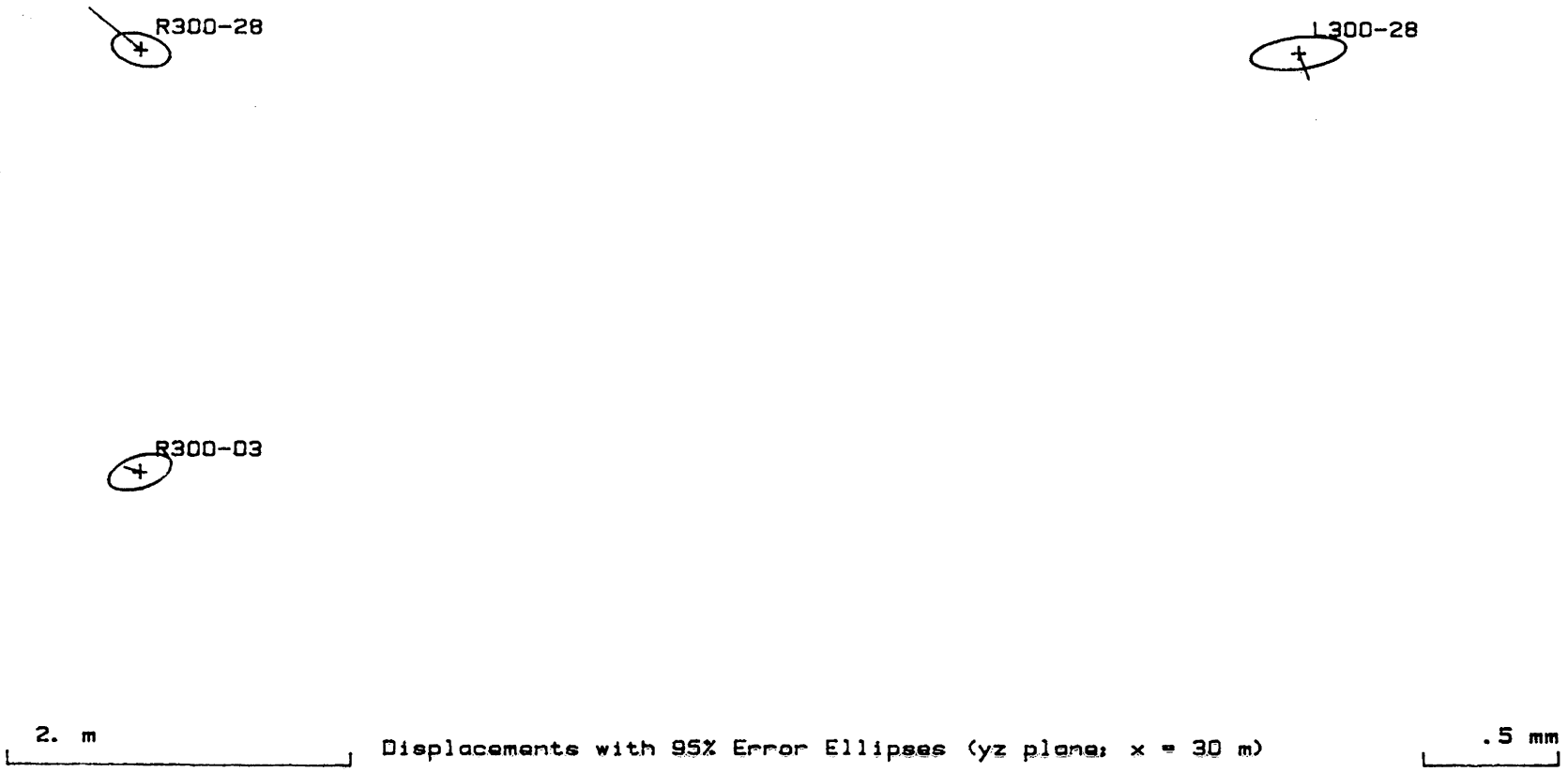
R300-28
L300-28
R300-03
2. m
Displacements with 95% Error Ellipses (yz plane; x = 30 m)
.5 mm

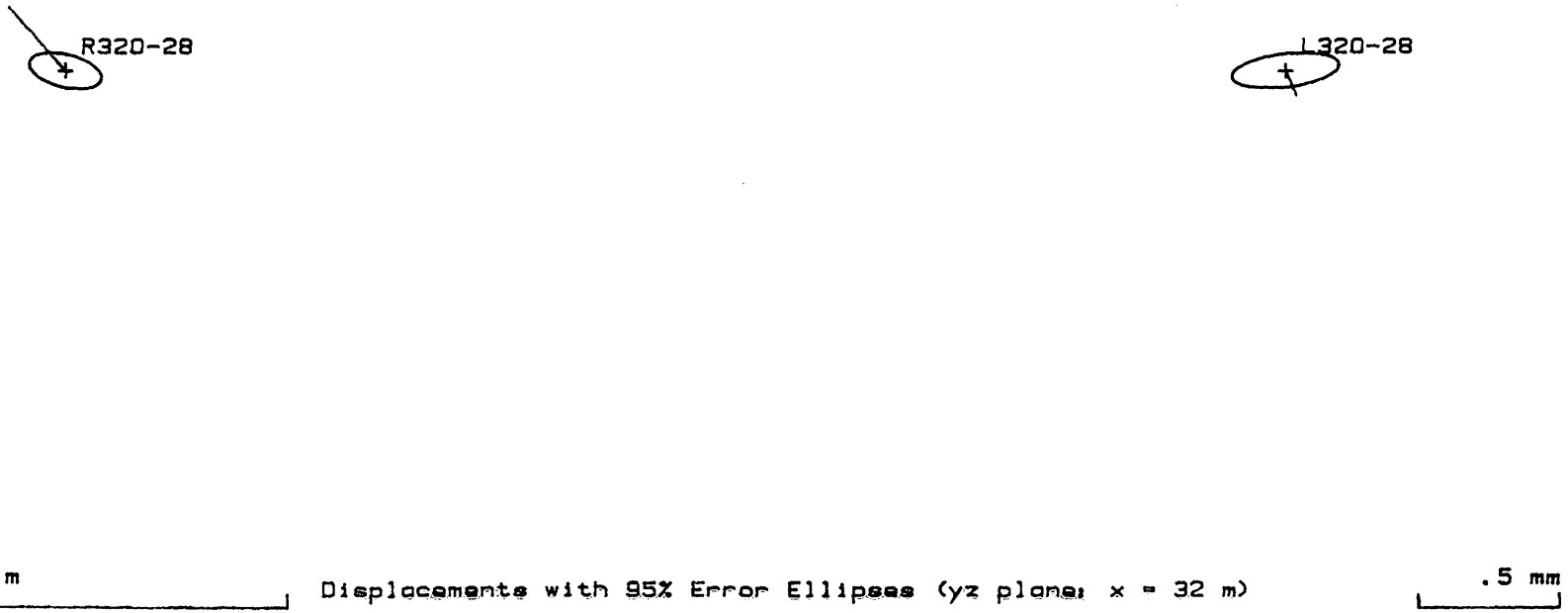
R320-28
L320-28
2. m
Displacements with 95% Error Ellipses (yz plane: x = 32 m)
.5 mm

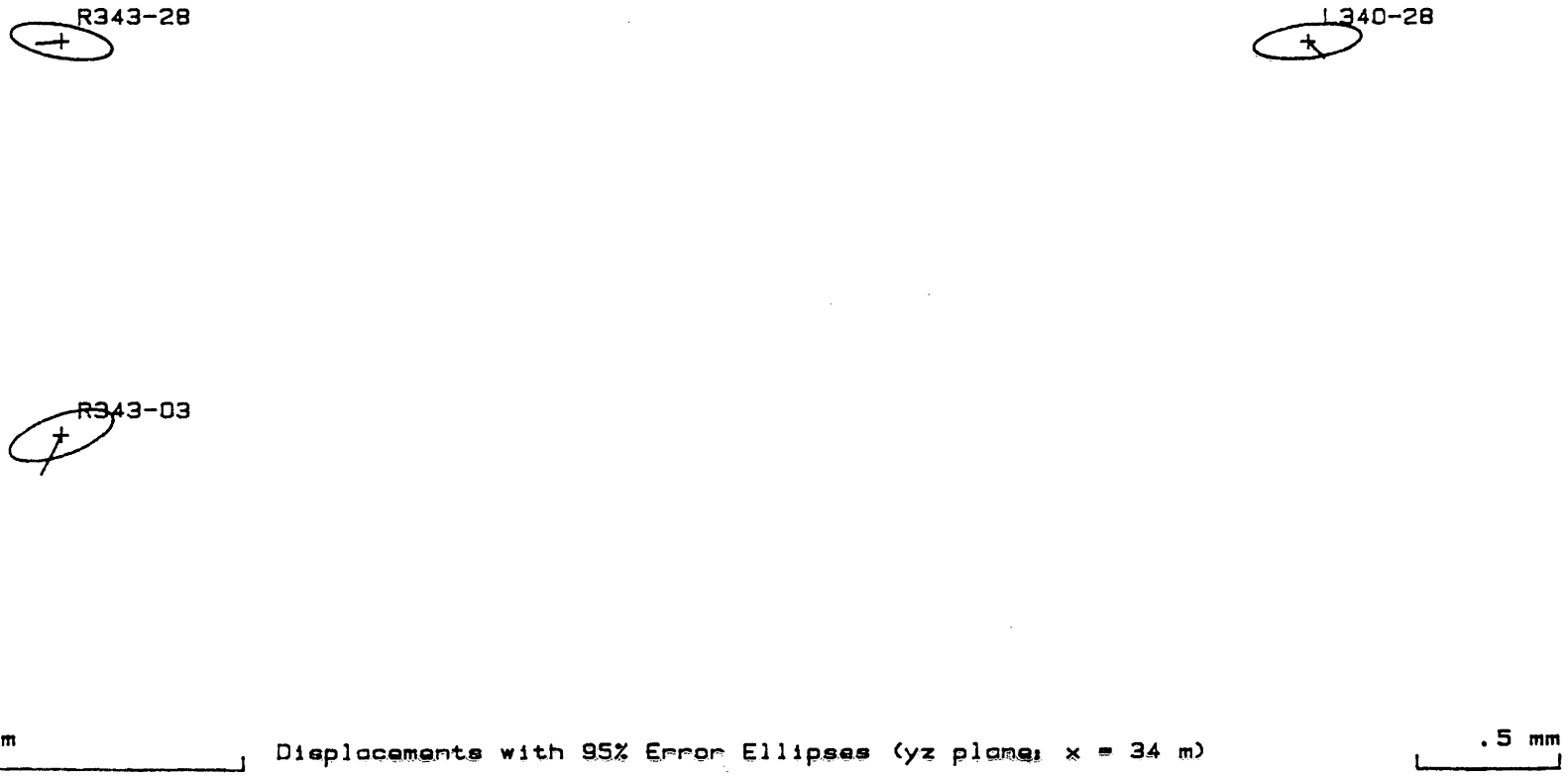
R343-28
L340-28
R343-03
2. m
Displacements with 95% Error Ellipses (yz plane; x = 34 m)
.5 mm

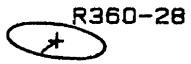

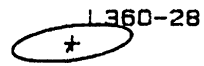

2. m

Displacements with 95% Error Ellipses (yz plane; x = 36 m)

.5 mm

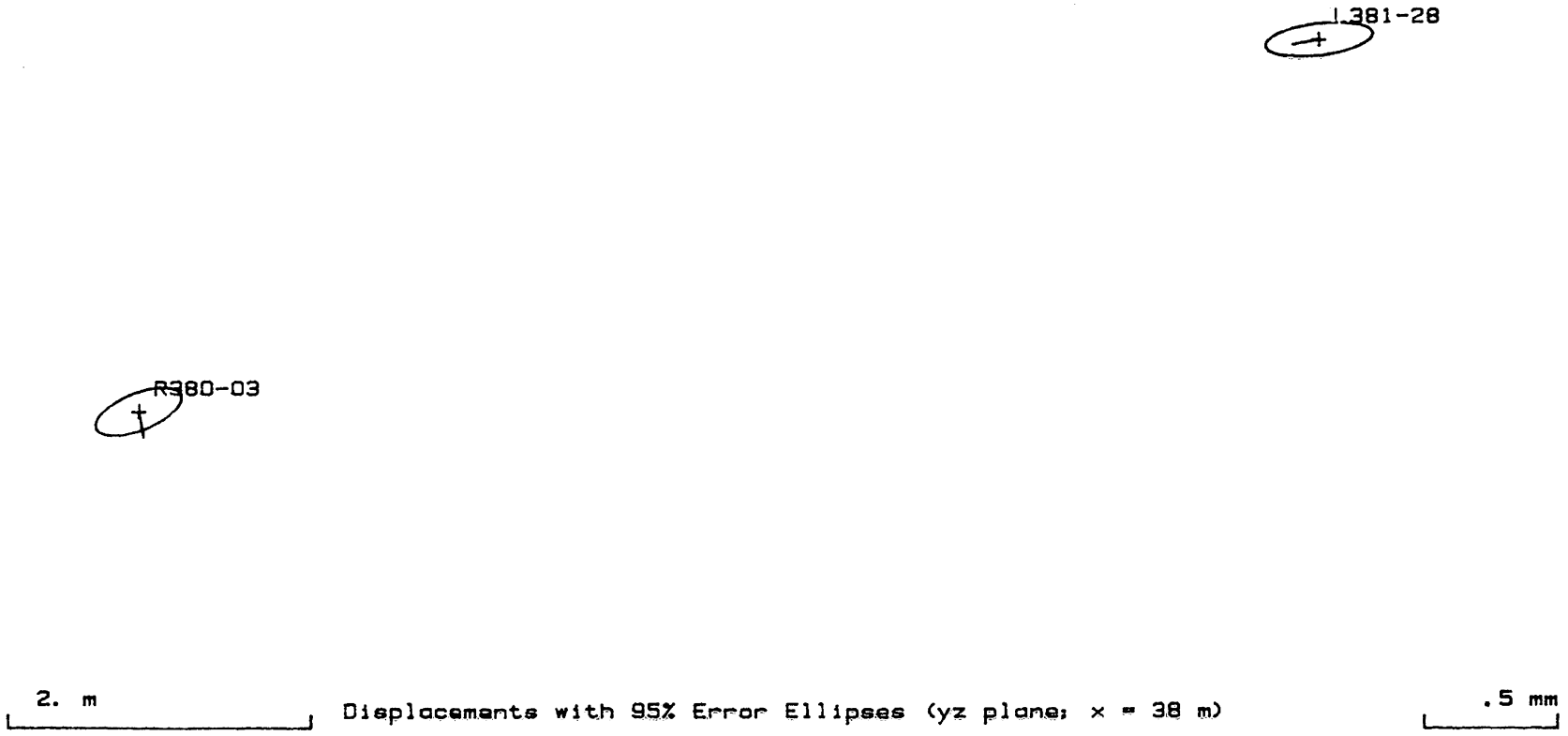
1381-28
R380-03
2. m
Displacements with 95% Error Ellipses (yz plane: x = 38 m)
.5 mm

2. m

Displacements with 95% Error Ellipses (yz plane: x = 40 m)

.5 mm

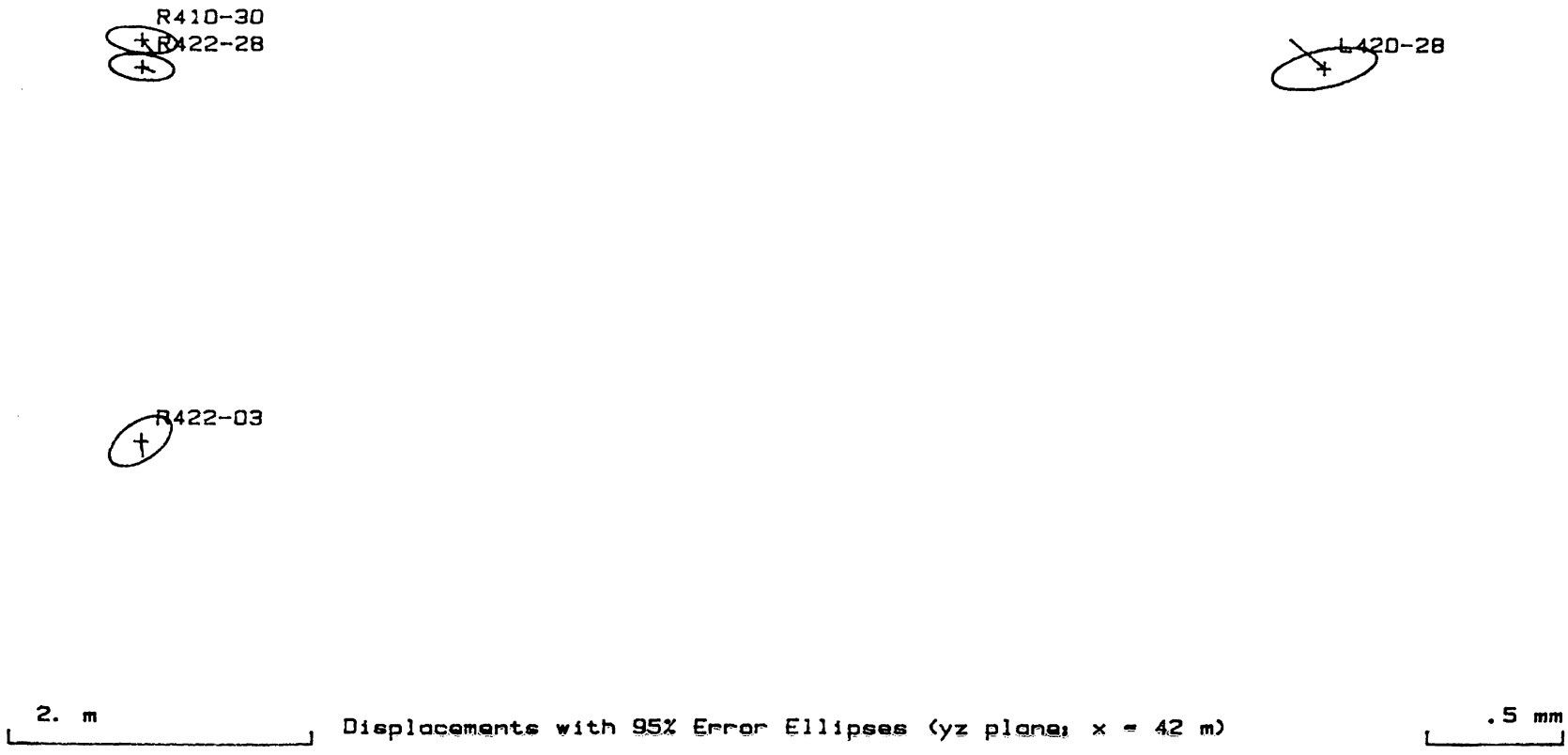
R410-30
R422-28
L420-28
R422-03
2. m
Displacements with 95% Error Ellipses (yz plane; x = 42 m)
.5 mm

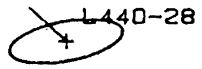

2. m

Displacements with 95% Error Ellipses (yz plane; x = 44 m)

.5 mm

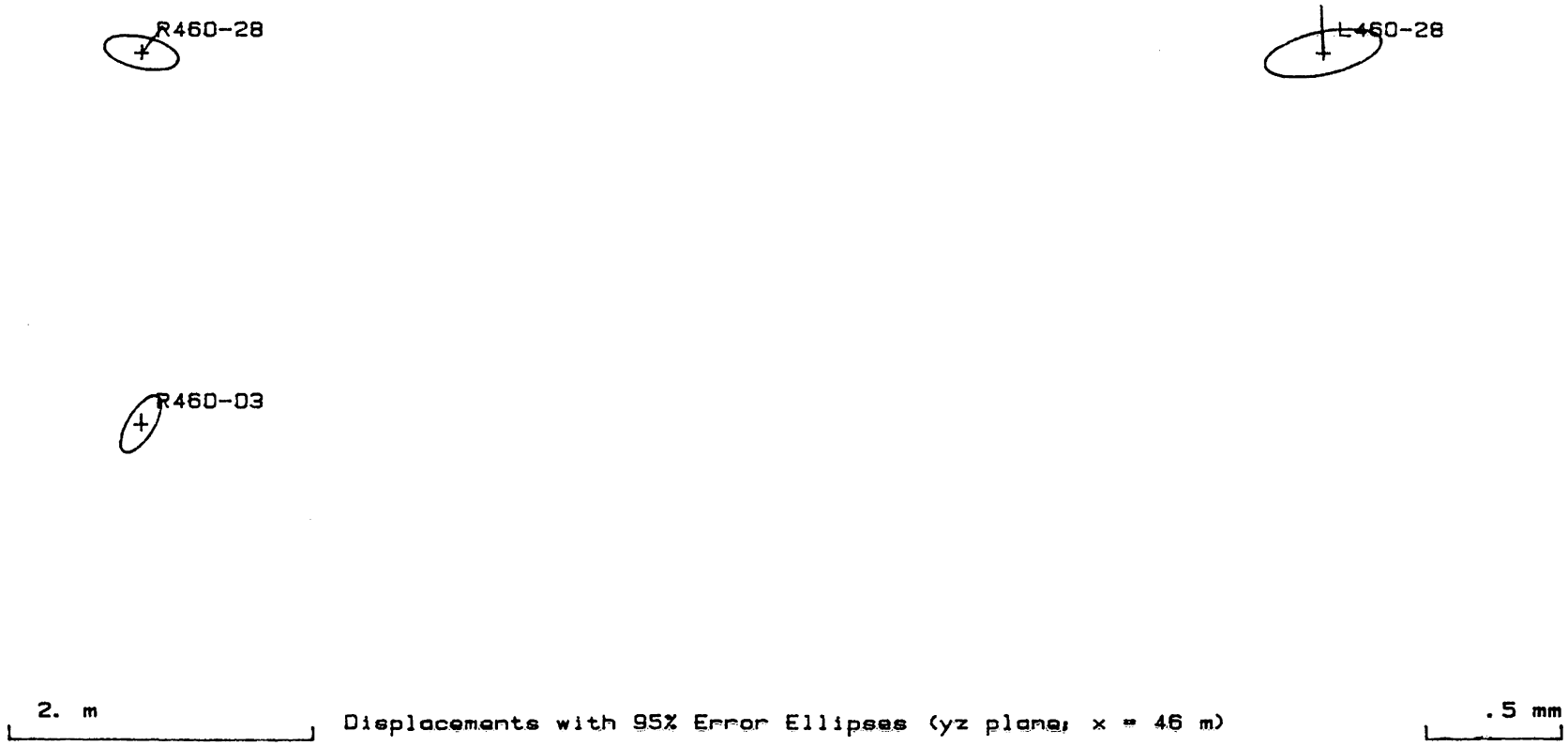
R460-28
L460-28
R460-03
2. m
Displacements with 95% Error Ellipses (yz plane; x = 46 m)
.5 mm